uOttawa

L'Université canadienne
Canada's university

FACULTÉ DES ÉTUDES SUPÉRIEURES ET POSTOCTORALES

uOttawa

L'Université canadienne
Canada's university

FACULTY OF GRADUATE AND POSDOCTORAL STUDIES

Mansour Navidpour

AUTEUR DE LA THÈSE / AUTHOR OF THESIS

M.A.Sc. (Civil Engineering)

GRADE / DEGREE

Department of Civil Engineering

FACULTÉ, ÉCOLE, DÉPARTEMENT / FACULTY, SCHOOL, DEPARTMENT

Shake Table Tests for Pulse-Generated Active-Seismic Control of Frame Structure

TITRE DE LA THÈSE / TITLE OF THESIS

Dr. Murat Saatchioglu

DIRECTEUR (DIRECTRICE) DE LA THÈSE / THESIS SUPERVISOR

CO-DIRECTEUR (CO-DIRECTRICE) DE LA THÈSE / THESIS CO-SUPERVISOR

EXAMINATEURS (EXAMINATRICES) DE LA THÈSE / THESIS EXAMINERS

Dr. Dan Palermo

Dr. N. Naumoski

Dr. David Lau

Gary W. Slater

Le Doyen de la Faculté des études supérieures et postdoctorales / Dean of the Faculty of Graduate and Postdoctoral Studies

Shake Table Tests for Pulse-Generated Active-Seismic Control of Frame Structure

by

Mansour Navidpour

A thesis
submitted in partial fulfillment
of the requirements for the degree of

Master of Applied Science
In
Civil Engineering

Department of Civil Engineering
University of Ottawa
Ottawa, Canada
May 2007

Your file Votre référence
ISBN: 978-0-494-49309-0
Our file Notre référence
ISBN: 978-0-494-49309-0

PLEASE NOTE THAT THERE ARE 2 PAGES 97.

Abstract

The majority of the existing infrastructure, designed prior to the enactment of modern seismic codes, is seismically deficient. Because it is not feasible to replace the entire inventory of seismically deficient infrastructure with new and seismically designed infrastructure, retrofitting remains to be the only viable option for seismic risk mitigation. Therefore, there has been significant research on the development of seismic retrofit technologies. The research project reported in this thesis is an effort towards developing a new seismic retrofit technique that utilizes pulse-based active force control. This approach involves the monitoring of structures during a seismic event and applying control forces through actuators beyond an acceptable range of deformations to minimize lateral drift and hence the potential structural and nonstructural damage.

The research project involves tests of small-scale frames on a shake table, with and without active force control. Two single-storey single-bal frames were manufactured for this purpose, with two different stiffnesses. Different magnitudes of mass were placed on the frames as part of experimental parametric investigation. The changes in stiffness and mass resulted in different vibration frequencies. Idealized ground motions in the form of sinusoidal wave functions were applied at different frequencies to assess the relationship between the dynamic characteristics of the structure and those of the ground excitation. A previously recorded earthquake record was also used to investigate the feasibility of the retrofit technique under realistic seismic excitations. The results indicate that pulse-control can be used as an effective methodology for seismic risk mitigation. The seismic drift was reduced between 65% and 95%, and the structural performance improved significantly. The control forces remained relatively low, indicating that it is possible to apply the techniques in practice, at full scale.

Acknowledgements

The author wishes to express his sincere appreciation and gratitude to his supervisor, Dr. Murat Saatcioglu who provided guidance, advice and encouragement throughout this research project. I also would like to thank Muslim Majeed, the technical officer at the structural laboratory, for his assistance and technical support during the experiments.

Special thanks are extended to my parents and my brother for their continuous encouragement and support.

Contents

List of tables

List of figures

CHAPTER 1

Introduction

1.1 General

The protection of structures against natural hazards, particularly earthquakes, has been one of the main challenges for structural engineers. The majority of current infrastructure was built prior to the enactment of modern seismic codes. Therefore, the safe performance of these structures during seismic events is not assured. Because it is economically not feasible to demolish and reconstruct these structures, seismic retrofitting remains to be the only viable approach to seismic risk mitigation.

There are different philosophies and approaches for retrofitting structures. Some retrofit techniques are done at the element level and call for strengthening and improving seismically deficient individual elements. The other approach is to attack the problem at the system level, aiming at controlling deformations and consequent inelastic response. The latter approach may be more suitable when the entire structure lacks seismic design and detailing techniques. A conventional approach to retrofitting non-ductile reinforced concrete frame structures involves building reinforced concrete structural walls between existing columns. Other types of lateral bracing systems have been used in the past, involving diagonal braces usually made up of structural steel sections.

Seismic retrofit techniques intended to be used at the system level can be categorized into three different groups: i) passive control systems, ii) semi-active control systems, and iii) active control systems. Adding shear-walls, braces, or installing base-isolation systems are examples of passive control methods. In a semi-active control method, the structure is equipped with a central processing unit that can adjust the properties of the structure according to the nature of the excitation. In this method, no actual control force is applied. Different types of controllable dampers are examples of this method. In an active control system, corrective control forces are directly applied to oppose the induced excitation. This method is highly sensitive to time lags, but if utilized properly, offers a great potential.

In this research program, the performance of an active control system utilizing a bounded state control algorithm and pulse-generated control forces is investigated. This method has been unexplored due to the lack of proper hardware. Recent technological advances have resulted in suitable actuators with significantly improved dynamic response capabilities, minimizing time lags. One of the advantages of active force control system is that it can be activated only when it is needed. This implies that the stiffness characteristics of the structure need not change and the consequence of increasing lateral stiffness at the expense of increasing seismic force demands can be avoided. Another benefit is the non-intrusive nature of the technique which allows the installation of control actuators without undergoing a major renovation of the building.

1.2 Research needs

During the past few decades a number of novel seismic retrofit techniques were introduced. The majority of these developments have involved passive and semi-active control of structures. Active control remains to be relatively unexplored. This is especially true for pulse-generated active seismic control systems. This type of seismic control offers a tremendous potential for use in practice but could not be developed further due to lack of research. There is clear lack of experimental verification of pulse-control systems in the literature, as evidenced by the literature survey presented in

Chapter 2. Therefore, it is necessary to conduct real-time shake table tests to evaluate the performance of frames equipped with pulse control actuators.

1.3 Objective and scope

The objective of the experimental research program carried out as part of this thesis is to investigate the feasibility of pulse-generated active force control method as a seismic retrofit technique utilizing electromechanical actuators with instantaneous response capability. The tests include two sets of small-scale model frames. The test variables include structural mass, stiffness, ground excitation, and control conditions. The expected outcome of tests is to achieve considerable reduction in frame displacement response through active pulse control while keeping control forces to a manageable level.

The following forms the scope of work:

- Literature review on available control systems.
- Preparation of test set-up capable of performing real-time experiments using the University of Ottawa Shake Table.
- Selection and design of model frames, representative of a realistic prototype building frame, for testing.
- Design and manufacturing of model frames.
- Identification of design parameters and the acquisition of necessary hardware, including an electromechanical actuator with sufficiently fast response time, a compatible load cell and other instrumentation.
- Development of necessary computer programs to run the tests.
- Execution of a large number of tests under different ground excitations and different structural mass.
- Analysis and interpretation of test results.
- Presentation of results and preparation of a thesis.

CHAPTER 2

Literature review

2.1 General

Over the past three decades, a great deal of effort has been spent on the use of structural protective systems to mitigate the effects of dynamic natural hazards, such as earthquakes and strong winds. Conventionally, structures have been designed to sustain seismic events by ensuring a combination of strength, deformability and energy dissipation capacity. Depending on the magnitude and nature of excitation, the structure may deform well beyond the elastic limit. Inelastic deformations do not necessarily lead to structural collapse. These structures, however, must be designed to possess sufficient inelastic deformability (ductility). While properly designed and detailed structures can withstand strong earthquakes within the inelastic range of deformations and life safety is ensured, buildings designed prior to the enactment of modern building codes do not possess the required energy absorption capacity upon exhausting their elastic capacities. These structures pose threat to public safety and have high seismic risk.

Because it is not economically feasible to demolish and rebuild a large volume of seismically deficient structures, retrofitting remains to be the only option. Among the many conventional techniques currently used in practice, the use of supplementary devices is emerging as a potentially promising new technique. One of the main challenges in structural engineering is to utilize innovative methods to develop novel seismic control techniques for more efficient protection of structures. Presently, different types of supplementary control devices are proposed to be implemented in structures to either function as the main and only seismic protective device, or to provide additional seismic resistance to a structure. The seismic vulnerability of older and non-code compliant structures, which form the majority of our buildings and bridges in the world, has made seismic retrofitting one of the popular topics for seismic risk mitigation.

The control devices can also be employed as part of the seismic resisting mechanism in new structures. Though the dissipation of seismic induced energy through inelasticity in structures has been accepted as the primary design philosophy worldwide, increased inelasticity in structures inevitably results in some damage that requires post-earthquake repair. Therefore, the protection of new structures through supplementary devices has been gaining recognition in recent years ensuring elastic behaviour with little interstorey drift, while protecting brittle non-structural element, sensitive equipments and building contents against seismic damage. This chapter provides an overview of the available literature on structural control systems.

2.2 Control systems

Structural control systems are designed and installed to reduce the energy demand on structures through absorbing or deflecting a portion of the vibration induced energy on the structure. Uang and Bestro (1988) applied the principle of the conservation of energy to explain the principle of a control system through Eq. 2.1.

$$E = E_k + E_s + E_h + E_d \tag{2.1}$$

Where;

E : Total input energy from environmental forces;

E_k : Absolute kinetic energy;

E_s : Recoverable elastic strain energy;

E_h : Irrecoverable energy dissipated by the structural system through inelastic deformation or other intrinsic forms of damping;

E_d : Energy dissipated by structural protective systems.

This equation indicates that during a seismic event with certain input energy, the demand on energy dissipation can be reduced by using a structural protective system (Yang 2001). During the last three decades, significant efforts have been made to develop and improve new supplementary structural protective systems. These concepts can be divided into four categories:

(i) Passive control systems

(ii) Semi-active control systems

(iii) Active control systems

(iv) Hybrid control systems

2.3 Passive control systems

A passive control system may be defined as a system which diminishes the energy dissipation demand on the primary structure by utilizing the motion of the structure to develop control forces without requiring any external power supply. The magnitude of control forces is a function of the response of the structure at the location of the passive control system. In other words, this system reduces possible structural damage by reflecting or absorbing a significant portion of the input energy, hence, reducing the demand on the structure. The interaction between a structure and a passive control system is shown in Fig. 2.1 (Housner et al. 1997, Symans and Constantinou 1999). However, it should be noted that passive control systems are unable to adapt to changes in external loading or usage pattern. For instance, a hospital building in Los Angeles equipped with a passive base isolation control system that survived the 1994 Northridge earthquake (Nagarajaiah and Sun 2000), may have been severely damaged if it had been located elsewhere in the city (Makris 1997).

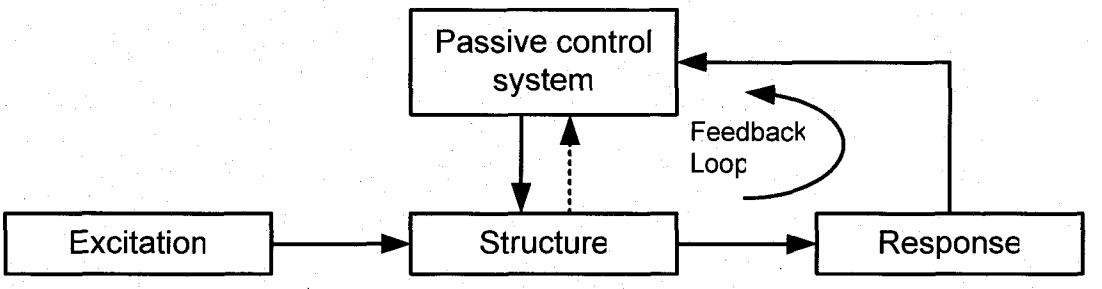

Fig. 2.1 Interaction between a passive control system and a structure (Housner et al. 1997)

When a structure is subjected to dynamic excitation, the structure will dissipate energy through cracking, yielding, friction, and plastic deformations in general. Having higher energy dissipation capability for the structure means a smaller portion of the input energy will act on the structure which consequently will lead to smaller vibration amplitudes for the structure. Many different control strategies have been proposed in the past, and they mainly aim at changing the damping characteristics of structures. Some buildings have little damping (damping ratio of about 1% of critical damping) with considerable deformations even when subjected to moderately strong earthquakes. Seismic induced energy can be dissipated with passive supplementary devices either by converting kinetic energy to heat or distributing energy among the modes of vibration. Frictional sliding, yielding of metals, phase transformation in metals, and deformation of viscoelastic solids or fluids are common methods used to convert kinetic energy to heat. Metallic yield dampers, friction dampers, viscoelastic dampers, and viscous fluid dampers are examples of such methods which utilize this approach in practice. Dynamic vibration absorbers are used to transfer the energy from one mode of vibration to another, with a view of distributing them approximately equally among the modes. Examples of devices using such method include tuned mass dampers and tuned liquid dampers (Housner et al. 1997). Comprehensive reviews of supplementary passive dampers are presented by Soong and Dargush (1997), Housner et al. (1997), Symans and Constantinou (1999), and Soong and Spencer (2002).

The theoretical concepts and behaviour patterns of these supplementary damping devices are well understood and their favorable performance in mitigating seismic damage is widely recognized. The following section introduces the base-isolation control system as one of the most debated passive supplementary device.

2.3.1 Base-isolation control system

Base-isolation control system, also referred to as seismic isolation system, is one of the most commonly debated technologies among engineers. The base-isolation system is typically installed at the foundation of a building as illustrated schematically in Fig. 2.2. The objective of the system is to isolate the structure from its base through a flexible energy dissipation system to keep the response of structure within acceptable limits. The performance level of a base-isolation system is mostly dependant on the level of flexibility that can be added to the structure to lengthen the natural period of vibration, as well as the energy dissipation characteristics of the system while providing sufficient rigidity against excessive deformations (Buckle and Mayes 1990). Typical base-isolation systems consist of elastometric bearings, lead rubber bearings, high damping rubber bearings, and sliding friction pendulum bearings (Soong and Constantinou 1994). During the past two decades, numerous structures have been equipped with base-isolation systems for seismic protection, especially in Japan and the United States of America.

After recent earthquakes, some researchers raised concerns about the reliability of base-isolation control systems (e.g. Hall et al. 1995, Heaton et al. 1995). The observations from the response of structures during the January 17, 1994 Northridge earthquake have suggested that this control system is susceptible to strong, impulsive, near-source ground excitations. Consequently, the requirements for base-isolation systems became stricter in the 1997 edition of the Uniform Building Code (ICBO 1997). This could potentially add to the complexities of base-isolation systems with potential ramifications on cost, making it more challenging to justify (Kelly 1999). The revisions in the code required the accommodation of larger base displacements to be mandatory. It was also recommended to use supplemental damping devices with simultaneous increase in strength to resist stronger earthquakes.

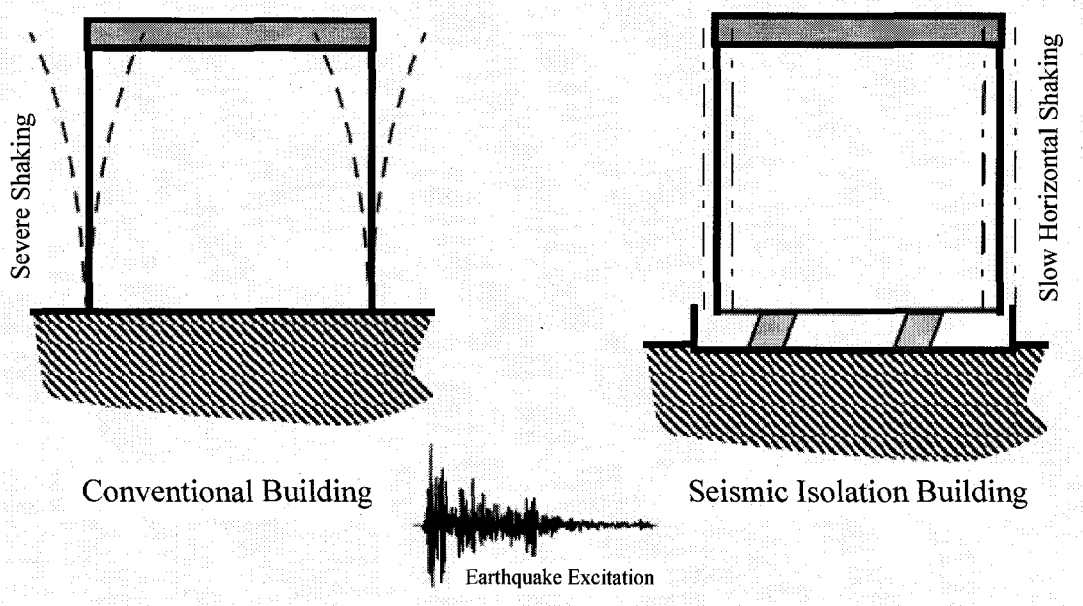

Fig. 2.2 Seismic base isolation system (Yang 2001)

2.4 Semi-active control systems

A semi-active control system may be defined as a system which cannot inject any mechanical energy to the structure and can optimally reduce the vibration amplitude by adjusting the structural properties. Since these devices do not apply any force to the structure, they do not have the potential to destabilize and/or damage the building. These control systems require a small power supply, i.e. a battery, to operate which is a big advantage since the external power supply may fail during an earthquake. Sensors are used to measure the excitation and/or the response of a structure. The sensors do not have to be installed on controllers and may be installed at locations remote from the control system. The readings from the sensors are used to monitor building response and adjust the mechanical properties of the control system to achieve required building response. Such devices are often referred to as controllable passive devices. The interaction diagram between a structure and a semi-active control system is shown in Fig. 2.3 (Housner et al. 1997, Symans and Constantinou 1999, Spencer and Nagarajaiah 2003).

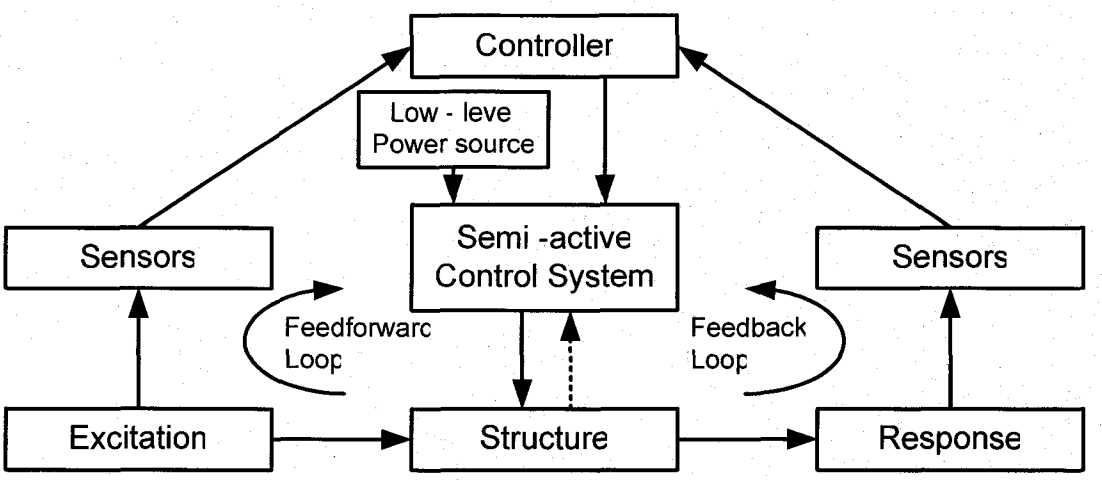

Fig. 2.3 Interaction diagram of a semi-active control system (Housner et al. 1997)

Research in the past two decades has indicated that semi active control systems, when appropriately installed, can show significantly better performance than passive control systems and have the potential to achieve the performance level of a fully active system. In fact, they demonstrated a good possibility for effective structural response reduction over a wide variety of dynamic loading conditions (Dyke et al. 1996, 1998; Spencer and Sain 1997, Spencer et al. 2000; Yi and Dyke 2000; Jansen and Dyke 2000; Yoshida et al. 2002; Ramallo et al. 2002; Johnson et al. 2003). Examples of such devices include variable-orifice fluid dampers, variable friction dampers, smart tuned mass dampers, tuned liquid dampers, variable stiffness devices, and controllable fluid dampers, as illustrated schematically in Fig. 2.4. Further details of semi-active control systems are provided in the following sections.

2.4.1 Variable – orifice dampers

In 1990, Feng and Shinozuka proposed a controllable, electromechanical, variable-orifice valve to adjust hydraulic fluid flow resistance. They suggested that the implementation of such a device on bridges can control the bridge movement during an earthquake. This approach was analytically and experimentally studied by a number of researchers, including Kawashima and Unjoh (1994), Sack and Patten (1993, 1998), Patten et al.

(1999), Symans and Constantinou (1999), Nagarajaiah (1994), Yang et al. (1995a), and Liang et al. (1995). A variable – orifice damper, shown schematically in Fig. 2.4 (a), requires about 50 watts of power to operate which can easily be supplied by a battery.

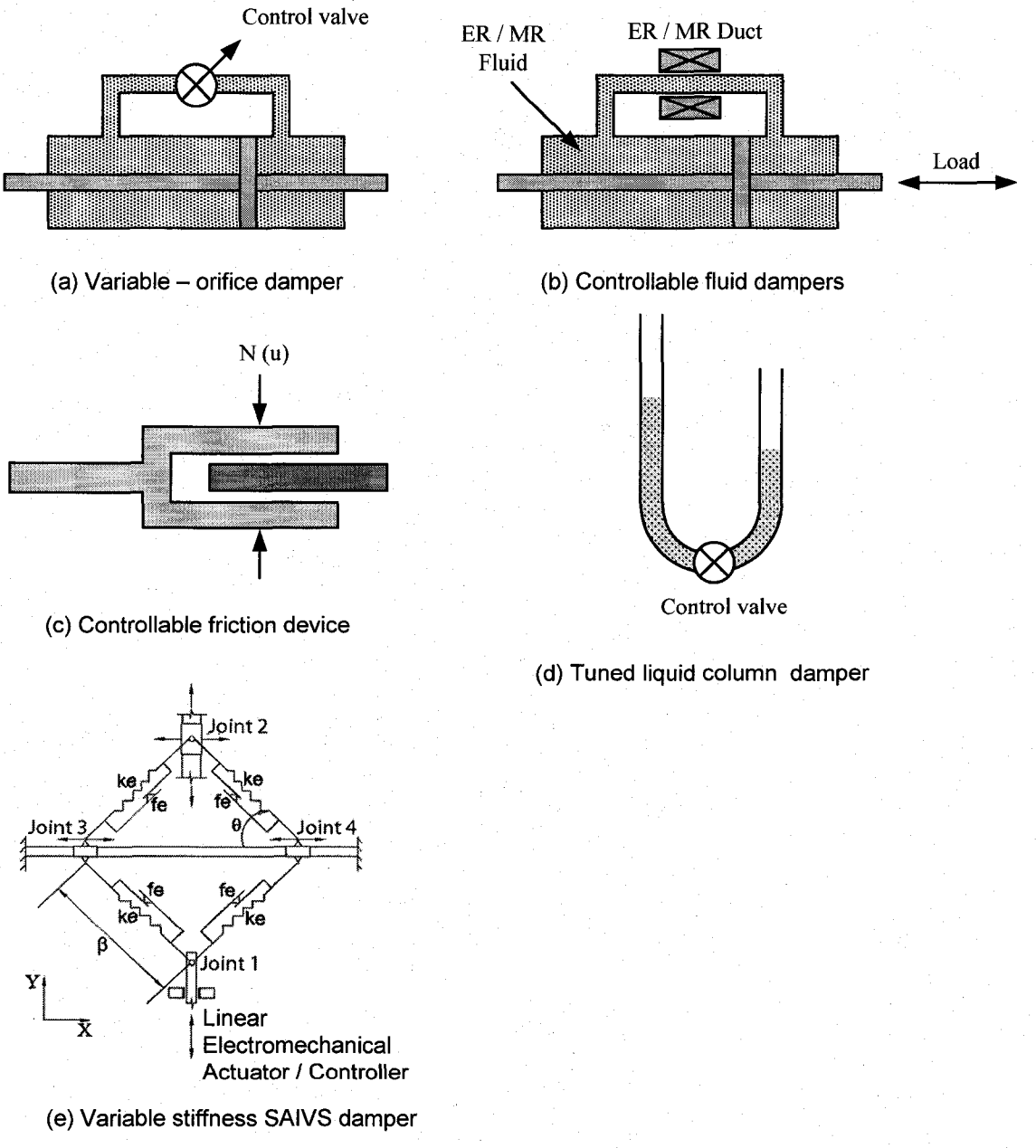

(a) Variable – orifice damper

(b) Controllable fluid dampers

(c) Controllable friction device

(d) Tuned liquid column damper

(e) Variable stiffness SAIVS damper

Fig. 2.4 Schematic view of semi active control devices

Shake table tests were conducted to evaluate the performance of a semi-active fluid damper presented by Symans et al. (1994). This semi-active fluid damper is nothing more than a passive fluid damper, modified by adding an external bypass loop with a controllable valve. The behaviour of this system is basically the same as that of a passive fluid damper, except for semi-active system having an adjustable damping property and enabling the system to deliver a wide range of damping levels. The tests indicate that this type of a semi-active control system can be effective for structures with low damping ratios (Symans and Constantinou 1997, Yang 2001).

Another semi-active variable stiffness system, using variable orifice dampers, was proposed by Kobori et al. (1993). The system was installed on a building at the Kobori Research Complex to investigate its vibration control performance. More recently, full-scale dampers of this type were installed in a five-story steel structure in the Kajima Shizuoka Building in Shizuoka, Japan (Kurata et al. 1999, 2000) as shown in Fig. 2.5. Each of the installed dampers in the building can produce up to a 1000 kN damping force, and requires only about 70 Watts of power to operate. After analyzing the response of structure, significant reductions were observed in both the storey shear forces and storey drifts (Yang 2001).

Sack and Patten (1993) designed a system to dissipate vibrations caused by vehicle traffic on bridges, using a hydraulic actuator, controlled by a motor operated valve. This system was first tested on a single-lane model bridge (Patten et al. 1994). It was then verified through a full-scale test of the Walnut Creek Bridge on Interstate Highway I-35 in Oklahoma, by Sack and Patten. The bridge is shown in Fig. 2.6. This system has a bi-stat control strategy and the test results showed that this semi-active control system can reduce as much as 70% of the vibrations. This bridge represents the first full-scale implementation of structural control in the United States (Newsletter of the International Association of Structural Control - 1997). An on-off controllable orifice hydraulic damper was also investigated as a resettable stiffness device by Jabbari and Bobrow (2002) and Yang et al. (2000).

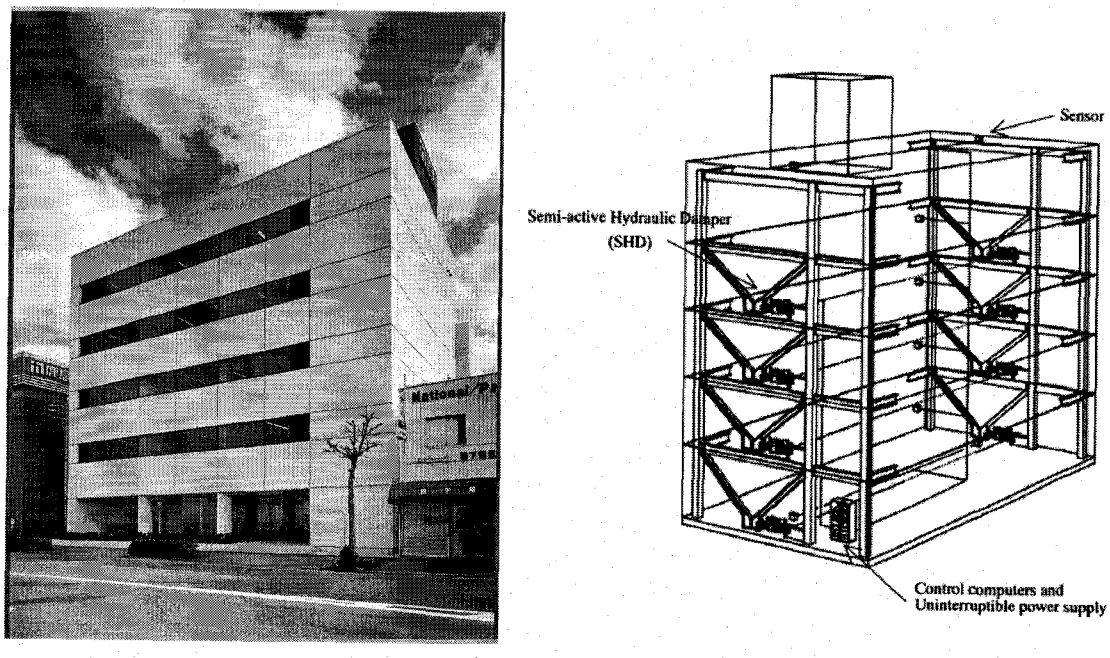

Fig. 2.5 Kajima Shizuoka Building equipped with semi-active hydraulic dampers

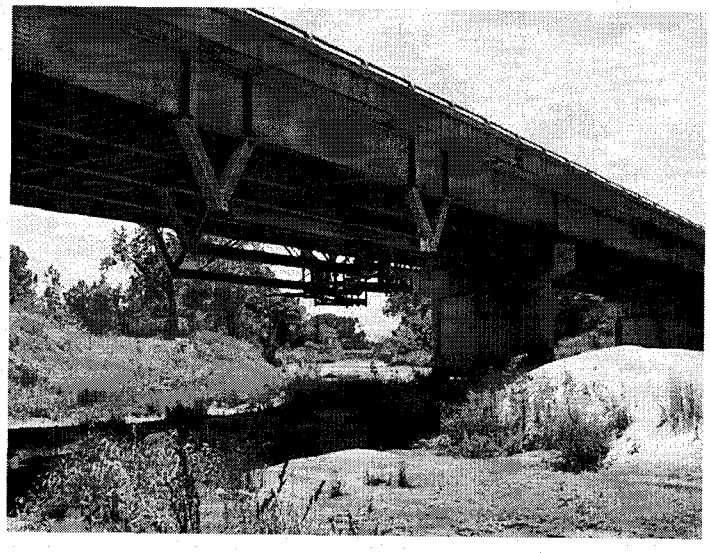

Fig. 2.6 Walnut Creek Bridge on Interstate Highway I-35 in Oklahoma

2.4.2 Variable friction dampers

Another semi-active control system was proposed by Akbay and Aktan (1991) and Kannan et al. (1995) which utilizes friction forces generated by surface friction to dissipate structural vibration. In this system, shown schematically in Fig. 2.4 (c), a friction shaft is rigidly connected to a structural bracing system and the magnitude of the

friction force is adjusted through changing the magnitude of the preload on the friction interface.

A similar device was presented at the University of British Colombia (Cherry 1994). Dowdell and Cherry (1994) developed a control device that used an "OFF-ON" algorithm. In this algorithm, the device maintains a constant pressure over the friction interface (ON) until the inter-storey velocity comes close to zero; then, the device releases the pressure (OFF) to let the brace position itself, and after that it returns to its original condition again (ON). Subsequently, Dowdell and Cherry (1994) proposed another approach using a full state feedback to actively control the friction force of the controller. Both systems were analytically and experimentally investigated and they both showed significant inter-storey drift reduction. While the "OFF-ON" algorithm seemed to be more appropriate for a single-degree-of-freedom (SDOF) structure, the second approach was shown to be effective for both SDOF and multi-degree-of-freedom (MDOF) structures.

Feng et al. (1993) and Yang et al. (1994a) installed a friction controllable fluid bearing in parallel with a seismic base-isolation system. Inaudi (1997) modeled the semi-active friction damper as a modulated homogeneous friction system and used only the deformation of the damper as a feedback signal for the controller. The use of piezoelectric friction dampers was experimentally investigated by Garrett et al. (2001). Recently, Yang and Agrawal (2002) studied the efficiency of variable-friction systems to reduce seismic response of non-linear buildings.

2.4.3 Smart tuned mass dampers

In this method, the motion of sloshing fluid or a column of fluid is used to dissipate the motion of the structure. This method is originally based on tuned sloshing dampers (TSD) and tuned liquid column dampers (TLCD) which are both passive control systems; known as tuned mass dampers (TMD). The design of TMD control system is very sensitive to the tuning frequency ratio, and in order to overcome this issue the idea of

using multiple mass tuned dampers (MTMD) was suggested. However, since the MTMD cannot be used in real-time, it is not practical.

The idea of TMDs with adjustable damping was introduced for the first time by Hrovat et al. (1983), offering a semi-active tuned mass damper (STMD). A decade after, Haroun et al. (1994) introduced a hybrid liquid damper (HLCD) which used a variable orifice damper in the TLCD to maintain an optimal damping condition. Another device based on TSD was designed by Lou et al. (1994) where the natural frequency of the damper can be adjusted by changing the length of the sloshing tank. Abe et al. (1996) and Yalla et al. (2001) have upgraded passive TLCD by modifying it with a variable orifice, hence, developing a STMD. Furthermore, Yalla and Kareem (2003) developed another STMD by utilizing an electro-pneumatic actuator driving a ball valve to change the cross section of a TLCD. Simulations showed an additional 15% to 30% extra response reduction in comparison with passive control systems.

2.4.4 Variable stiffness devices

The main goal of most of the designed control systems is to enhance the structure to sustain excitations against strong winds and moderate earthquakes. During 1980's, researchers in Kobori Research Complex concentrated on finding a method capable of handling strong earthquakes. Kobori et al. (1993) designed a variable stiffness device by installing a variable-orifice damper in a semi-active variable stiffness system (AVS). In order to investigate the performance of this device, a full-scale damper was installed on Kajima Research Institute building to control vibrations. Even though a variable orifice damper can be used to manufacture a variable stiffness device, the device will only work in on-off states; where it will either have high stiffness due to hydraulic fluid compressibility primarily due to entrapped air when the valve is closed or has no stiffness when the valve is open. In other words, by using variable orifice dampers, the stiffness cannot vary continuously between different states.

Nagarajaiah and Varadarajan (2000) developed a semi-active tuned mass damper, with variable stiffness that functions in real time with the capability of continuously adjusting

building stiffness and damping (Nagarajaiah 2000, US Patent No. 6,098,969). The effectiveness of this semi-active continuously and independently variable-stiffness device (SAIVS), illustrated in Fig. 2.7 (a), was studied by Nagarajaiah and Mate (1998) in a scaled structure. The force-displacement hysteretic loops of this scalable device are shown in Fig. 2.7 (b). The test results displayed smooth changes in the stiffness of structure and produced a non-resonant system. Varadarajan and Nagarajaiah (2003) research on the efficiency of this system in a tall benchmark building showed competence to reduce responses comparable to active control systems. The effectiveness of this type of control system in base isolated bridges subjected to near fault earthquakes was investigated (Sahasrabudhe and Nagarajaiah 2005). Recently, an experimental and numerical study on seismic control of smart sliding isolated buildings using variable stiffness systems was conducted by Nagarajaiah and Sahasrabudhe (2006).

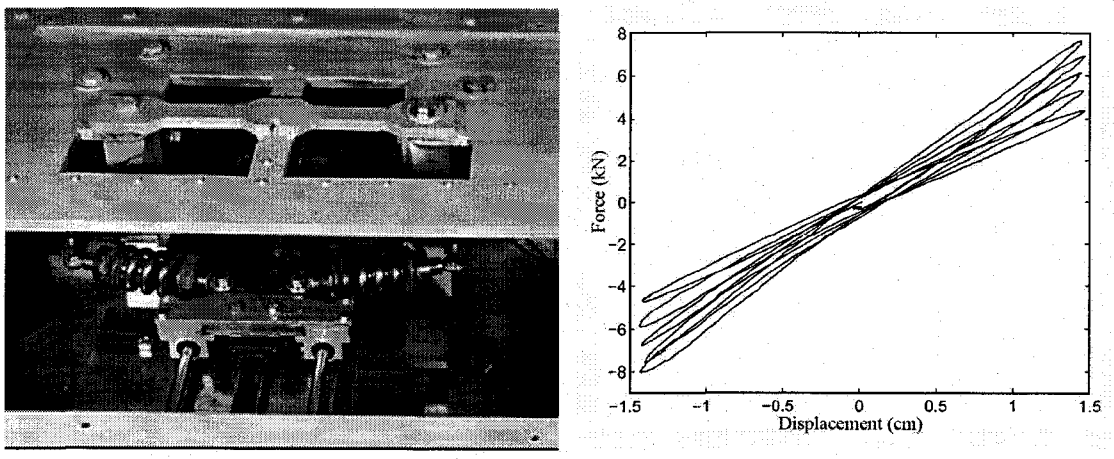

(a) **(b)**

Fig. 2.7 Semi-active independently variable Stiffness (SAIVS) device

2.4.5 Controllable fluid dampers

In the previously mentioned semi-active devices, the characteristics of structures were adjusted through some electrically controlled valves or mechanisms. A new generation of semi-active controllers uses a unique controllable fluid in a fixed orifice damper to mitigate the vibrations of structures. The mechanical simplicity of this device without any

moving part except the damper's piston makes it advantageous in terms of maintenance and reliability. This type of damper is illustrated schematically in Fig. 2.4 (b).

There are two types of fluid that have the characteristics suitable for use in such dampers, i) electrorheological (ER) fluid and ii) magnetorheological (MR) fluid. These types of fluid have the capability to change reversibly from free-flowing linear viscous fluids to semi-solid with a controllable yield stress, in a matter of few milliseconds when exposed to an electric field for ER fluid or magnetic field for MR fluid. Among these two types of fluid, only the MR fluid is suitable for civil engineering applications (Spencer and Sain 1997). The behaviour of fluid can be modeled as Newtonian, in the absence of a magnetic field. It can be modeled as visco-plastic (Phillips 1969) when the field is applied. MR fluid appears in the form of micron-sized, particles that are magnetically polarized. They are dispersed in mineral or silicon oil. Their yield strength is not sensitive to variations in temperature and they can operate between -40°C and 150°C with little change in yield stress. In addition, MR fluid dampers can be operated with approximately 50 Watts of power which can be provided with batteries. This adds to the reliability of system in terms of independency from external power supply sources.

Even though the discovery of MR fluid dates back to 1940s, only recently it has been applied to civil engineering. The performance of MR dampers has been thoroughly studied analytically and experimentally by a number of researchers during the last decade (Spencer and Sain 1997; Spencer et al. 1997, 2000; Spencer 2002; Dyke et al. 1996, 1998; Nagarajaiah et al. 2000; Sahasrabudhe et al. 2000; Xu et al. 2000; Gavin et al. 2001; Yi et al 2001; Ramallo et al. 2002; Yoshioka et al. 2002; Madden et al 2002, 2003; Hiemenz et al. 2003; Johnson et al. 2003; Ni et al. 2004; Yang et al. 2004; Ying et al. 2004; Jin et al. 2005; Yan and Zhang 2005; Karkoub and Zribi 2006; Jung et al. 2006; Loh and Chang 2006; Zhou et al. 2006; and Yan and Zhou 2006).

Test results indicated that MR dampers significantly outperform comparable passive control devices. In addition, the technology has been demonstrated to be scalable to devices large enough for civil engineering structures. For instance, a 20 ton capacity MR

damper shown in Fig. 2.8 (b), appropriate for full-scale applications, was developed and tested by a number of research groups (Carlson and Spencer 1996, Spencer et al. 1999, and Yang et al. 2002a). Figure 2.8 (a) shows the force – displacement hysteretic loops of this damper (Spencer and Nagarajaiah 2003).

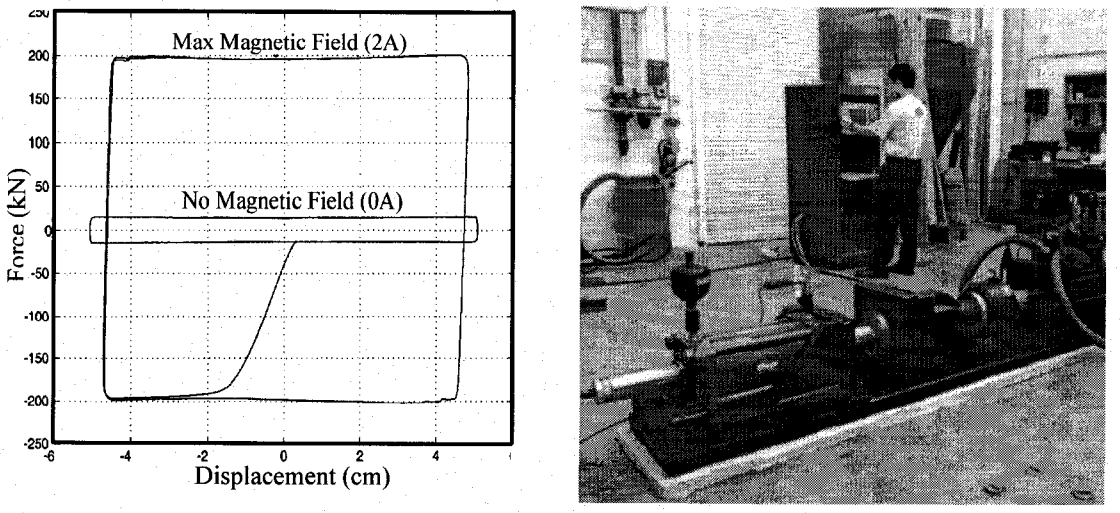

(a) **(b)**

Fig. 2.8 Large-scale 20 ton MR fluid damper

2.5 Active control systems

An active control system may be defined as a system in which a control actuator applies control forces to the structure in a prescribed manner with real-time processing. The control forces are a function of the measured responses of structures and/or ground excitations, depending on the algorithm used to calculate control forces.

As illustrated in Fig. 2.9, Sensors that are not necessarily mounted on the controller are used at a remote location to measure the response of structure. The data is then sent to the controller as feedback. In other words this control system acts simultaneously with a seismic excitation in order to ensure structural safety. The actuator(s) used in the system is normally supported by an external source of power due to the high operational power demand of the electrohydraulic or electromechanical system (Housner et al. 1997, Symans and Constantinou 1999).

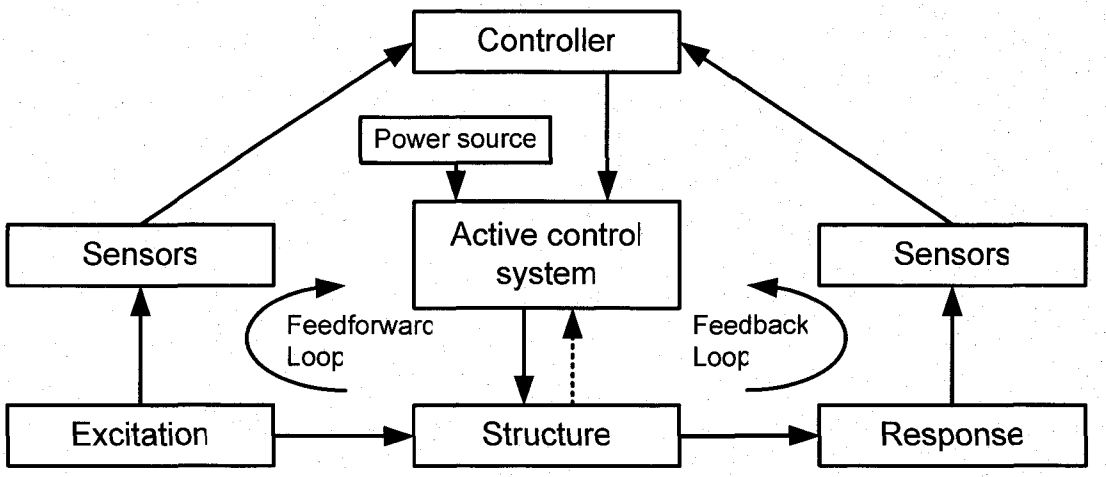

Fig. 2.9Interaction diagram of an active control system

(Housner et al. 1997)

2.5.1 Control algorithms

There are different control strategies and algorithms to calculate control forces that should be applied on structures and some of these algorithms are specifically proposed for civil engineering applications. The dynamic response of an n-degree-of-freedom structure when subjected to seismic excitation is represented by its state-space equation written in the form of Eq. 2.2. This equation is also referred to as equation of motion.

$$M\ddot{x} + C\dot{x} + Kx = E\ddot{x}_g(t) \tag{2.2}$$

After implementing an active control system, the state-space equation is modified as in Eq. 2.3.

$$M\ddot{x} + C\dot{x} + Kx = E\ddot{x}_g(t) + Du(t) \tag{2.3}$$

Where; M, C and K are mass, damping and stiffness matrices, respectively; and $\ddot{x}$, $\dot{x}$ and x represent acceleration, velocity and displacement, respectively. $\ddot{x}_g(t)$ is the ground excitation and E is a vector representing the degree-of-freedom in which the ground acceleration is applied. D is the matrix representing the location of control forces and $u(t)$ is the control vector corresponding to the magnitude and number of control forces for the structure. If Eq. 2.3 is solved for $\ddot{x}$, then the following expression is obtained:

$$\ddot{x} = -M^{-1}C\dot{x} - M^{-1}Kx + M^{-1}E\ddot{x}_g(t) + M^{-1}Du(t) \tag{2.4}$$

Combining Eq. 2.4 with $\dot{x}$, an equation known as state-space equation, is derived, as shown below.

$$\dot{Z}(t) = AZ(t) + W_1\ddot{x}_g(t) + Bu(t) \tag{2.5}$$

Where; $Z(t)$ and $\dot{Z}(t)$ are given in Eq. 2.6. $Z(t)$ is referred to as the state vector.

$$Z(t) = \begin{bmatrix} x \\ \dot{x} \end{bmatrix} \quad ; \quad \dot{Z}(t) = \begin{bmatrix} \dot{x} \\ \ddot{x} \end{bmatrix} \tag{2.6}$$

And matrices A, W_1, and B are defined as:

$$A = \begin{bmatrix} 0 & I \\ -M^{-1}K & -M^{-1}C \end{bmatrix} \quad ; \quad W_1 = \begin{bmatrix} 0 \\ M^{-1}E \end{bmatrix} \quad ; \quad B = \begin{bmatrix} 0 \\ M^{-1}D \end{bmatrix} \tag{2.7}$$

There are different control strategies and algorithms to calculate the control force, and each one has its own advantages and disadvantages. In other words, each approach provides a better treatment for a different parameter. The most important step in the entire control process is the selection of the most appropriate control algorithm for the problem at hand. Some of the most common control algorithms include:

(a) Optimal linear control (also called classical linear optimal control)

(b) Pole assignment

(c) Independent model space control (IMSC)

(d) Instantaneous optimal control

(e) H_∞ Method

(f) Sliding mode control

(g) Bounded state control

(h) Fuzzy logic control

(i) Predictive control

(j) Neural network systems

Among the above, there are several algorithms that are more suitable for civil engineering structural control applications. Those methods are discussed in the following section.

2.5.1.1 Optimal linear control

In the optimal linear control algorithm, a J function (also referred to as "cost function" or "pay-off-function") is introduced as illustrated in Eq. 2.8 (Soong 1990). The control vector, $u(t)$, is chosen in such a way that J index would be minimized.

$$J(t) = \int_0^{t_f} \left[Z^T(t) Q Z(t) + u^T(t) R u(t) \right] dt \tag{2.8}$$

In the above expression, superscript ^{T} indicates vector or matrix transpose. Q and R matrices are referred to as weighting matrices, and the magnitude of them is chosen by control system designer. If a large value is assigned to Q, relative to matrix R, a higher priority is given to the reduction of structural response over the magnitude of control force. The opposite is also true when Q is assigned a large value relative to R. The designer can assign a higher priority to response control if there is no need to limit the energy consumption of control device or any concern over exceeding the capacity of the control device. Similarly, where special needs for structural response reduction dictates the situation, such as in the case of nuclear power plants, then a higher weight is assigned to Q. This implies that the relative magnitude of Q and R introduces a proper trade-off between the effectiveness of control and the consumption of control energy (Soong 1990). It should be noted that the time span defined in Eq. 2.8, $\left[0 \quad t_f \right]$ should be longer than the duration of external excitation.

2.5.1.2 Pole assignment

Matrix A in the state-space equation defined in Eq. 2.7, describes system dynamics. Its eigenvalue provides modal damping and stiffness properties. In this method, the control force is calculated by linear state feedback from the structure, as shown below:

$$u(t) = GZ(t) \tag{2.9}$$

Where, G is a constant gain matrix. After substituting the above equation in Eq. 2.5, the state-space equation is written in the following form:

$$\dot{Z}(t) = (A + BG) Z(t) + W_1 \ddot{x}_g(t) \tag{2.10}$$

A comparison between Eq. 2.5 and the above equation shows that the state matrix has changed from (A) in Eq. 2.4 to (A+BG) in Eq. 2.9. The main goal in this strategy is to find a gain matrix, G, such that the system is changed to be completely controllable and observable.

The two conditions mentioned above should be examined in order to use this method: (i) controllability, and (ii) observability. A system is called completely controllable if for every time step of response, the initial state $Z(t_0)=Z_0$ at initial time (time t_0) and it can be transferred to final state $Z(t_1)=Z_1$ during a limited time increment of (t_1-t_0).The easiest method to check the controllability of a system is to find a range for matrix P expressed below:

$$P=\left[A\vdots AB\vdots A^2B\vdots\cdots\vdots A^{n-1}B\right] \tag{2.11}$$

Where, A and B matrices are shown in Eq. 2.6. If the rank of matrix P is equal to the number of degrees-of-freedom of the system "n", then the system is completely controllable (Shooshtari 2005).

A system is referred as an observable system if for every initial time t_0 of incremental response the initial state $Z(t_0)=Z_0$ can be determined from a measured parameter $y(t_1)$ during time increment (t_1-t_0). In the pole assignment method, vector $y(t)$ is a function of measured response of structure and is introduced and expressed as:

$$y(t)=CZ(t) \tag{2.12}$$

Then, Matrix S, illustrated in Eq. 2.13, is formed to determine the observability of a linear system.

$$S=\begin{bmatrix} C \\ CA \\ CA^2 \\ \vdots \\ CA^{n-1} \end{bmatrix} \tag{2.13}$$

If the rank of the above matrix matches to the number of degrees-of-freedom of the system, n; then the system is completely observable. It should be mentioned that if a system is not completely observable, it does not satisfy the above condition. (Shooshtari 2005)

Pole assignment method was used to calculate control forces in a long-span bridge under moving loads, and reported to have resulted in a significant reduction in bridge response (Abdel-Rohman and Leipholz 1978).

2.5.1.3 Independent modal space control (IMSC)

The equation of motion of an n-degree-of-freedom system subjected to an external excitation force $F(t)$, in the absence of any control force, is written as given in Eq. 2.14.

$$M\ddot{x} + C\dot{x} + Kx = F(t) \tag{2.14}$$

Where; M, C and K are mass, damping and stiffness matrices respectively; and x is the geometric coordinate of the structure. This expression can be rewritten in terms of the generalized coordinate, y, where;

$$x = \Phi y \tag{2.15}$$

Matrix Φ is $n \times n$, and contains the mode shapes of the structure. It is well-known that the equation of motion of an n-degree-of-freedom system can be converted into n decoupled single-degree-of-freedom system in modal coordinates. In order to find the decoupled system of equation of motion, in generalized coordinate, y, the following steps are taken. First, x from Eq. 2.15 and its derivative and second derivative are substituted into Eq. 2.14, and then multiplied by Φ^T. This results in the uncoupled equation of motion shown in Eq. 2.16.

$$\bar{m}_i \ddot{y}_i + \bar{c}_i \dot{y}_i + \bar{k}_i y_i = f_i(t) \qquad i = 1, 2, ..., n \tag{2.16}$$

Where; $\bar{m}_i$, $\bar{c}_i$ and $\bar{k}_i$ are generalized mass, generalized damping and generalized stiffness, respectively; and $f_i(t)$ is the i^{th} column of matrix $\Phi^T \times F(t)$.

This form of equation of motion, expressed in generalized coordinates, was used by Martin and Soong (1976) to solve the problem of active control for a multi-storey building. They expressed the generalized force acting on the structure, $f_i(t)$, in terms of ground acceleration and generalized control force up to mode p, as illustrated in Eq. 2.17.

$$\bar{m}_i \ddot{y}_i + \bar{c}_i \dot{y}_i + \bar{k}_i y_i = g_i(t) + v_i(t) \qquad i = 1,2,...,p \quad (2.17)$$

Where; $g_i(t)$ and $v_i(t)$ are the ith elements of $G(t)$ and $V(t)$ vectors, respectively, which are defined as follows:

$$G(t) = C^T E \ddot{x}_g(t) \quad (2.18)$$

$$V(t) = C^T D u(t) = L u(t) \quad (2.19)$$

Where; C is an $n \times p$ sub-matrix of Φ matrix, including the first p mode shapes. The first p modes can then be used to represent the system in a state-space form. Next, by solving this state-space equation, control forces required to restrain the equivalent p-degree-of-freedom system are found. Any one of the previously discussed methods can be used to compute these control forces. For instance, if optimal linear control method is applied, the J index that should be minimized is expressed as Eq. 2.20.

$$J = \sum_{i=1}^{p} J_i \quad (2.20)$$

Where; p is the number of modes considered, and J_i is as shown below.

$$J_i = \int_0^{t_f} \left[q_{1i} y_i^2(t) + q_{2i} \dot{y}_i^2(t) + r_i v_i^2(t) \right] dt \quad (2.21)$$

In this method, the control force for the ith mode, $v_i(t)$, and the response of the structure in terms of general coordinates, y_i and $\dot{y}_i$, are obtained. The results for all the desired modes can be put together to find matrix $V(t)$. The final step in this method of calculating control forces in geometric coordinates, $u(t)$, is to find L from Eq. 2.19 (Shooshtari 2005).

There are three different cases to solve for L matrix, which has the dimension of $p \times m$:

Case 1. If the number of p modes considered is equal to the number of control forces, m; then L is a square matrix and the control force can be found from the following expression:

$$u(t) = L^{-1}V(t) \tag{2.22}$$

Case 2. If m > p, then L is not a square matrix. By using pseudo-inverse technique, the control force, $u(t)$, can be calculated as below:

$$u(t) = L^T\left(LL^T\right)^{-1}V(t) \tag{2.23}$$

The accuracy of the result is verified through the following calculation.

$$V(t) = Lu(t) = LL^T\left(LL^T\right)^{-1}V(t) = V(t) \tag{2.24}$$

Case 3. If m < p, then L is not a square matrix and another pseudo-inverse technique can be used to calculate $u(t)$.

$$u(t) = \left(L^TL\right)^{-1}L^TV(t) \tag{2.25}$$

After checking the accuracy of the above equation it is observed that this equation offers an approximate solution for the latter case.

$$V(t) = Lu(t) = L\left(L^TL\right)^{-1}L^TV(t) \approx V(t) \tag{2.26}$$

As a solution for the final case, it is recommended to consider number of modes such that $m \geq p$ to avoid such inaccuracy in calculations. Baruh and Meirovitch (1982) have studied the effect of using a varying number of controllers and indicated that the stability margin of the structure decreases with decreasing number of controllers (i.e. actuators). On the other hand it should be noted that there is no practical use in having more controllers than the number of modes to be controlled (Soong 1990).

2.5.1.4 Instantaneous optimal control

The optimal control system was discussed previously in Section 2.5.1.1. In that method, no feedback from the ground was used. Therefore, the control system could have been optimized even further if the ground acceleration feedback was considered, $\ddot{x}_g$. In 1986, Yang, Akbarpour and Ghaemmaghami introduced a new algorithm, referred to as

instantaneous optimal control by modifying the optimal control algorithm. They redefined J factor from optimal control algorithm, which should have been minimized over a period of time between zero and t_f in such a way that it could be minimized at every time step t for all $0 \le t \le t_f$. This is illustrated below:

$$J(t) = Z^T(t) Q Z(t) + u^T(t) R(t) \tag{2.27}$$

The state-space equation is defined as expressed in Eq. 2.27.

$$Z(t) = Td(t - \Delta t) + \frac{\Delta t}{2}\left[Bu(t) + W_1 \ddot{x}_g(t)\right] \tag{2.28}$$

Where; T is a modal matrix whose columns are the eigenvectors of state matrix A. Also, the $d(t-\Delta t)$ is expressed as follows:

$$d(t - \Delta t) = e^{\Omega \Delta t} T^{-1}\left[Z(t - \Delta t) + \frac{\Delta t}{2}\left[Bu(t - \Delta t) + W_1 \ddot{x}_g(t - \Delta t)\right]\right] \tag{2.29}$$

Where; Ω is assumed as shown below:

$$\Omega = T^{-1} A T \tag{2.30}$$

In this method, Hamilton function, H, is defined as follow:

$$H = Z^T(t) Q Z(t) + u^T(t) R u(t) + \lambda^T\left\{Z(t) - Td(t - \Delta t) - \frac{\Delta t}{2}\left[Bu(t) + W_1 \ddot{x}_g(t)\right]\right\} \tag{2.31}$$

Where; $\lambda(t)$ is the Lagrange multiplier, and Q and R are the weighting matrices, defined in Section 2.5.1.1. The J function is minimized through calculating the derivatives and setting them equal to zero:

$$\frac{\partial H}{\partial Z} = 0 \quad ; \quad \frac{\partial H}{\partial u} = 0 \quad ; \quad \frac{\partial H}{\partial \lambda} = 0 \tag{2.32}$$

The resulting equations from the above calculations are shown below:

$$2QZ(t) + \lambda(t) = 0 \tag{2.33}$$

$$2Ru(t) - \frac{\Delta t}{2} B^T \lambda(t) = 0 \tag{2.34}$$

$$Z(t) = Td(t - \Delta t) + \frac{\Delta t}{2}\left[W_1 \ddot{x}_g(t) + Bu(t)\right] \tag{2.35}$$

The Lagrange multiplier, $\lambda(t)$, can be defined differently depending on the feedbacks of the control algorithm and used to find control forces. The three possible cases are indicated below:

1. Closed-loop control
2. Open-loop control
3. Closed-open-loop control

In a closed-loop control system, $\lambda(t)$ is only a function of structural response; whereas, in open-loop control system, $\lambda(t)$ is only a function of ground excitation. In closed-open-loop control system, both the structural response and ground excitation are incorporated to obtain $\lambda(t)$.

2.5.1.5 H_∞ method

For civil engineering applications, most important goals in applying the optimal linear control algorithm are to retain the stability of the structure and also to attain specific performance criterion. As an example, this criterion can be the control efficiency of the system facing random excitations. There are issues that prevent the optimal linear control to perform in its best possible way. These issues are the consideration of nonlinear actuator saturation effects, pre-specified levels of robustness, and random, time-varying parametric uncertainties which should be addressed concurrently.

Actuator saturation happens when the demand from the actuator is greater than the designed peak output of the actuator. This results in a clipped control that consequently leads to changes in the optimal linear control algorithm input and if this non-linearity is not accounted for; then, neither performance nor stability of the system can be guaranteed. The solution to this problem is to either perform extensive simulation to find the absolute maximum required control force for different cases, which is impractical, or to develop a control algorithm that can guarantee stability even if the saturation occurs (Chase and Smith 1996).

Under large magnitudes of loads, the structural parameters may change along with the state-space equation. These changes may vary as unknown functions of time or structural response. To account for these uncertainties, the variations can be assumed to take place within the framework of a linear model. Afterwards, the inherent modeling errors in defining state-space representative equation can be corrected by implementing this linear model to achieve a robust control method (Chase and Smith 1996).

H_∞ control algorithm was first presented by Zames (1981) and was further developed based on the work of Golver and Doyle (1988), Petersen (1987), Doyle et al. (1988), and Khargonekar et al. (1990). Yang et al. (1994b) improved the feasibility of the system for civil engineering applications.

In a Robust control strategy; as in the case of robust H_∞ control algorithm, the control system guarantees quadratic stability of otherwise uncertain system over all combinations of uncertain parameters (Chase and Smith 1996). In this method, the solution of a definite algebraic Riccati equation is necessary to obtain the control force. Hollet et al. (1980), Petersen et al. (1986), and Petersen (1985, 1987) confirmed the stability of the robust H_∞ system through their research. Research conducted by Veillette et al. (1989) and Xie et al. (1992) indicated that the robust H_∞ control system not only guarantees stability, but also ensures the prescribed performance level while facing time-varying uncertainties. Other researches that utilized the H_∞ method include Schmitendorf et al. (1994); Smith et al. (1994); Jabbari et al. (1995); Kose et al. (1996, 1998); Yang et al. (1996a, 2002b); Khot and Oz (1997); Sun and Shahin (1999); Alt et al. (2000); Du et al. (2004); and Bai and Grigoriadis (2005).

2.5.1.6 Sliding mode control (SMC)

The sliding mode control (SMC) algorithm, also referred to as variable structure control (VSC), has been studied since early sixties and it was developed to control uncertain nonlinear systems (Taran 1964; Utkin 1977, 1992). The objective of SMC control system

is to force the response trajectory into the sliding surface. This surface is designed to remain stable and to maintain the trajectory on the sliding surface for all times. In a regular sliding mode control system, there is no systematic design approach; although, through designing the sliding surface, the variation of control effort is attained (Wu and Yang 2004). Yang et al. (1997) introduced a novel systematic approach for the modulation of control effort by using a compensator. Another systematic approach was presented by Wu and Yang (2004) through using a pre-filter.

SMC system application to nonlinear and hysteretic structures, and also shake-table experimental verification for both linear and nonlinear cases was conducted by: Yang et al. (1994c, 1995 b, c; 1996 a, b), Agrawal et al. (1998), and Wu (2003).

SMC has been effectively applied to control systems such as:

(i) Active variable damper systems (Yang et al. 1994c, 1995c)

(ii) Active variable stiffness systems (Yang et al. 1996b)

(iii) Hybrid control systems installed on building using rubber-bearings or sliding-bearing and actuators (Yang et al. 1995bc, 1996b)

(iv) Hybrid control systems installed on bridges using rubber bearings and actuators or rubber bearings and active variable dampers (AVD) or sliding bearings and actuators (Yang et al. 1995b)

The SMC was used in the past with active, semi-active and hybrid control systems. Its application in either nonlinear dynamics or hysteretic behavior or parametric controls showed promising response. Civil engineering applications of SMC control strategies were investigated by a number of researchers and the results showed remarkable performance levels (Yang et al. 1994c, 1995 b, c; Spencer et al. 1998; Wu et al. 1998; Wu and Yang 1998; Cao et al. 1998; Wu 2003). Full-scale applications of this method include:

1) Nanjing TV transmission tower (310 m height) in 1998.
2) A full-scale experimental building in 2003.
3) A 76-story wind excited benchmark building in 2004.

2.5.1.7 Bounded state control

In general, the main goal of a control system is to limit a set of response variables to permissible range established by codes and standards to ensure structural safety and human comfort. Among the parameters of structural response, displacements and accelerations are of interest for structural safety and the comfort of the occupant, respectively. Consequently, control algorithms are proposed to limit state variables to prescribed limits for civil engineering structures. The limits are not necessarily zero displacement or zero acceleration and may vary with applications. For example, a structure may be permitted to respond freely until a limit is exceeded; and then the control system is activated to ensure that structural response is maintained within the prescribed limits. All pulse control systems are categorized under this method.

2.5.1.8 Other control algorithms

Other control algorithms, not discussed above, include neural network systems, predictive control algorithms, and fuzzy logic control algorithms. Fuzzy logic control has similarities to H_∞ control algorithm in terms of capabilities of handling nonlinearities, and uncertainties of the system (Ahlawat and Ramaswamy 2004). Researchers who developed fuzzy logic control include: Iiba (1994), Joghataei and Ghaboussi (1994), Subramaniam et al. (1996), Battaini et al. (1998), Symans and Kelly (1999), and Ahlawat and Ramaswamy (2001, 2002, 2004).

2.5.2 Active control systems

A variety of active control systems were designed, developed and modified during the past few decades. Depending on the proposed approach, either a single or several control algorithms may be applicable to calculate the direction and magnitude of control forces. The most common active control systems include:

(a) Active mass damper and Active mass driver (AMD)

(b) Active tuned mass dampers (TRIGON)

(c) Active variable stiffness system (AVS) or active variable damping system (AVD)

(d) Aerodynamic appendages
(e) Active bracing system
(f) Pulse generator
(g) Active tendon control

The procedure for each control system, previous researchers in the area, and in a few cases actual applications are presented in the following sections.

2.5.2.1 Active mass damper and Active mass driver (AMD)

The principals of this method are based on passively tuned mass dampers (TMD). A conventional TMD is made-up of a spring and a damper to absorb structural vibrations. This passive system shows best performance when the frequency of the seismic excitation matches the natural frequency of the structure. On the other hand if a non-resonant dynamic excitation occurs, TMD system is generally ineffective since the response of the structure is not sufficiently strong. However, it should be noted that the modification introduced through a TMD system may change the natural frequency of the overall system such that the frequency of the excitation may approach to that of the modified structure. If this happens, the response of structure may increase and may even exceed that of the uncontrolled structure (Collins et al. 2006).

The control performance of TMD is improved by adding extra actuators, as illustrated in Fig. 2.10. The active vibration control approach was theoretically compared to conventional passive TMD by Morison and Karnopp (1973). Lund (1979) investigated the feasibility of this method by using an actuator and a pneumatic spring. His thoughts were pursued further by Chang and Soong (1980). The researchers employed a linear quadric optimum control algorithm. However, they did not optimize the TMD parameters to find control forces. The performance of this method was discussed and compared with regular TMD systems by Nishimura et al. (1992).

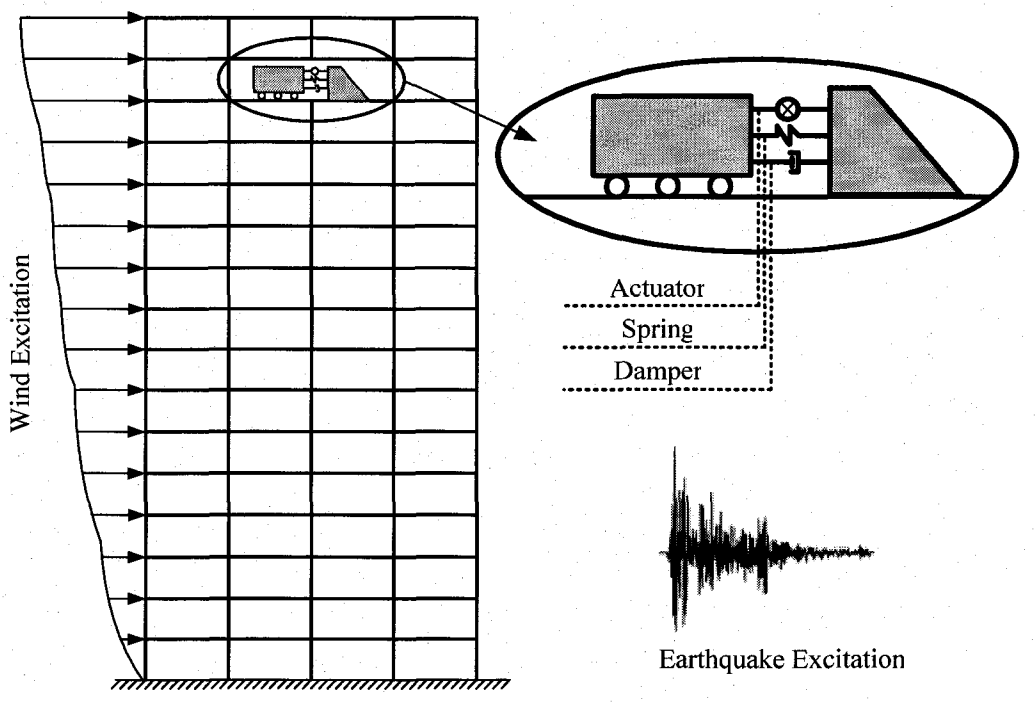

Fig. 2.10 Concept of the AMD control system

In 1987, Kuroiwa and Aizawa mounted an AMD device on top of a four-storey model frame with a varying moving mass ranging from 1% to 2% of structural weight. The dimensions of the structure were 1m width × 1m depth × 2m height, and weighed 970kg. This specimen was tested using a shake table. The experimental results showed 50% reduction in displacements of the top floor, but only 5-7% reduction in accelerations.

In another study, an AMD system was mounted on top of a 0.5m wide × 3m high three-storey steel frame. The experimental results showed two-third reduction in maximum acceleration and displacement. Further investigation on the AMD control systems was performed by a number of researchers, including; Dyke et al. (1994), Chang and Yang (1995), Ankireddi and Yang (1996), Mackriell et al. (1997), Yan et al. (1999); Li et al. (2003), Li (2004), Li and Zhou (2004), Li and Zhang (2004), Guclu and Sertbas (2005), Collins et al. (2005).

The first full-scale field application of the active control system was Kyobashi Seiwa Building, Tokyo, Japan, in 1989. The control system was designed by Kyobori Research Company and consisted of a large mass acting as a pendulum which was controlled by an actuator, as shown in Fig. 2.11(a). In this eleven-storey building, two AMD systems were used as shown in Fig. 2.11(b). These masses consisted of one 4200 ton mass at the center of the gravity of the eleventh floor, and another 1200 ton mass positioned at the same level with some eccentricity from the center of gravity.

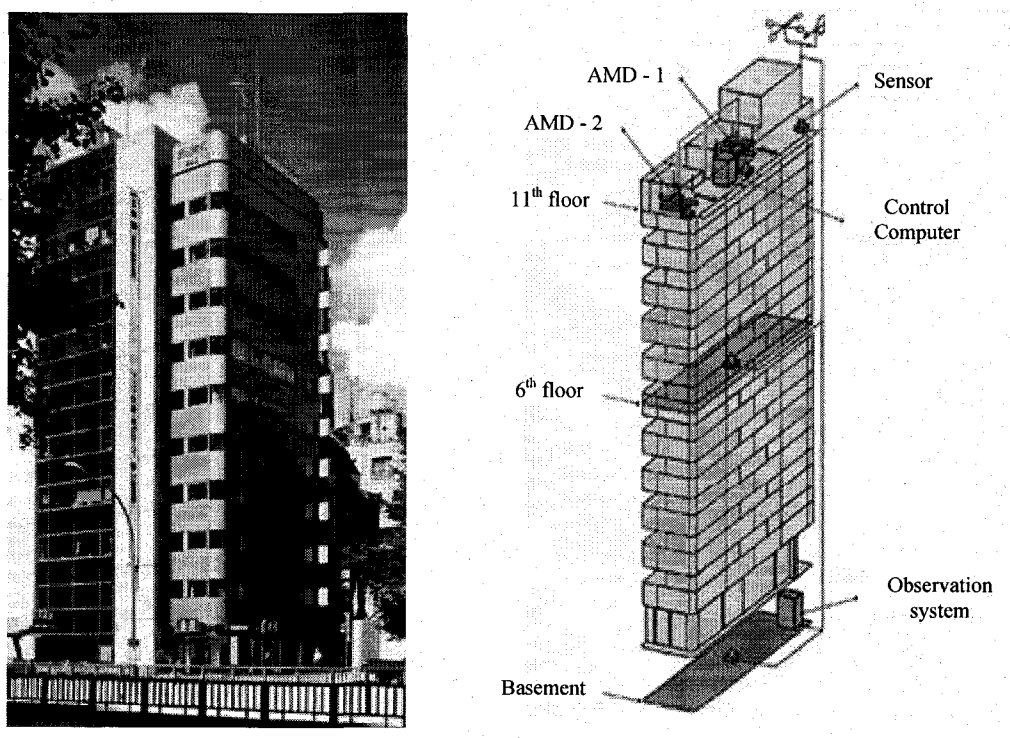

(a) **(b)**

Fig. 2.11 Kyobashi Seiwa Building with AMD Installation.

Nanjing tall communication tower (340 m height) also uses AMD protective system. The design details of the AMD control system of this tower can be found in Cao et al. (1997).

2.5.2.2 TRIGON – active tuned mass dampers

Kajima Corporation introduced a new device for structural response control in early 1990's. This device was named "TRIGON" and was a modified version of a conventional AMD device. The modification of this system allows the amplitude of pendulum to be

extended when necessary to enable better performance. The concept of the system is shown in Fig. 2.12.

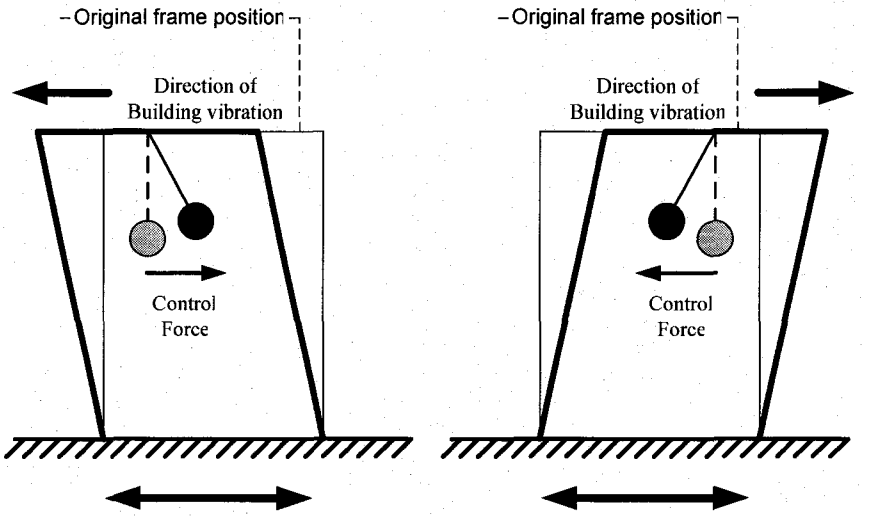

Fig. 2.12 Concept of TRIGON device (Lynch 1998)

The inertia force applied on the mass, illustrated in Fig. 2.12, functions as the control force on the structure. The TRIGON device consists of a V shaped rail on which the device is mounted, as illustrated in Figure 2.13. The angle of the rail is adjustable, allowing the adjustment of the period of structure. This device was installed in 1994 for the first time on the Shinjuku Park Tower, Tokyo, Japan. This high-rise building is a 52-storey building and is considered as one of the tallest buildings in Japan. The TRIGON device is located on the 39th floor. The control system establishes the direction and magnitude of control force, based on feedbacks from the sensors positioned on the 1st, 10th, 20th, 30th, and 39th floors.

2.5.2.3 Aerodynamic appendages

Klein et al. (1972) suggested using aerodynamic appendages to reduce wind-induced motion of tall buildings for the first time. The approach was further developed by Klein and Salhi (1980). The most attractive attribute of this method is the ability of the control system to utilize the energy of the same wind, effects of which are being controlled. In other words, there is no need for an external energy source to produce the control force.

The only external power supply necessary to run this system is the power required to operate the appendages positioning mechanism (Fig. 2.14).

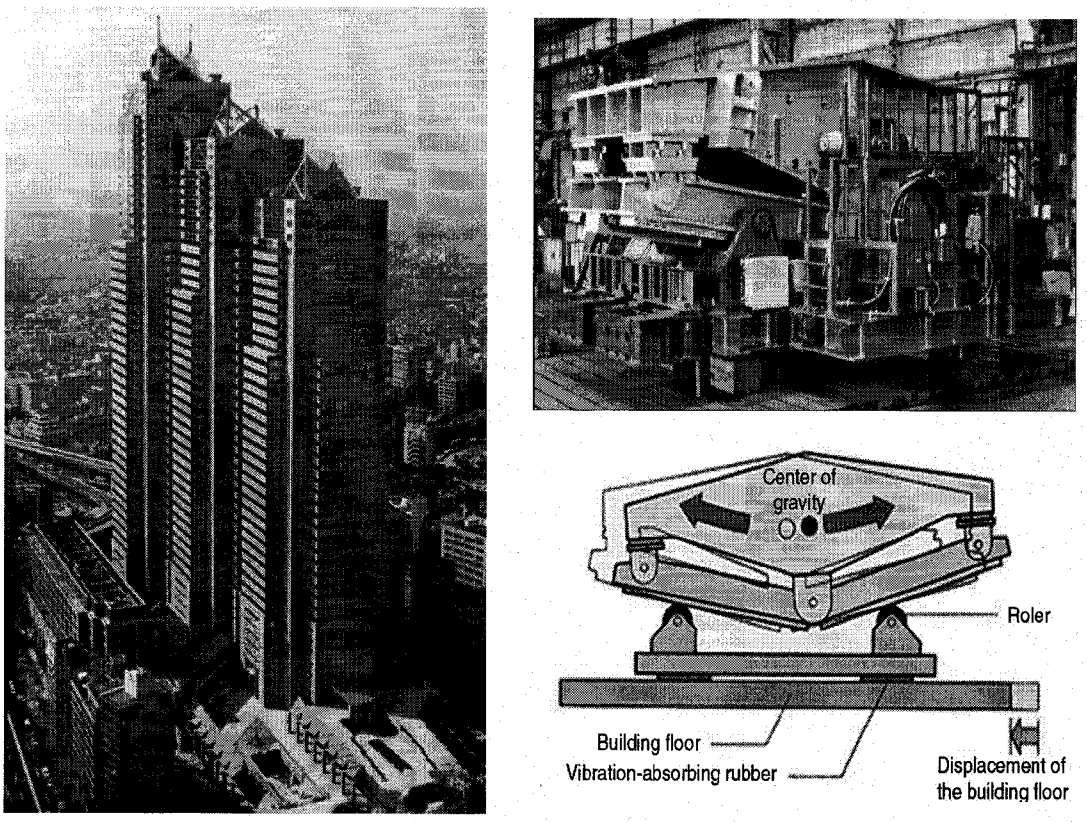

(a) Shinjuku Park Tower, Tokyo, Japan

(b) TRIGON control device

Fig. 2.13 TRIGON control device implemented in practice

Further research on this method was performed by Chang et al. (1980) and Abdel-Rohman (1983, 1984) who utilized the optimal control algorithm. Moreover, the technique was studied experimentally by conducting wind-tunnel tests (Soong and Skinner 1981). For simplicity the researchers used a suboptimal control algorithm, which functioned as an on-off function. The appendages in this case fully extended when the controller was on, applying control forces, and fully retracted otherwise. The area of the appendages was approximately 2% of the structural frontal area when fully extended. The test results indicated approximately 50% reduction in displacement response.

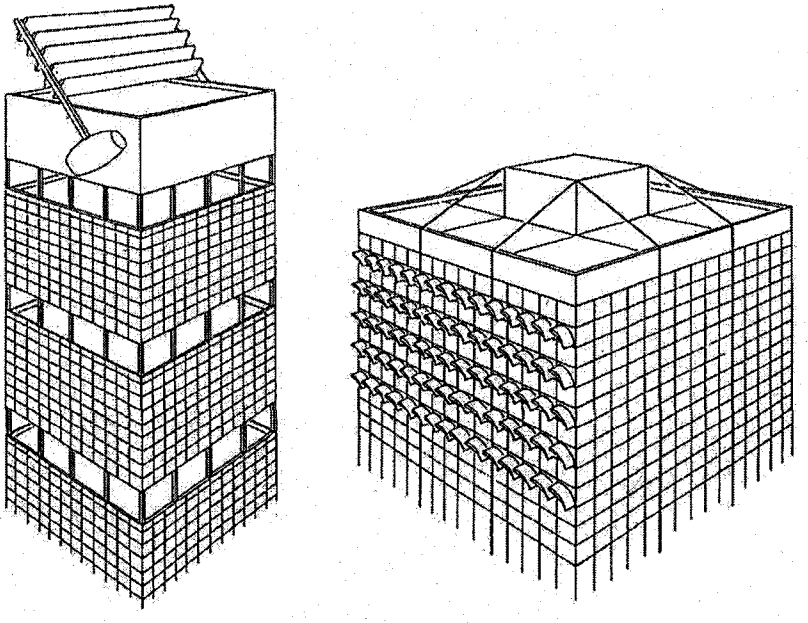

(a) (b)

Fig. 2.14 Examples of appendage design (Soong 1990)

(a) Venetian blind-type appendage; (b) Symmetrically placed appendages

The feasibility of this method in reducing wind-induced vibration and increasing structural stability was studied on long suspension bridges (Arco and Aparicio 1999, 2001; and Nissen et al. 2004).

2.5.2.4 Pulse generator

Masri et al. (1980, 1981, 1982), and Udwadia and Tabaie (1981 a, b) introduced a simple control strategy based on pulse generation. In this system short-interval high-energy pulses are applied to the structure to limit deformations beyond a certain tolerable level and/or destroy the gradual rhythmic build-up of structural responses in the case of resonance. The system requires constant instantaneous feedback from the structure. When the response of the structure exceeds a certain threshold value, defined by the designer of the system, the control force is applied in the opposite direction of the motion. The magnitude of the control force is determined as a function of the instantaneous velocity of the structure. The value of the control force has to minimize a non-negative cost function.

The actuator is then trigged whenever a zero-crossing of the relative displacement at the point of interest is observed. Then, the control pulse, p_i, expressed in Eq. 2.36, is applied on the structure at a selected location.

$$p_i(t) = -c_i \operatorname{sgn}(v_i)|v_i|^{n_i} \quad , \quad t_{0i} < t < t_{0i} + \Delta t_i \qquad (2.36)$$
$$= 0 \quad \text{otherwise}$$

Where; c_i is a pulse scaling coefficient at location i, sgn( ) represents the algebraic sign if its argument, v_i is relative velocity at location i, t_{0i} is the zero-crossing time at location i, and Δt_i is the pulse width at location i. An appropriate value for n_i has to be chosen based on modeling preferences. $n_i = 0$ is selected when control forces act as Columbus friction forces, with the magnitude of $\pm c_i$; whereas, $n_i = 1$ represents an active viscous damper with the coefficient of c_i; and finally, $n_i > 1$ corresponds to nonlinear velocity dampers (Soong 1990).

This control system was tested on a 6-storey model frame in a lab (Miller et al. 1988, Traina et al. 1988). A pneumatic actuator was used to thrust the frame. A sample measurement from the thruster indicated the time delay between the time that the control signal was sent to the pneumatic actuator and the time that the actuator responded to deliver the thrust action on the frame. Also, some inevitable deviations from an ideal rectangle pulse shape is observed, shown in Fig. 2.15. In this test, $n_i = 0$ was chosen, the results showed 15% reduction of structural response. The result may have been improved if the time-delay was minimized and the control force was determined more precisely.

Another pulse control system was introduced by Prucz and Soong (1983), and Reinhorn et al. (1987a). In their method, the control system tries to predict the motion of the structure, and applies the control pulse shortly prior to the expected threshold crossing time. The performance of the system is dependent on how good the algorithm employed

can predict the state of structure. This control system is efficient for both resonant and non-resonant excitations.

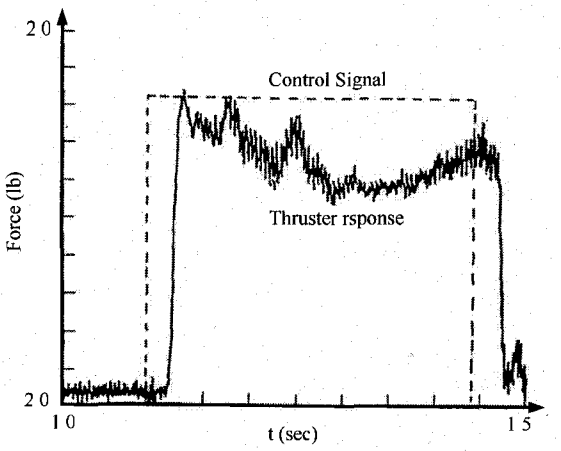

Fig. 2.15 Experimental control pulse (Traina et al. 1988)

In general, pulse control mechanisms have a lot of attractive features which give them high-potential for field applications. First, they are relatively simple to implement. Second, they require less complicated on-line computational effort in comparison with other control techniques. They are suitable for the treatment of both elastic and inelastic structures. Furthermore, they consume less control energy to control buildings. This can be explained with the force application procedure used in these methods. Since small levels of vibrations are tolerated in this system, control forces need to be applied only when necessary, and relatively smaller amount of energy might be sufficient to perform corrective actions on the structure periodically.

2.5.1.9 Active tendon control

In 1960, Freyssinet introduced the concept of active control system for the first time. This system consists of a set of prestressed tendons connected to the structure. The magnitude of tension is adjusted by an electrohydraulic servomechanism. One advantage of this

method is that it can operate under both pulse mode control as well as continuous-time mode control.

The effectiveness of active tendon system for different types of structures has been studied in a number of research projects involving slender structures (Roorda 1975, Yang and Giannopoulos 1978), tall buildings (Abdel-Rohman and Leipholz 1983; Abdel-Rohman 1987; Juang et al. 1980; Samali et al. 1985 a, b; Yang 1982; Yang and Lin 1983, Betti and Panariello 1995), bridges (Yang and Giannopoulos 1979 a, b; Carotti et al. 1987), and offshore structures (Prucz and Soong 1983; Reinhorn et al. 1986, 1987b). In 1994, Dyke et al. experimentally verified the acceleration feedback control strategies for active tendon systems.

A comprehensive study was carried out in 1987 by Soong et al. to investigate the performance of active tendon control systems using a shake table. This test consisted of three stages. In stage one, a single-degree-of-freedom structure was modeled and tested as illustrated in Fig. 2.16 (a). In stage two, a three-degree-of-freedom structure was examined as shown in Fig. 2.16 (b), and in stage three, a six-degree-of-freedom structure was investigated as illustrated in Fig. 2.16 (c). Closed-loop optimal linear control algorithm was used to calculate the control force for these tests.

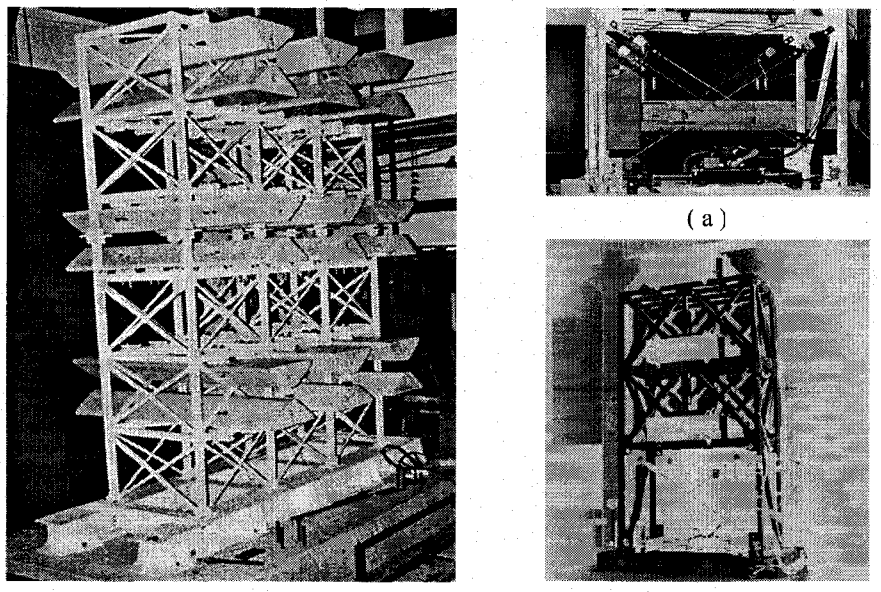

Fig. 2.16 (a) **SDOF model;** (b) **3-DOF model;** (c) **6-DOF model. (Soong 1990)**

Different tendon arrangements were used for the six-degree-of freedom structure as shown in Fig. 2.17. The results for all these tests can be found in Chung et al. (1986, 1988). A sample test result is shown in Fig. 2.18.

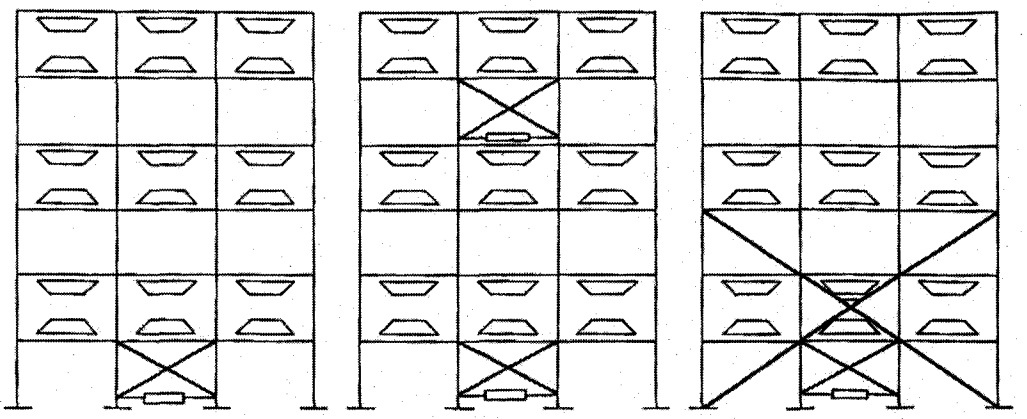

Fig. 2.17 Examples of tendon arrangements

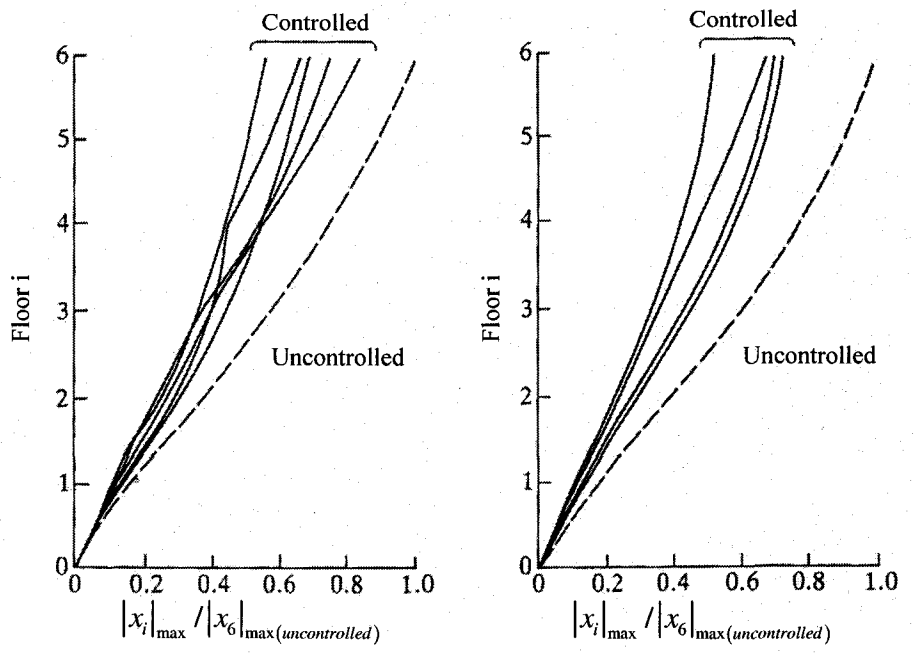

(a) Experimental results **(b) Simulation results**

Fig. 2.18 Reduction of maximum response normalized to uncontrolled top displacement

2.6 Advantages and disadvantages of active control systems

The performance of active control systems is not sensitive to the characteristics of dynamic excitation. In addition, these systems can adapt to structural modifications and patterns of loading. Furthermore, they can be programmed to behave according to the unique demands of each project. Due to these abilities to adapt, the performance of a properly designed and implemented active control system can not be matched by other systems.

In order to develop confidence for an active control system, a number of challenges have to be addressed (Soong 1990). These include; i) capital cost and maintenance, ii) reliability of the external power supply, iii) fear of unknown in a non-traditional technology, iv) system robustness. These concerns are expanded below.

Capital cost and maintenance: The initial cost of some of the active control systems can be prohibitively high. Furthermore, the system is only used during an earthquake and it is likely that it would not be activated frequently. Because the reliability of operation depends on the performance level of the system after a long period of standby time, maintenance is an important factor. In spite of the high cost of active control systems, it has recently been shown that, when used as a retrofit technique the cost can be relatively low due to the non-invasive nature of the technology. However, more research is needed to clarify issues pertaining to cost.

Dependence on external power and its reliability: The possibility of a power failure is quite high during a seismic event. This increases the vulnerability of the structure to potential power loss with a risk of leaving it unprotected during a seismic event. However, recent research led to new developments to overcome this problem. The duration of a seismic excitation is usually around one minute for each episode. If the control system is provided with a secondary power supply to operate independently of the primary power supply during this duration, then the system reliability can be improved. Fortunately, the magnitude of the power requirement is such that it can be supplied with currently available accumulators.

Non-traditional technology: Since the application of active control to civil engineering infrastructure has been proposed rather recently and it is outside the conventional fields of application, it has faced obstacles for widespread acceptance. The acceptance of technology will be achieved through more research and verification.

System robustness: In order to facilitate the application of active control systems in practice, simplicity is promoted. However, civil engineering structures are complex systems. Therefore, the design of a proper and robust system with sufficient controllability and effectiveness becomes a major challenge.

2.7 Hybrid control systems

A hybrid control system is typically defined as a system that utilizes a combination of passive and active devices. In such systems, higher levels of performance can be achieved because of the involvement of multiple control systems, acting simultaneously on the structure. In addition, some of the restrictions and limitations associated with a single system are alleviated. Also, the hybrid control systems can be more reliable, though designing and debugging these systems can be more challenging, requiring ful knowledge of both systems. To date, the majority of controlled buildings and bridges that have active control devices utilize hybrid control systems. DUOX system is an example of a hybrid control mechanism.

2.7.1 Active/passive composite tuned mass dampers (DUOX)

Another one of the innovative control systems introduced by Kajima Corporation was named "DUOX". This control approach, shown schematically in Fig. 2.19, has a small active mass damper (AMD) on top of a passive tuned mass damper (TMD). In general, a TMD passive control system contains a large mass, and hence it functions slowly. It starts moving very slowly upon the application of induced force and also stops slowly after the removal of external forces. The deficiency of this system was addressed through adding an AMD mass to the primary TMD mass. This adjustment enables the control device to

react instantly upon the onset of loading. The device was employed in two buildings: Ando Nishikicho Building in Tokyo, a 14-storey building; and Dowa Kasai Phoenix Tower in Osaka, a 29-storey building (145 m height) shown in Fig. 2.20 (Ohrui et al. 1994, Kobori 1994, Imazeki et al. 1995). The Ando Nishikicho Building was subjected to an earthquake having Richter magnitude of 7.1 in 1993 and resisted the earthquake with 70% reduction in maximum response acceleration. Devices similar to DUOX were also studied by Iemura and Izuno (1994).

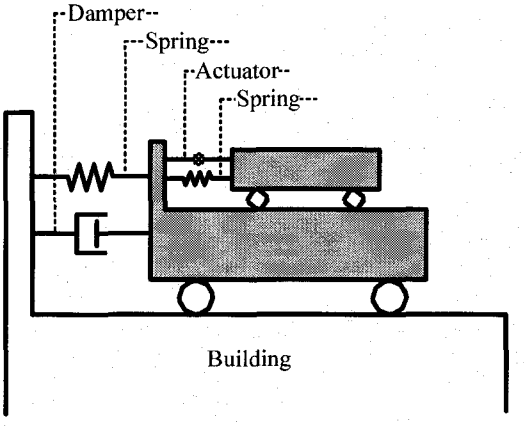

Fig. 2.19 Concept of DUOX device

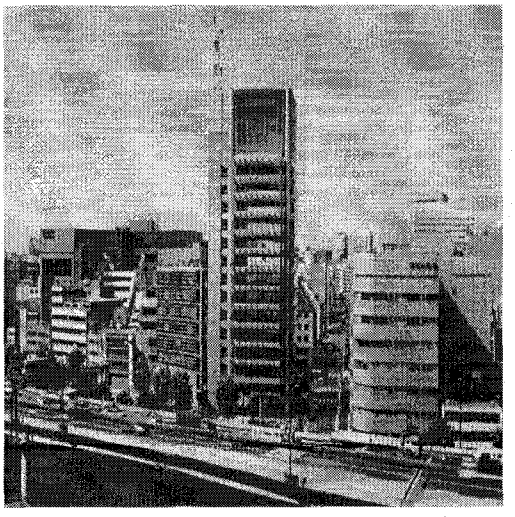

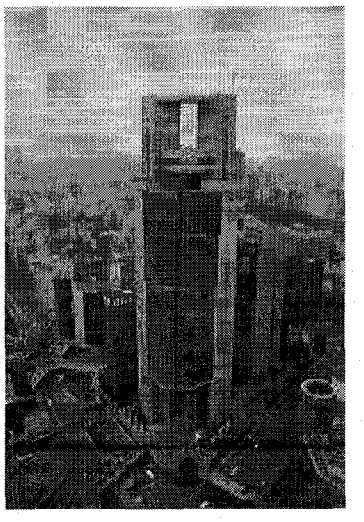

(a) Ando Nishikicho Building **(b) Dowa Kasai Phoenix Tower**

Fig. 2.20 Towers utilizing DUOX control system in Japan

2.8 Field applications

A summary of buildings and towers in the world, equipped with control devices that utilize smart supplementary control technology (active, semi-active or hybrid control systems) for seismic hazard mitigation, is listed in Table 2.1. The properties of each building, such as height, occupancy, control system, and location are indicated in the Table. Table 2.2 contains a list of actively controlled bridges. The vast majority of these structures employs hybrid control systems, and is mainly located in Japan. Table 2.4 provides a list of key structures equipped with supplementary passive control systems, each of which has introduced a new system. Recently completed applications of control devices in Tokyo, Japan are listed in Table 2.4.

It is noteworthy mentioning that the tallest building in the world; Taipei 101 in Taipei, Taiwan, illustrated in Fig. 2.21; is using tuned mass damper to mitigate induced vibrations to the building. This building is 509.2 m tall, has 101 floors, and was finished in 2004. The damper weighs used is 800-ton and helps stabilize the tower in high winds and earthquakes.

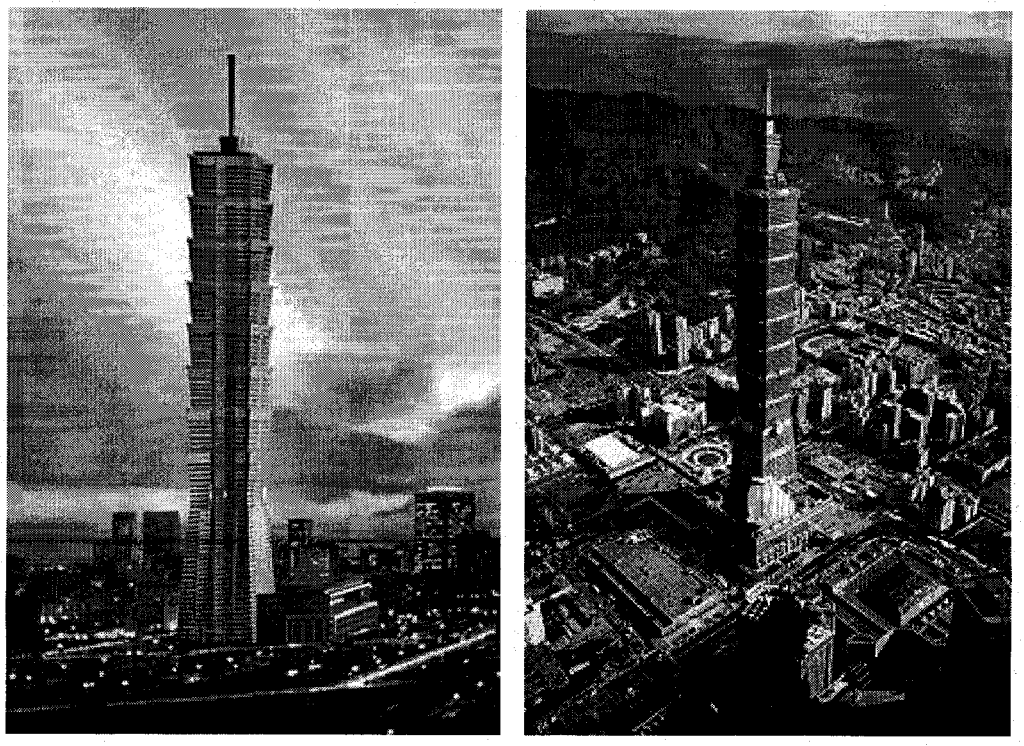

Fig. 2.21 Taipei-101, Taipei, Taiwan (509.2 m)

Table 2.1 Summary of controlled buildings and towers

Name of structure	Location	Completion Year	Building usage	Scale of building	Control system	AMD/HMD		Actuation mechanism
						Number	Mass (ton)	
Kyobashi Seiwa Buildind	Tokyo	1989	office	33 m, 400 ton, 11 stories	AMD[a]	2	5	hydraulic
Kajima Technical	Tokyo	1990	office	12 m, 400 ton, 3 stories	AVS[b]			variable-orifice
Research Institute No. 21 Sendagaya INTES	Tokyo	1991	office	58 m, 3,280 ton (1st mode), 11 stories	AMD	2	72	hydraulic damper
Shimizu Tech. Lab	Tokyo	1991	laboratory	30 m, 364 ton, 7 stories	HMD[c]	1	4.3	servo motor
Applause Tower (Hankyu Chayamachi Bldg.)	Osaka, Japan	1992	office/hotel/ theater	165 m, 62,660 ton, 34 stories	AMD	1	480	hydraulic
Kansai Int. Airport Control Tower	Osaka, Japan	1992	control tower	86 m, 2,570 ton, 5 stories	HMD	2	10	servo motor
ORC 200 Bay Tower	Osaka, Japan	1992	office/hotel	200 m, 56,680 ton, 50 stories	HMD	2	230	servo motor
High-rise Housing Experiment Tower	Tokyo	1993	experiment	108 m, 730 ton, 36 stories	AGS[d]	1	0.8	servo motor
Landic Otemachi	Tokyo	1993	office	130 m, 39,800 ton, 21 stories	HMD	1	195	hydraulic
Nishimoto Kosan Nishikicho Bldg.	Tokyo	1993	office	54 m, 2,600 ton, 14 stories	HMD	1	22	servo motor
NTT Kuredo Motomachi Bldg.	Hiroshima, Japan	1993	office/hotel	150 m, 83,000 ton, 35 stories	HMD	1	78	servo motor
Yokohama Land Mark Tower	Yokohama, Japan	1993	office/hotel	296 m, 260,600 ton, 70 stories	HMD	2	340	hydraulic
Hamamatsu ACT Tower	Hamamatsu, Japan	1994	office/hotel/ commercial	213 m, 107,534 ton, 45 stories	HMD	2	180	servo motor
Hikarigaoka J-City Tower	Tokyo	1994	office	112 m, 25,391 ton, 24 stories	HMD	2	44	servo motor
Hirobe Miyake Bldg.	Tokyo	1994	office/residential	31 m, 273 ton, 9 stories	HMD	1	2.1	servo motor
MHI Yokohama Bldg.	Yokohama, Japan	1994	office	152 m, 61,800 ton, 34 stories	HMD	1	60	servo motor
Penta-Ocean Exp. Bldg.	Tochigi, Japan	1994	experiment	19 m, 154 ton, 5 stories	HMD	1	0.5	servo motor
Porte Kanazawa	Kanazawa, Japan	1994	office/hotel	131 m, 27,600 ton, 30 stories	AMD	2	100	hydraulic
Yokohama Land Mark Tower (Hotel Nikko Kanazawa)	Yokohama, Japan	1993	office/hotel	296 m, 260,600 ton, 70 stories	HMD	2	340	hydraulic
Riverside Sumida Central Tower	Tokyo	1994	office/residential	134 m, 52,000 ton, 33 stories	AMD	2	30	servo motor
Sheridan Grande Ocean Resort	Miyazaki, Japan	1994	hotel	154 m, 83,650 ton, 43 stories	HMD	2	240	servo motor
Shinjuku Park Tower	Tokyo	1994	office/hotel	235 m, 130,000 ton, 52 stories	HMD	3	330	servo motor
Nissei Dowa Phoenix Tower	Osaka, Japan	1995	office	145 m, 26,800 ton, 29 stories	HMD	2	84	servo motor
Osaka WTC Bldg.	Osaka, Japan	1995	office	256 m, 80,000 ton, 55 stories	HMD	2	100	servo motor
Plaza Ichihara	Chiba, Japan	1995	office	58 m, 5,760 ton, 12 stories	HMD	2	14	servo motor
Kaikyo Dream Tower	Yamaguchi, Japan	1996	communication/ observatory deck	153 m, 5,400 ton	HMD	1	10	servo motor
Rinku Gate Tower North Bldg.	Osaka, Japan	1996	office/hotel	256 m, 65,000 ton, 56 stories	HMD	2	160	servo motor
Herbis Osaka	Osaka, Japan	1997	hotel/office	190 m, 62,450 ton, 40 stories	HMD	2	320	hydraulic
Itoyama Tower	Tokyo	1997	office/residential	89 m, 9,025 ton, 18 stories	HMD	1	48	servo motor

Table 2.1 Summary of controlled buildings and towers (Cont'd)

Name of structure	Location	Completion Year	Building usage	Scale of building	Control system	AMD/HMD		Actuation mechanism
						Number	Mass (ton)	
Nisseki Yokohama Bldg.	Yokohama, Japan	1997	office	133 m, 53,000 ton, 30 stories	HMD	2	100	servo motor
TC Tower	Kau-Shon, Taiwan	1997	office/hotel	348 m, 221,000 ton, 85 stories	HMD	2	100	servo motor
Bunka Gakuen New Bldg.	Tokyo	1998	school	93 m, 43,488 ton, 20 stories	HMD	2	48	servo motor
Daiichi Hotel Ohita Oasis Tower	Ohita, Japan	1998	office/hotel	101 m, 20,942 ton, 21 stories	HMD	2	50	hydraulic
Kajima Shizuoka Bldg.	Shizuoka, Japan	1998	office	20 m, 1,100 ton, 5 stories	SAD [e]	—	—	variable-orifice hydraulic damper
Odakyu Southern Tower	Tokyo	1998	office/hotel	150 m, 50,000 ton, 36 stories	HMD	2	60	linear motor
Otis Shibayama Test Tower	Chiba, Japan	1998	laboratory	154 m, 6,877 ton, 39 stories	HMD	1	61	hydraulic
Yokohama Bay Sheraton Hotel and Towers	Yokohama, Japan	1998	hotel	115 m, 33,000 ton, 27 stories	HMD	2	122	servo motor
Century Park Tower	Tokyo	1999	residential	170 m, 124,540 ton, 54 stories	HMD	4	440	servo motor
JR Central towers	Nagoya, Japan	1999	hotel/office/ commercial	hotel: 226 m; office: 245 m, 300,000 ton	HMD	4(H) 2(O)	60(H) 75(O)	servo motor (H) hydraulic (O)
Laxa Osaka	Osaka, Japan	1999	hotel/office	115 m, 33,000 ton 27 stories	Semi-active TMD	2	330	variable-orifice hydraulic damper
Nanjing Tower	Nanjing, China	1999	communication	310 m	AMD	1	60	hydraulic
Shin-Jei Bldg.	Taipei, Taiwan	1999	office/commerce	99 m, 22 stories	AMD	3	120	servo motor
Shinagawa Intercity A	Tokyo	1999	office/ commerce	144 m, 50,000 ton, 32 stories	HMD	2	150	servo motor
CEPCO Gifu Bldg.	Gifu, Japan	2000	office	47 m, 18,000 ton, 11 stories	SAD [e]	—	—	variable-orifice hydraulic
Incheon Int. Airport Air-Traffic Control Tower	Incheon, Korea	2000	air-traffic control	100 m	HMD	2	12	servo motor
Keio University Engineering Bldg.	Tokyo	2000	office/laboratory	29 m, 25,460 ton, 9 stories isolated	smart base isolation	—	—	variable-orifice damper
Cerulean Tower Tokyu Hotel	Tokyo, Japan	2001	hotel/office/ parking	184 m, 65,000 ton, 40 stories	HMD	2	210	hydraulic
Harumi Island Triton Square (3 buildings)	Tokyo	2001	office/commerce	195 m, 45 stories; 175 m, 40 stories; 155 m, 34 stories	couple building control	—	—	servo motor
Osaka International Airport Air-Traffic Control Tower	Osaka, Japan	2001	air-traffic control	69 m, 3,600 ton, 5 stories	HMD	2	10	servo motor
Dentsu New Headquarter Office Bldg.	Tokyo, Japan	2002	office/commerce/ parking	210 m, 130,000 ton 48 stories	HMD	2	440	servo motor
Hotel Nikko Bayside Osaka	Osaka, Japan	2002	hotel/parking	138 m, 37,000 ton, 33 stories	HMD	2	124	servo motor

[a] Active mass damper; [b] Active variable stiffness system; [c] Hybrid mass damper; [d] Active gyroscopic stabilizer; [e] Semi-active dampers.

Table 2.2 Summary of actively controlled bridges

Name of structure	Year employed	Height (m)/ Weight (tonf)	Frequency range (Hz)	Moving mass, mass ratio (%) [a]	Control algorithm	Number of controlled model
Rainbow Bridge: Pylon 1	1991–1992	119/4,800	0.26–0.95	6 ton*2 (0.6)	Feedback control	3
Pylon 2	1991–1993	117/4,800	0.26–0.55	2 ton (0.14)	DVFBb	1
Tsurumi-Tsubasa Bridge	1992–1993	183/3,560	0.27–0.99	10 ton*2 (0.16)	Optimal regulator DVFB	1
Hakucho Bridge Pylon 1	1992–1994	127.9/2,400	0.13–0.68	9 ton (0.4)	Suboptimal feedback control	1
Pylon 2	1992–1995	131/2,500	0.13–0.69	4 ton32 (0.36)	DVFB	1
Akashi Kaikyo Bridge Pylons 1 and 2	1993–1995	293/24,650	-0.127	28 ton*2 (0.8)	Optimal regulator DVFB	1
Meiko-Central Bridgec: Pylon 1	1994–1995	190/6,200	0.18–0.42	8 ton*2 (0.98–1.15)	H_∞ feedback control	1
Pylon 2	1994–1995	190/6,200	0.16–0.25	(0.17–0.38)		1
First Kurushima Bridge: Pylon 1	1995–1997	112/1,600 t	0.23–1.67	6 ton*2 (0.15–2.05)	Suboptimal regulator control	3
Pylon 2	1995–1997	145/2,400 t	0.17–1.70	10 ton*2 (0.3–2.6)	H_∞ feedback control	3
2nd Kurushima Bridge: Pylon 1	1994–1997	166/4,407	0.17–1.06	10 ton*2 (0.41)	DVFB/ H_∞	2
Pylon 2	1995–1997	143/4,000	0.20–1.45	10 ton*2 (0.54–1.01)	Fuzzy control	0.3
Third Kurushima Bridge: Pylon 1	1995–1996	179/4,500	0.13–0.76	11 ton*2 (0.3–2.4)	Variable gain DVFB	1
Pylon 2	1994–1996	179/4,600	0.13–0.76	11 ton*2 (0.3–2.4)	H_∞ output feedback control	1
Nakajima Bridge	1995–1996	71/580	0.21–1.87	3.5 ton*2 (1.0-10.6)	Fuzzy control	3

[a] Percent of first mode mass.

[b] Direct velocity feedback.

[c] Cable-stayed bridge. Others are suspension bridges.

Table 2.3 Summary of typical passive response-control buildings in Japan

Name of the building	Completion year	Structure type [a]	Number of stories [b]	Height (m)	Building usage	Location	Classification [c]	Control device [d]	Objective
Hitachi Head Office	1984	S	+18, −3	72.6	Office	Tokyo	ED	HD	Earthquake
Chiba Port Tower	1986	S	—	125	Tower	Chiba	ME	TMD (RS)	Earthquake / Wind
Yokahama Marine Tower	1987	S	—	101.3	Tower	Yokohama	ME	TLD	Wind
MHS Bldg	1988	S	+8, −1	26.8	Office	Tokyo	ME	TMD (PE)	Earthquake / Wind
Sonic-City Office Bldg	1988	S	+31, −4	136.5	Office	Saitama	ED	FD	Earthquake
Gold Tower	1988	S	—	144	Tower	Kagawa	ME	TLD	Wind
Higashiyama Park Tower	1989	S	—	134	Tower	Nagoya	ME	TMD (PE)	Wind
Kajima KI Bldg	1989	SRC	+9, −1	34.3	Office	Tokyo	ED	HD	Earthquake
Fukuoka Tower	1989	S	—	150.7	Tower	Fukuoka	ME	TMD (RS)	Earthquake / Wind
Asahi Beer Tower	1989	S	+22, −2	94.9	Office	Tokyo	ED	FD	Earthquake
Crystal Tower	1990	S	+37, −2	157.0	Office	Osaka	ME	TMD (PE)	Wind
Fujita Corp. Head Office	1990	S	+20, −4	81.2	Office	Tokyo	ED	LD	Earthquake
Pipe Lab.	1990	S	+12	33.8	Laboratory	Kanagawa	ME	TLD	Earthquake
Shibaura Sea Vance S-bldg	1991	S	+24, −2	97.7	Office	Tokyo	ED	VED	Earthquake
Shinyokohama Prince Hotel	1991	S	+42, −3	149.3	Hotel	Yokohama	ME	TLD	Wind
House Tembos Tower	1992	S	—	105.0	Tower	Nagasaki	ME	TMD (MR)	Wind
Sato Bldg	1992	S	+7, −1	20.8	Complex	Tokyo	ED	VD	Earthquake
Chiba Portside Tower Bldg.	1992	S	+29 −3	121.6	Office	Chiba	ED	VED	Earthquake / Wind
Haneda Airport Tower	1993	S	—	77.6	Tower	Tokyo	ME	TLD	Wind
Shimura 3-chome Dormitory	1993	S	+10, −2	30.1	Dormitory	Tokyo	ED	OD	Earthquake
Rokko-island P&G	1993	S	+31, −2	117.0	Office	Kobe	ME	TMD (PE)	Wind
Chiba City Gymnasium	1993	S	+29, −3	121.6	Office	Chiba	ED	VED	Earthquake / Wind
TV Shizuoka Media City	1994	S	+14, −2	64.7	Complex	Shizuoka	ED	VD	Earthquake
JAL Bldg.	1996	S + SRC	+26, −1	108.0	Office	Tokyo	ED	OD	Earthquake / Wind
Asuru Esaka	1997	SRC	+14	39.25	Apartment	Osaka	ED	HD	Earthquake
Nissei Okayama Shimoshakujii	1997	S + CFT	+14, −1	55.54	Office	Okayama	ED	HD	Earthquake
Osaka Keizai Univ. G-bldg.	1997	S + CFT	+7, −1	29.6	School	Osaka	ED	HD	Earthquake
Saitama Koiki Godo-chosha E-2	2000	S + SRC	+31, −2	142.7	Office	Saitama	ED	HD	Earthquake
Saitama Koiki Godo-chosha H	2000	S + SRC	+26, −3	119.4	Office	Saitama	ED	HD	Earthquake
Shin-chuo Godo-chosha 2	2000	S + SRC	+21, −4	95.05	Office	Tokyo	ED	HD	Earthquake
Kanto-yuseikyokutou Chosha	2000	S + SRC	+28, −2	116.3	Office	Saitama	ED	VD	Earthquake / Wind

[a] **S**: steel structure, **SRC**: steel reinforced concrete structure, **CFT**: concrete filled steel tube

[b] +: number of floors above the ground, −: number of basement floors.

[c] **ME**: Mass Effect, **ED**: Energy dissipation.

[d] **FD**: friction damper (energy dissipation using friction force), **HD**: steel hysteretic damper (energy dissipation using inelastic behavior of steel), **LD**: lead damper (energy dissipation using hysteretic behavior of lead), **MR**: multiple rubber bearing system (combination of laminated rubber bearings), **OD**: oil damper (energy dissipation using orifice resistance of moving piston in oil-filled cylinder), **PE**: pendulum system (application of swing of pendulum), **RS**: roller and spring system (combination of roller and spring), **TLD**: tuned liquid damper (application of sloshing of fluid), **TMD**: tuned mass damper (application of inertia force of moving mass), **VED**: visco-elastic damper (energy dissipation using shear resistance of visco-elastic material), **VD**: viscous damper (energy dissipation using viscous resistance of viscous fluid).

Table 2.4 Buildings recently completed in Tokyo employing semi-active hydraulic dampers

Name of structure	Stories	Height (m)	Number of SAD *	Completion date
Chuden Gifu Building	11	56.0	42	March 2001
Niigata B-project	31	140.5	72	December 2002
Siodome M-Building	25	119.9	38	January 2003
Siodome N-Building	28	136.6	60	March 2003
Siodome Tower	38	172.0	88	April 2003
Mori Tower	54	241.4	356	May 2003
Siodome T-Building	19	98.9	27	May 2003
S-Hotel	30	104.9	66	December 2004
H-Building	23	100.4	28	August 2004

* Semi-active dampers.

CHAPTER 3

Experimental Program

3.1 Introduction

The scope of current research includes experimental investigation of a small-scale test frame subjected to active force control under shake-table generated seismic excitations. This chapter discusses the test procedure and related control algorithm employed. In addition, the apparatus used to perform these experiments is presented with a discussion of the necessity and importance of real-time experiments. Also included in the chapter are descriptions of computer programs which were either developed or used as available software for running the shake table.

3.2 Experimental program

During a seismic event structures are subjected to lateral forces, magnitudes of which depend on the level of ground acceleration. The lateral forces can cause significant drift in uncontrolled structures. Depending on the design and detailing of structures, they can deform up to a certain limit without damage. Beyond this limit, however, the buildings are likely to sustain damage, and in extreme cases, partial or total collapses. Buildings designed based on the seismic provisions of modern codes are capable of responding in a

ductile manner during strong earthquakes. This ensures satisfactory performance of structures and safety of the occupants. Unfortunately, since the majority of existing buildings were constructed before the enactment of modern seismic codes, they do not satisfy the necessary standards to ensure safe performance of structures during earthquakes. Therefore, these structures should be enhanced by using one of the available retrofit techniques. Among the available techniques, active force control appears to offer potentials for future applications.

One of the active force control systems is pulse control. Pulse control, accompanied with bounded state control, offers an attractive protective device. This system, however, has special hardware requirements which pose a challenge. Due to the development of improved instrumentation and faster and cheaper computer processors, as well as electronic equipments, the possibility of utilizing pulse control systems is no longer out of reach.

The attractive aspects of pulse control with bounded state algorithm can be pointed out as follows:

(1) The magnitude of control forces is smaller than those used in other active control mechanisms because of immediate incremental response of the control system in the form of force pulses. In a regular control mechanism the control force is computed on the basis of measured structural deformation which can be substantial, by the time the control forces are activated. In pulse control, which is used the current research project, a small threshold value is defined, and as soon as the deformation level passes this predefined critical point, the actuator applies a pulse, as in instantaneous force control system. The entire system is monitored continuously and correctional forces are applied in smaller incremental pulses at every few ten milliseconds. Since large deformations are prevented, the magnitude of each individual control pulse is small.

(2) Better deformation control can be attainable. This is especially true when compared against conventional passive control systems, such as shear walls or lateral braces. In latter systems the magnitude of the control force has direct

relation to the deformation level attained. In other words, it is impossible to develop control forces without lateral drift. In the pulse control system, however, the magnitude of control force is completely independent of lateral displacements, forces being generated without significant deformation of the structure. This can be extremely important for tall buildings and long bridges where deformation control may be needed for human perception purposes, rather than structural safety. The stringent deformation control may also be necessary for special structures, such as nuclear power plants where functional safety may be sensitive to small deformations.

(3) Because of significant reductions in deformations, the pulse system allows complete protection of the structure against damage such that the structure may not need any repair after the seismic event, including brittle non-structural elements. Should the force capacity of the actuators is exceeded, the actuators will remain undamaged at a load level equal to the actuator capacity, unlike other bracing elements, which may experience inelasticity during a seismic event, and hence may have to be repaired after the earthquake.

The experimental program consists of tests of a small-scale steel frame, as proof of concept. It is also intended to asses the feasibility of the control system selected within the available technology.

Testing is done in three stages:

(1) Uncontrolled test – performed on bare frame;

(2) Uncontrolled test – performed while the actuator is connected to the frame via sliding bearing;

(3) Controlled tests – executed when the actuator is fully connected to the frame, programmed to react to lateral excitations.

For the uncontrolled test of bare frame, the frame is mounted on top of the shake table and then excited. A schematic view of test set-up is shown in Fig. 3.1. This test is performed to determine the response of an uncontrolled frame. The frame response due to

different types of ground excitations is investigated and analyzed. The test also gave experimentally established period of the structure.

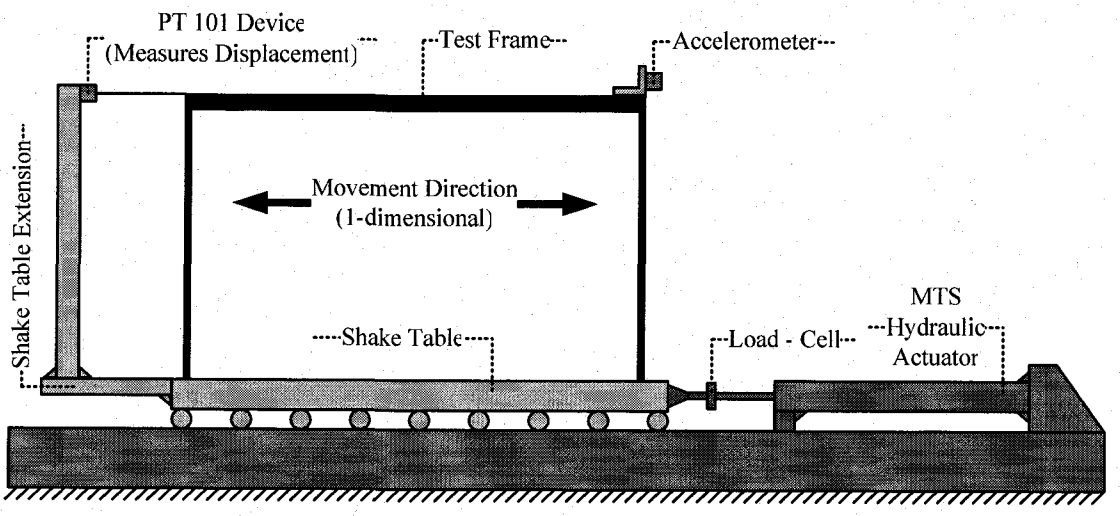

Fig. 3.1 A schematic view of an uncontrolled test set-up of a bare frame

Next, the uncontrolled test of the frame was performed with the actuator connected through a sliding bearing (without exerting any force) to incorporate the effects of mass and damping of the actuator. A schematic view of this set-up is shown in Fig. 3.2. The frame response under different types of ground excitations is investigated and analyzed.

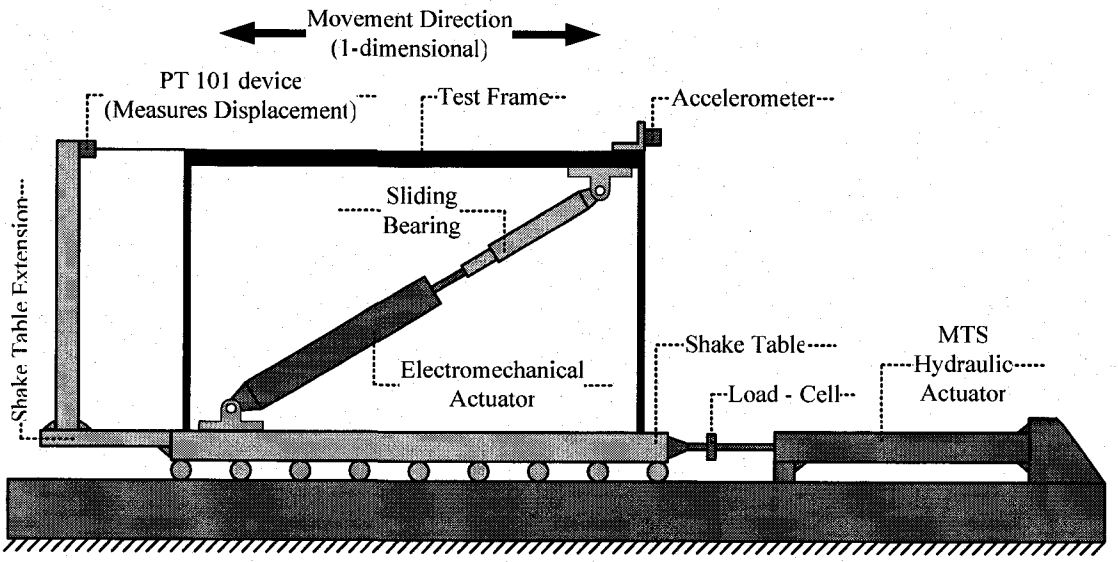

Fig. 3.2 A schematic view of an uncontrolled test set-up where the actuator is connected via a sliding bearing

The sliding bearing used is a simple tool that allows the frame to slide back and forth without interfering with the movement of the frame. It consists of a piston and a shaft where the piston can easily slide in the lubricated inner surface of the shaft.

The controlled tests were performed with the actuator connected to the frame diagonally through a pin-pin connection. A schematic view of this set-up is shown in Fig. 3.3. Since the actuator was shorter than the diagonal length of the frame, a solid circular steel section was used as an extension piece. The slenderness of the extension piece and the possibility of buckling under compression were considered when choosing the section size of the extension. Also, a load cell was used to measure the magnitude of the force in the diagonal member.

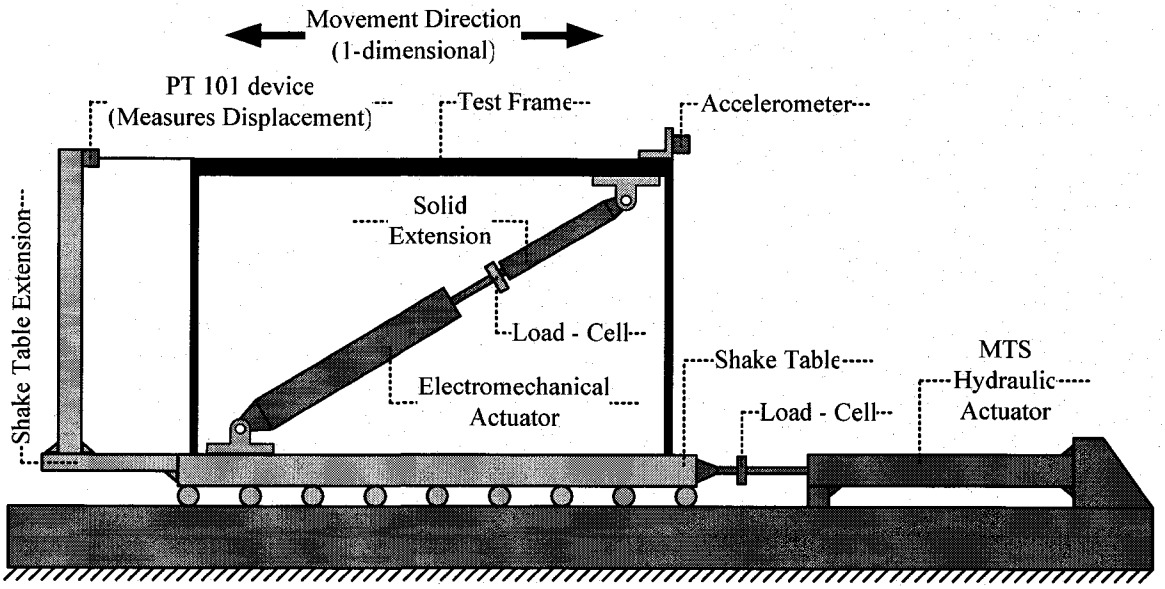

Fig. 3.3 A schematic view of a controlled test set-up

The shake table was programmed to simulate different ground excitations. The magnitude of ground excitation was established with due considerations given to the frame displacements and the magnitude of control forces in limiting deformations. The performance of the system was completely dependent on performance levels of individual components used and their connections in carrying out the real-time

experiments. The experimental parameters included; structural mass, stiffness and ground excitation characteristics. As for the results, the most important response quantities recorded and analyzed were frame displacements and control forces.

3.3 Apparatus

This section provides the description and rationale for all test apparatus utilized. Most of the equipments were purchased specifically for this test program, with required sensitivity levels for real-time testing. The list of apparatus includes: (1) shake-table; (2) data acquisition system; (3) load-cell; (4) electromechanical actuator; (5) PT-1A measurement device; and (6) accelerometer. The details of each one of these devices are presented in the following sections.

3.3.1 Shake table

A small-size, one-dimensional shake-table was used to simulate ground excitations. A schematic view of the shake-table is shown In Fig. 3.4. The top platform of the table consists of an aluminum piece which is supported on bearing rails. It is driven by an MTS hydraulic actuator. The actuator, shown in Fig. 3.5 is MTS model 244, with 25 kN force capacity and a 250 mm (10 in.) stroke length. It is designed for highly dynamic fatigue rated tests and is capable of moving the shake table back and forth at high frequencies. The actuator is mounted on a rigid floor, with the direction of loading constrained to the geometric centre of the shake-table. The actuator is hooked up to a hydraulic pump. An MTS controller and computer software is used to control hydraulic pressure to apply the required forces on the shake-table. This ensures the proper functioning of the shake table.

The controller receives two feedback signals from the actuator, to ensure accurate movements defined by the computer program. One signal is for displacements, through an internal LVDT measurement device, and the other is the applied load, which is monitored by a load-cell mounted at the tip of the moving rod. These feedbacks are used to form a close-loop, accurately determining the status of the actuator. This shake-table

was manufactured prior to the initiation of this project and was designed to move a mass of up to one ton, in addition to its own self-weight.

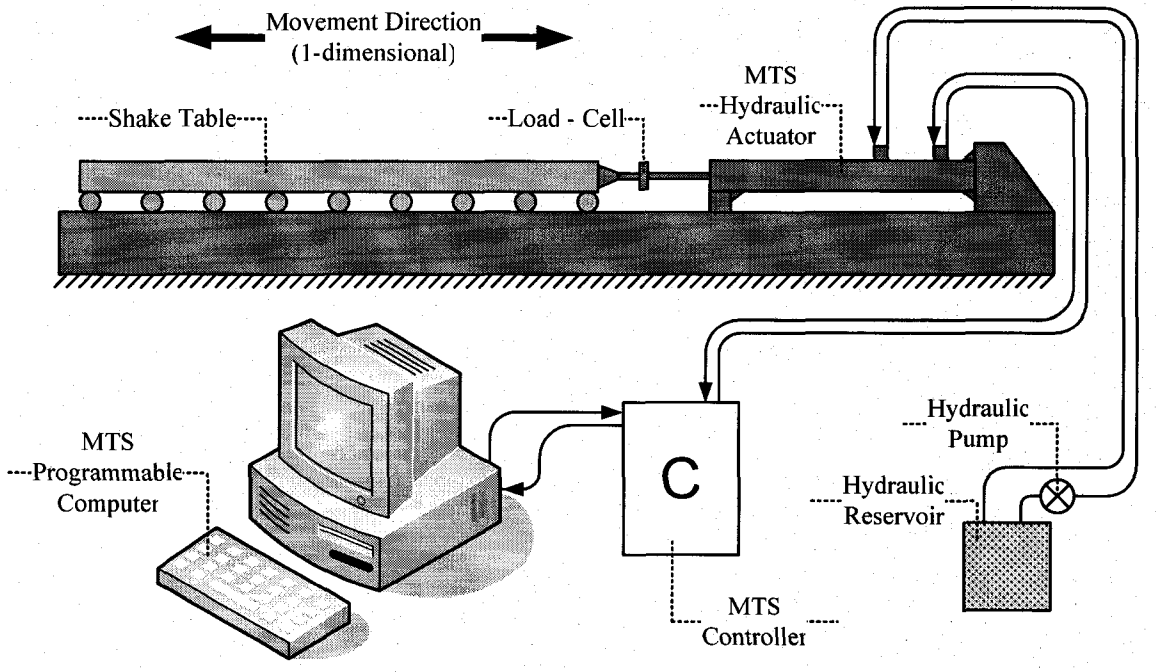

Fig. 3.4 A schematic view of the shake-table.

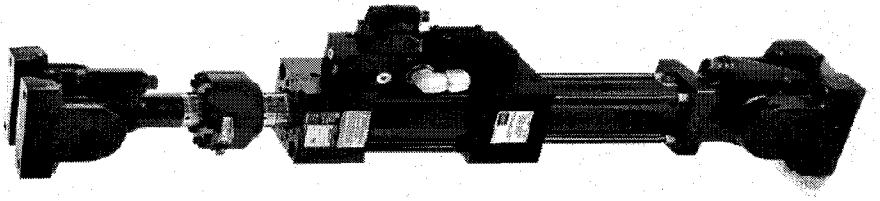

Fig. 3.5 MTS actuator - model 244 used to run the shake table

3.3.2 Data acquisition System

A data acquisition system (DAQ) manufactured by National Instruments was used to monitor and record data during testing. This DAQ employed had the necessary precision for real-time tests of this type with full compatibility LabView software which was developed by the same company and used extensively in the experimental program. A schematic view of the DAQ is shown in Fig. 3.6. A PCI–NI 6229 DAQ card was

purchased for use in the experiment. The card can be installed on a regular PC and is capable of supporting up to 32 analog inputs (AI), 4 analog outputs (AO), and 48 Digital input/output (DI/O). This card is suggested by the manufacturer as being ideal for the type of tests conducted in the current research program. The specifications of the card are presented in Table. 3.1.

A conditioner module was implemented in the DAQ system to have accuracy in readings. Depending on the intended use, a conditioner module contains one or more of the following units; amplifiers, filters, power supply unit to provide the excitation voltage for sensors, resistances, and capacitors. For this experiment, accelerometer modules and high rate analog input modules were implemented in addition to the conventional feed-through modules. The accelerometer module contains an amplifier with a gain of two, one high-pass filter, and one low pass filter. These modules were mounted on a connector block, which was then connected to the DAQ card via shielded cable.

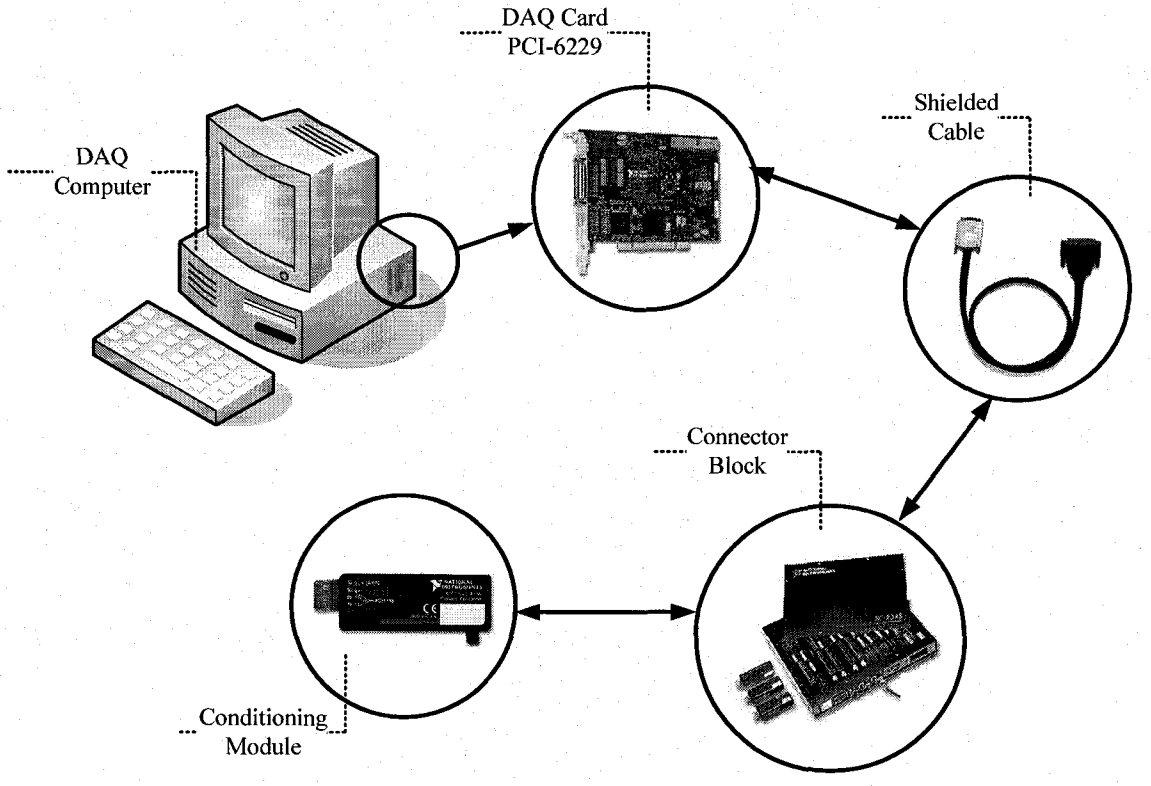

Fig. 3.6 A schematic view of a data acquisition system (DAQ)

Table 3.1 DAQ card specifications

Family	NI – 6229	Bus	PCI
Analog inputs	32	**AI resolution (bits)**	16
Analog output	4	**AO resolution (bits)**	16
Max output rate (kS/s)	833	**Output range (V)**	±10 V
Digital I/O	48	**DIO clock**	32 up to 1 MHz

3.3.3 Load – cell

A load-cell was used to measure the control force in the diagonal member of the frame. Different types of load cells are available for different loading conditions, such as static or dynamic loads. In the case of dynamic loading, it is essential to have the capability of reading fast-paced varying load in real-time with minimal or close to zero time-delay. As for the load capacity, it should be higher than the maximum probable load while maintaining sufficient level of sensitivity during experiments, with least possible noise in readings. The mounting system is usually governed by geometry and location. A number of load-cells were tested to assess their suitability. It was finally decided to select MLP-500 *Transducer Techniques*, shown in Fig. 3.7. This load cell is for dynamic in-line loading, with a capacity of 2.2 kN (500 lbs). The specifications of the load-cell are presented in Table 3.2.

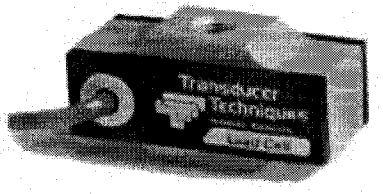

Fig. 3.7 MLP-500 dynamic in-line load cell

The output response voltage of the load-cell was small for the magnitude of load applied during the experiment. Therefore, it was decided to use an amplifier to increase the output voltage up to a level that could be read precisely by the data acquisition system with practically close to zero noise level. The load cell was re-calibrated after installing

the amplifier and the new calibration sheet, shown in Fig. 3.8, was used to translate the response voltage to the load in test. The calibration test was done in two stages; tension and compression calibration. Both sides of the calibration curve follow a linear load-response pattern with the same slope.

Table 3.2 MLP-500 load-cell specifications

Nonlinearity	**0.1% of R.O.**	**Temp. Effect on Output**	**0.005% of Load/°F**
Hysteresis	0.1% of R.O	**Temp. Effect on Zero**	0.005% of R.O./°F
Nonrepeatability	0.05% of R.O.	**Terminal Resistance**	350 ohms nominal
Zero Balance	1.0% of R.O.	**Excitation Voltage**	10 VDC
Compensated Temp. Range	60° to 160°F	**Safe Overload**	150% of R.O.
Safe Temp. Range	-65° to 200°F	**Calibration**	Compression & Tension
Natural Ringing Frequency	5,200 (Hz)	**Deflection**	0.003 in.

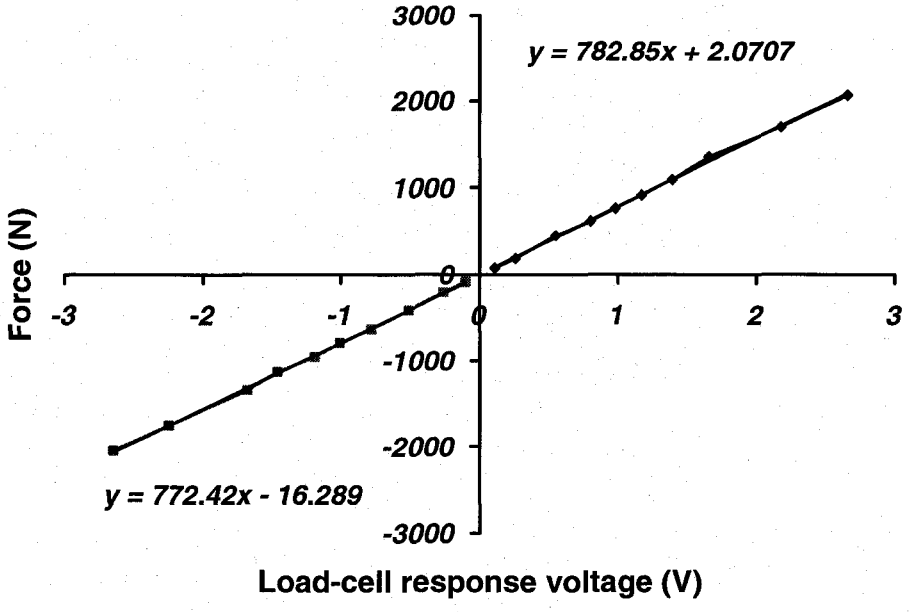

Fig. 3.8 Load-cell calibration sheet

3.3.4 Electromechanical actuator

Finding an appropriate actuator for the specimen size, the dynamic nature of loading, and the magnitude of loading was a challenging task. The actuator had to be sufficiently compact to be installed diagonally in the test frame. Also, due to the technological

constrains on manufacturing actuators that perform at high frequency movements while requiring minimal response time and power, a number of characteristics were important. The first challenge was the response time. The capability to respond to the excitation signal within milliseconds was essential. The second challenge was the size, which had to be compact enough to be fitted inside the frame easily, with sufficient room for the rod to extend and shorten according to the frame movement. The third challenge was the force capacity. The selected actuator was expected to provide enough thrust power while moving at high speeds, since at high-speeds the maximum thrust power drops as illustrated in Fig. 3.9. When selecting an actuator, one can not only focus on force or speed demand, but should consider them concurrently. In reversed cyclic loading, such as those caused by earthquakes or sinusoidal excitations, the change in movement direction requires the actuator to come to a complete stop at peak deformation and then to reverse its direction. Therefore, the acceleration and deceleration rates become important factors in high frequency excitations. Also, the time required to come to complete stop and to reverse the direction usually takes about half of the time needed for a complete cycle in high frequency excitations.

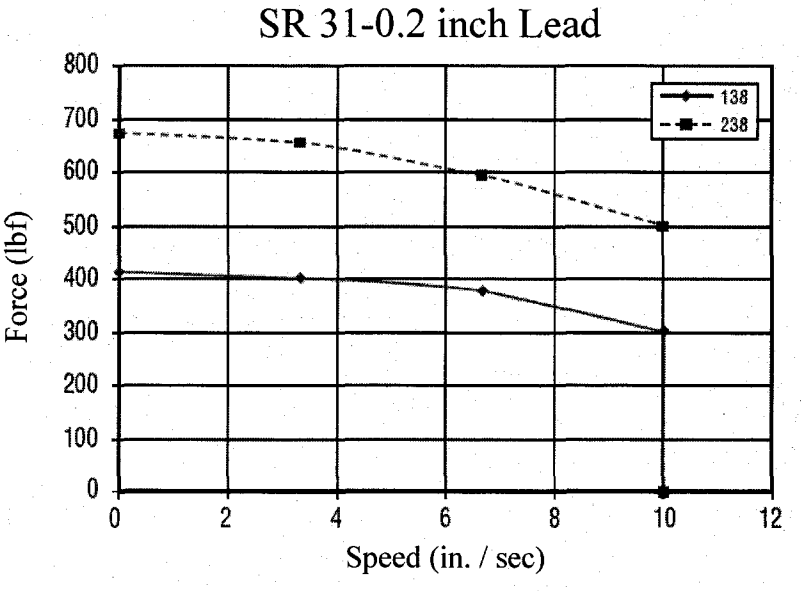

Fig. 3.9 An example of typical force-speed relationship in actuators.

The actuators available in the market can be categorized into; i) piezoelectric, ii) hydraulic, iii) pneumatic, and iv) electromechanical. Piezoelectric actuators respond almost instantly to the excitation command but because of limitations on their deformation capacity they are not suitable for civil engineering applications. They also need high voltages to operate. Hydraulic actuators are very strong and powerful and can be fast, but normally the time lag of response to a movement command becomes an issue in the control process. This issue becomes especially important if the structure is stiff, with a short period. Furthermore, they need high-pressure hydraulic fluid to operate. The required hydraulic pump for this purpose may suffer from a power loss during seismic events. The installation of such pumps creates other problems. Innovative methods were suggested in the past to maintain high-pressure without running the pump all the time. However, these methods increase the primary capital cost and may not be practical.

Pneumatic actuators are fast but they have the controllability issue; meaning they can move in steps but they are incapable of stopping between these predetermined steps.

Electromechanical actuators come in different sizes and capacities and can be manufactured to work with battery power, eliminating difficulties associated with possible power failure during seismic events. In addition, they can provide sufficient power at high-speed movements. It was decided that the electromechanical actuators was the best choice for this experiment. Hence, after conducting market search, *EXLAR* SR_31 actuator, illustrated in Fig. 3.10, was purchased.

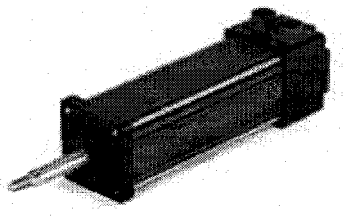

Fig. 3.10 *EXLAR* SR-21 electromechanical actuator

The electro-mechanical actuators need about a 1000 W power to run. This necessitates an amplifier and/or regulator unit, which was provided in the controller unit of the actuator

used. A digital controller system was used to control the actuator and was connected to a computer through an Ethernet port. The control program was downloaded into this unit through this connection. This unit had the capability of functioning completely independently after downloading the program into its memory chip, and did not need to be connected to a computer afterwards. A signal was sent to the controller to control the actuator. Consequently this signal was translated into an excitation voltage. PicPro program was used to communicate and program the controller through Ethernet cable. The schematic views of all the essential components for running the *EXLAR* actuator are shown in Fig. 3.11.

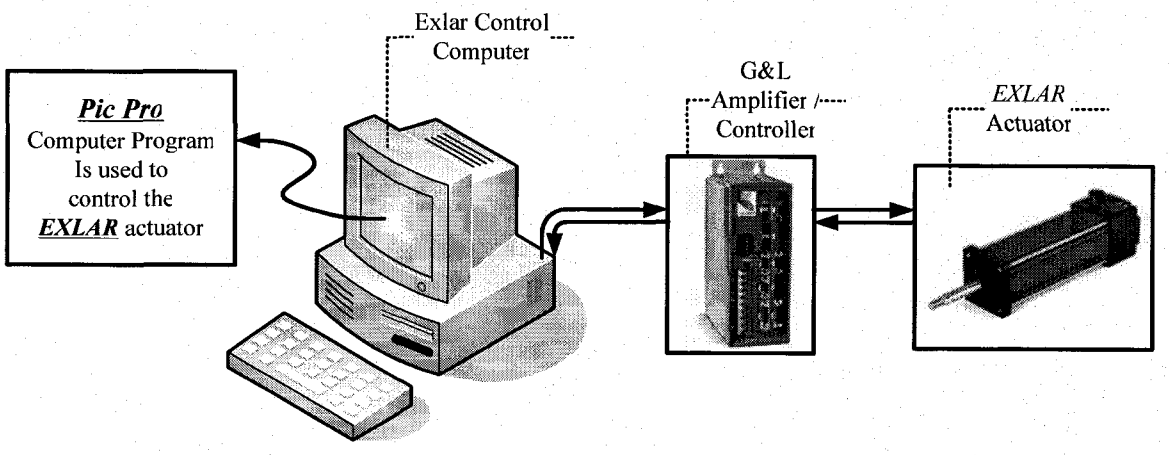

Fig. 3.11 Schematic view of *EXLAR* actuator control system

Different signals with different voltages were sent to the actuator and the corresponding force values were measured and recorded. These values were used to obtain the calibration sheet for the actuator, as shown in Fig. 3.12. This calibration sheet was used to determine the excitation voltage associated with a specific magnitude of force.

The response time of this actuator is quite short (fast) and it needs about few milliseconds to respond to the excitation signal. Basically, there are two time lags that have to be overcome before the initiation of movement. These time lags depend on the mechanical and electrical characteristics of actuator and are called mechanical time constant and

electrical time constant. The summation of both of these time constants for this *EXLAR* actuator adds up to less than ten milliseconds. The detailed specifications for *EXLAR* actuators are presented in the Table 3.3.

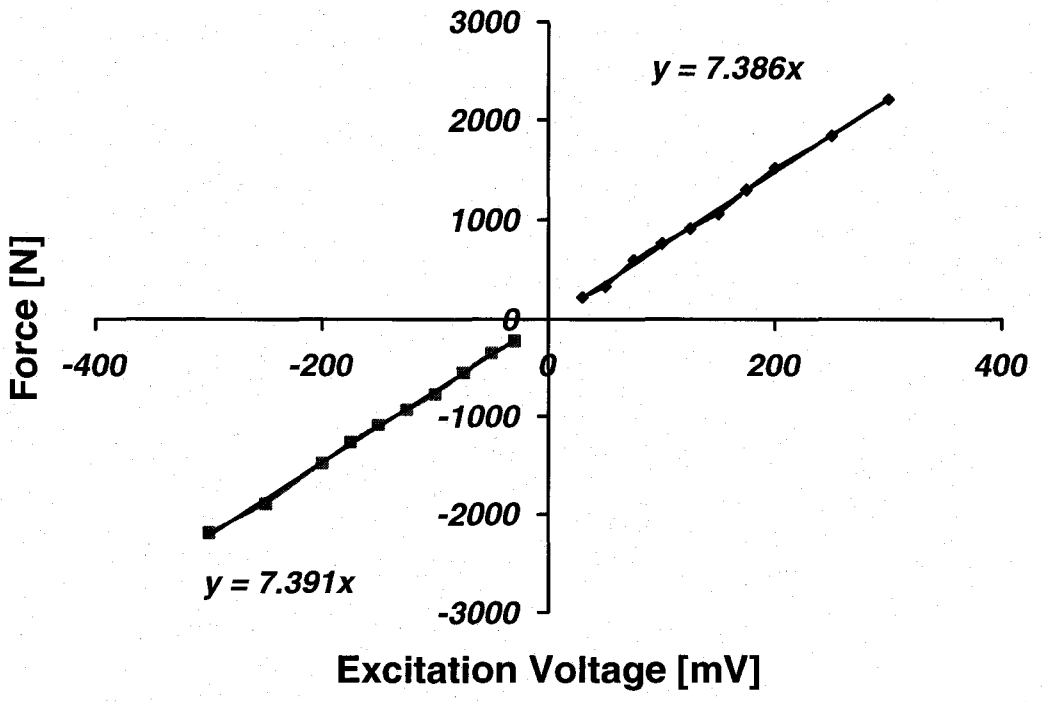

Fig. 3.12 *EXLAR* actuator calibration sheet

Table 3.3 *EXLAR* actuator specifications

Manufacturing Company	EXLAR
Actuator model	SR31-1201-238-AR
Stroke length	12 (in.)
Mechanical time constant	From 2.6 up to 4.3 (ms)
Electrical time constant	3.3 (ms)
Accessories	Anti-rotation mechanism
Length	485 mm
Height	83.8 mm
Width	83.8 mm
Weight	10 kg

3.3.5 PT – 1A

After reviewing different types of displacement measurement instruments it was decided to use PT-1A in the test program. This device, shown in Fig. 3.13, consists of a main body which is mounted on a support (used as the origin point) and a non-stretchable non-deformable wire which is connected to the frame. The wire is always under a small amount of tension provided by a small spring, preventing the sagging of wire, thereby following any movement accurately. The deformation of the frame changes the wire length outside the main body. This changes the response voltage of the unit. By using a calibration sheet, the output voltage is translated into the corresponding lateral deformation. The calibration sheet presented in Fig. 3.14 is provided by the company and was verified in the lab. The specifications of this unit are given in Table 3.4.

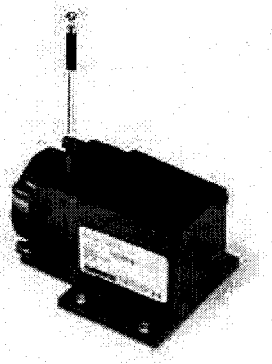

Fig. 3.13 PT-1A (displacement measuring device)

One of the other common devices to measure displacements is LVDT (Linear Variable Differential Transducer). In an LVDT, instead of a wire, a rod is used to measure the displacements. Depending on the model, it can be supported by a spring, or it can work with gravity. There are a couple of reasons that make PT-1A a more suitable choice for the tests conducted in the current project. One is that the measurement length of an LVDT is more limited than a PT-1A. The other is that a PT-1A is better suited for following the movement of the frame than a rigid rod of an LVDT.

Table 3.4 PT-1A specifications

Full stroke length	0-20 inches
Accuracy	±0.25% to ±0.10% full stroke
Repeatability	±0.02% full stroke
Resolution	Essentially infinite
Measuring cable	0.19 in. diameter nylon coated stainless steel
Enclosure material	ABS plastic and black anodized aluminum
Sensor	Plastic-hybrid precision potentiometer

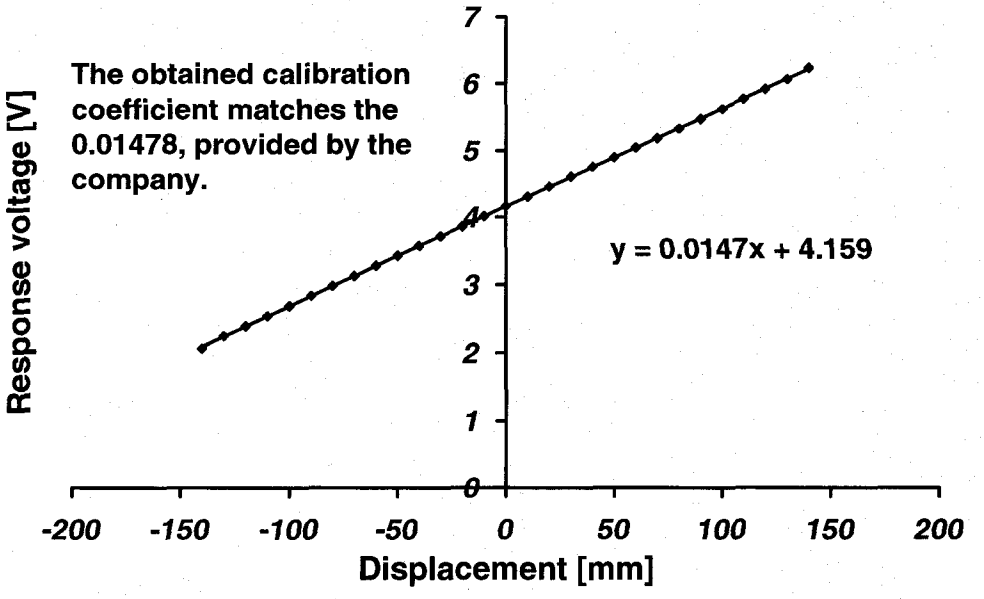

Fig. 3.14 PT-1A calibration sheet

3.3.6 Accelerometer

A number of accelerometers were reviewed, including high and low frequency piezoelectric accelerometers and AC and DC-coupled accelerometers, to find an appropriate accelerometer for the specific application at hand. When choosing an accelerometer, it is important to determine whether it is selected to measure motion or vibration. Depending on the nature of the excitation, accelerometers have been categorized in four different categories, including:

- Motion
- High-frequency vibration
- Low-frequency vibration
- Shock

When an accelerometer is utilized to measure the motion accurately, it must be ensured to have zero offset errors. Even a very small amount of zero offset in output measurements can lead to large velocity and displacement calculation errors after numerical integration. Measuring a slow-moving robotic arm or an elevator are instances of motion measurement accelerometers.

Measuring high-frequency accelerations in cases such as turbine vibration or high-speed rotary machinery requires an accelerometer with precise high-frequency characteristics. Due to the physical constraints of spring-mass type transducers they usually have very low output sensitivity. Additionally, the proper mounting technique for this type of accelerometer plays an important role in obtaining accurate results.

A low-frequency accelerometer is required for modal analysis or building and bridge monitoring. The ideal accelerometer should have no phase shift within frequency range of interest. It has been shown that DC-coupled accelerometers have an advantage over the AC-coupled ones. Also, distinguishing between vibration signals and base-strain sensitivity cannot be done easily, especially for low-frequency excitations. Therefore, the ideal accelerometer should have very low strain sensitivity. In addition, the error induced by significant environmental temperature changes usually affect low-frequency readings which are combined with low-frequency excitation readings, reducing the accuracy of readings significantly. Thermal protective boots can be used to protect accelerometers with high thermal transient sensitivity. To improve the accuracy of readings, a low-pass filtering unit can be installed on an accelerometer to minimize the effect of high-level high-frequency components in the desired low-frequency monitoring range.

In cases such as automotive crash-testing or package drop-testing, a special accelerometer with shock measurement capabilities is required. A common mistake among novice shock-testing mechanism developers is to wrongly assume that the shock measurement of an object can be approximated using a rigid body model, and forget to consider the localized material response. In high acceleration shock-testing, where structural response is usually non-linear and difficult to characterize accurately, choosing the right accelerometer can be critical.

The *ENDEVCO* accelerometer, model 7593A, shown in Fig. 3.15, was used in the current research program to measure accelerations in low-frequency shake-table experiments. This accelerometer is an economical variable capacitance accelerometer with built-in signal conditioning. It has been shown that this unit is suitable for measuring low-frequency vibrations in civil engineering applications, such as low-level low-frequency vibrations of buildings, bridges and other structures.

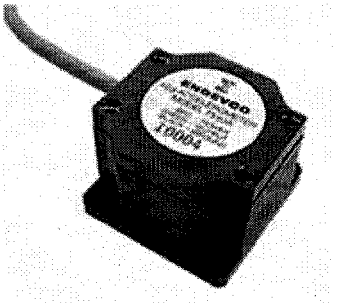

Fig. 3.15 *ENDEVCO* 7593A variable capacitance accelerometer

The *ENDEVCO* 7593A accelerometer has a full-scale range of ±2 g with a frequency response from 0 to 50 Hz. Low milli-g noise filter provides high measurement resolution. It features a rugged thermoplastic case with an integral cable and operates over a temperature range of -40°C to +125°C. The accelerometer's shape and size make it easy to mount on large and small structures. Complete specifications are reproduced in Table 3.5.

Table 3.5 *ENDEVCO* 7593A specifications

	Unit	7593A
Range		±2 g
Sensitivity	V/g	1.0 ± 0.03
Frequency response	Hz	0 to 50 Hz.
Transverse sensitivity	% max % Typ.	3.0 1.5
Non-linearity and Hysteresis	% FSO	±0.5
Thermal zero shift	mV/°C	1.0 (Typical)
Thermal sensitivity shift	ppm/°C	500 (Typical)
Case, material		Thermoplastic
Acceleration limits (in any direction)		400g
Shock (340 micro-sec)		400g
Temperature (Operating and Storage)		-40°C to +125°C

3.4 Computer programs

A number of software had to be used to perform the experiments. The main purpose of these computer programs is to drive various equipments needed during testing. Some of the software needed to run the shaking table was supplied by MTS (the manufacturer of the shake-table actuator). These computer programs were used to generate (a) sinusoidal excitation functions and (b) earthquake simulation for any given acceleration record. In addition, two other programs had to be developed to monitor and control the system for uncontrolled and controlled tests. For the latter programs LabView, PicPro and OPC-Server programs were used. The details of these computer programs are presented in the following sections.

3.4.1 Computer programs for shake table

Sinusoidal excitation: The MTS Company that supplied the hydraulic actuator used to run the shake table also provided a user friendly computer program to control the actuator. The program generates sinusoidal excitation patterns. A screenshot of this program is shown in Fig. 3.16. The amplitude of excitation (in mm), the location of the neutral point (zero point for the amplitude), and the frequency of excitation can be adjusted by the program. The amplitude of excitation is dependent on the maximum stroke length. The full stroke length is 250 millimeters, which translates into a cyclic

motion with maximum amplitude of 125 mm. The amplitude of 100 mm was utilized in the experiments. This particular actuator is capable of running the shake-table up to 10 Hz of excitation frequency. These quantities were verified by test runs prior to the experimentation.

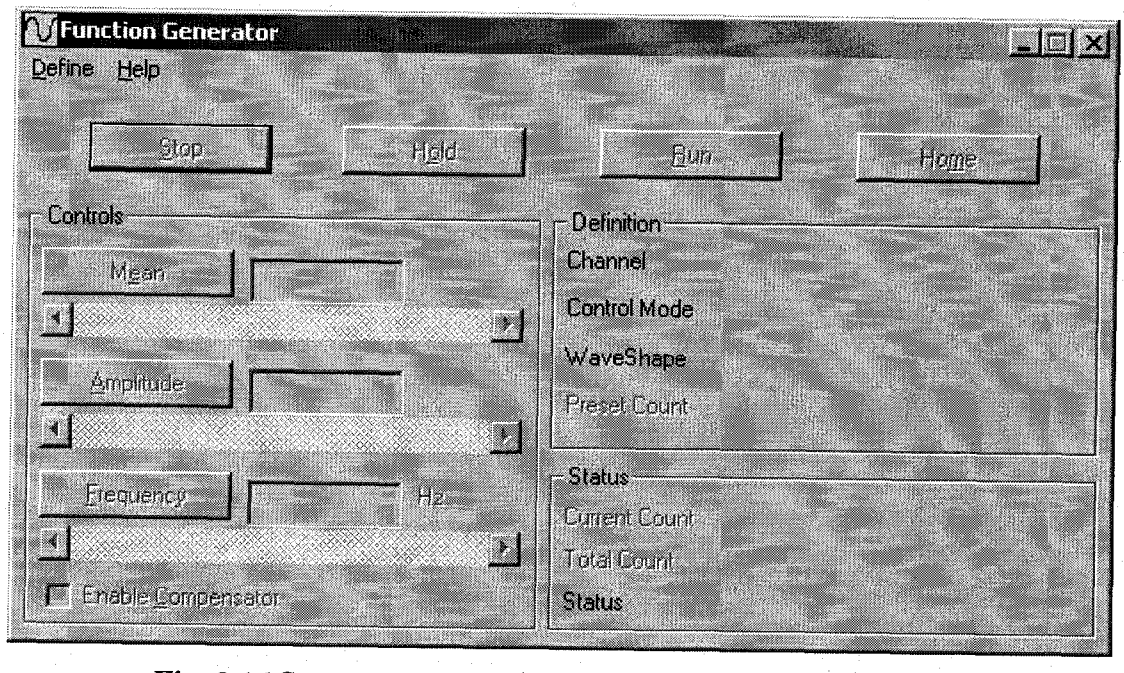

Fig. 3.16 Screenshot of MTS sinusoidal excitation software.

Earthquake simulation: Another MTS program is used to read accelerations from a data file created during earthquake simulation and generating the same records on the shake table. A screenshot of the set-up page of this program is presented in Fig. 3.17. This program has the option of amplifying the magnitude of acceleration by any given scale, as long as the actuator is capable of performing the given task. Also, it offers the option to shorten or lengthen the duration of the earthquake using a multiplier factor. Finally, it can repeat the earthquake record for as many times as desired.

3.4.2 Software for structural monitoring during uncontrolled tests

Uncontrolled tests involve a bare-frame or a frame with a non-reacting actuator attached to the structure via a sliding bearing. A program was developed to monitor the displacement response of the structure by converting the PT-1A voltages to

corresponding displacements through the calibration information. It was developed in LabView environment. The output voltage coming from the PT-1A device is fed into the DAQ system, and then this output is sent to the LabView program. The displacements represent lateral drift of the frame. All the deformations are stored in a history file for further processing after the experiments. A schematic view of the flowchart explaining the steps involved is shown in Fig. 3.18 (a). In addition, a screenshot of the interface of this LabView program is shown in Fig. 3.18 (b).

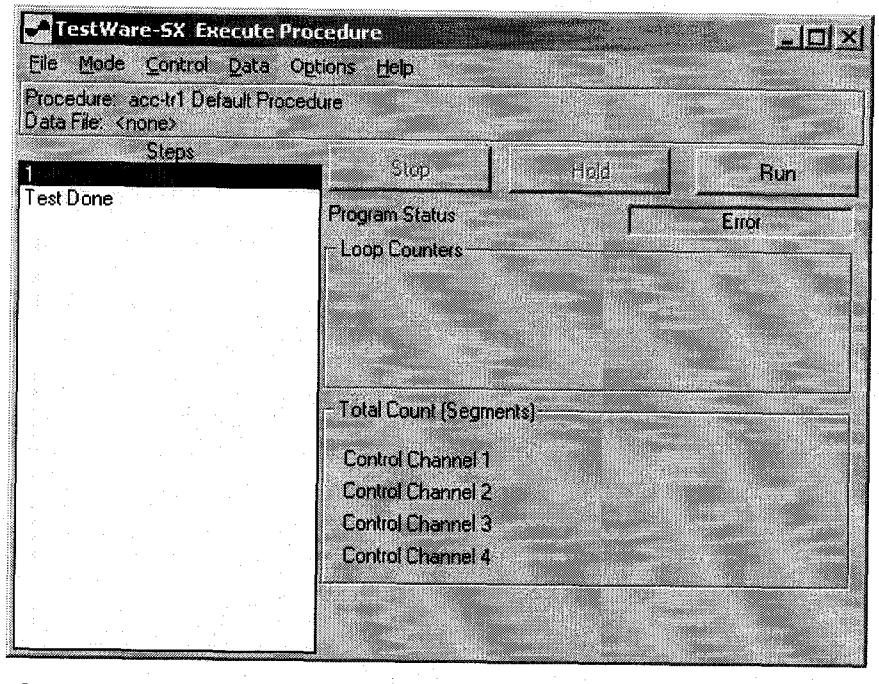

Fig. 3.17 Screenshot of MTS earthquake simulator software.

The input options can be adjusted by the program through its interactive menu. "Zero displacement calibration" input is used to indicate the neutral position of the frame at the beginning of the test. The option called "rate" indicates the refreshment rate of data read from the DAQ system by LabView. These data are stored in a file for further processing. And finally, the "number of samples" input item is used to specify the number of samples to be stored in memory temporarily, before getting stored in a file or displayed on the screen.

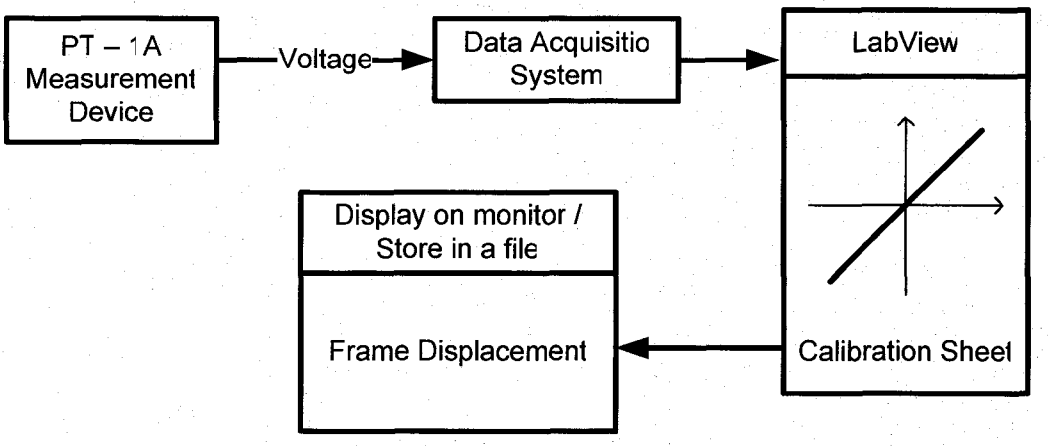

(a) Uncontrolled test schematics

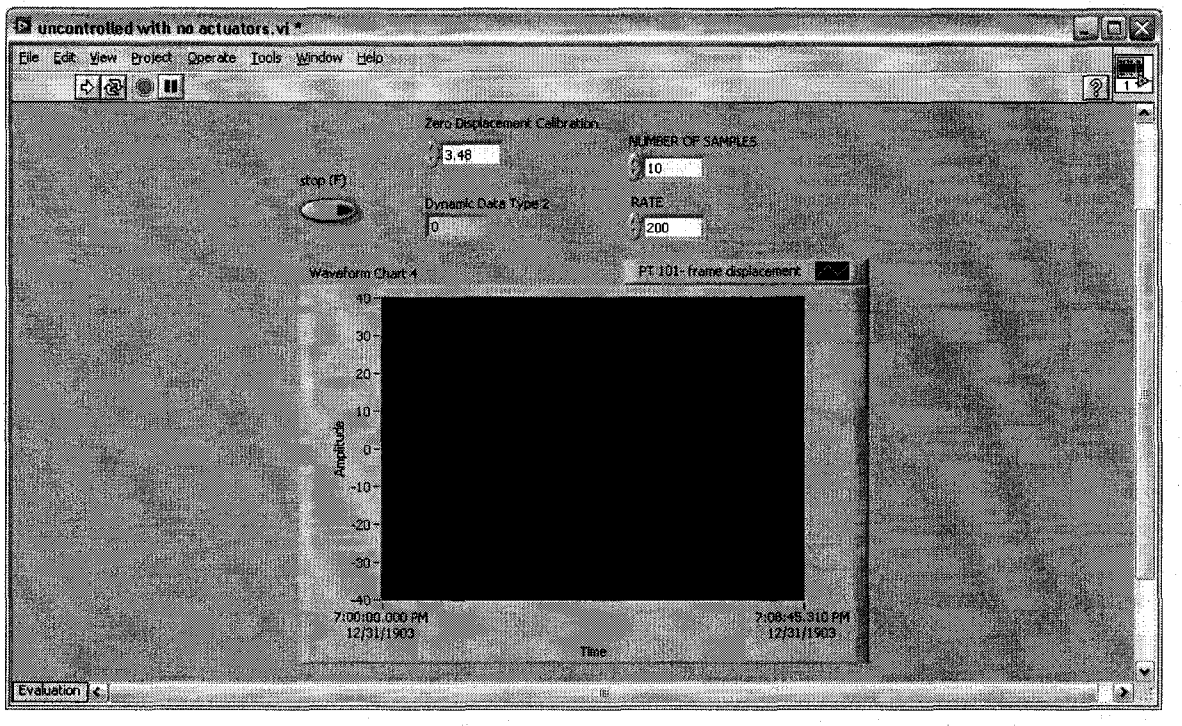

(b) Uncontrolled LabView program interface

Fig. 3.18 Uncontrolled test software

3.4.3 Software for monitoring and driving the electro-mechanical actuator for structural control

Controlled tests involved three computer programs. These include a program; i) to continuously monitor structural displacements and accelerations (LabView Interface Program), ii) to drive the actuator to apply control forces (PicPro Program), and iii) to link structural response data to the software that controls the actuator (OPC-Server Program). The first program is written in LabView environment and records structural response and control force data. The program that drives the actuator was developed using PicPro, which is an industrial programming language to provide commends to operate machinery. The information recorded by the LabView program needs to be used by the PicPro program that drives the actuator. The environment in which this linkage is enabled is provided by an OPC-Server program. The OPC-Server program allows the integration of PicPro and LabView programs so that one can access the data file generated by the other. This operation is illustrated in the flowchart depicted in Fig. 3.20.

3.4.3.1 LabView interface program

A computer program in LabView environment was developed for controlled testing to continuously monitor the status of the frame. The data collected through this program is to be shared with the control program, discussed in the next section, to perform corrective measures by applying control forces to the structure, as necessary. The information on the system is refreshed and the latest status of the frame is updated continuously. The information includes feedbacks from the accelerometers installed on the shake table and frame, in addition to the displacement measurements recorded by PT-1A device for lateral displacements of the frame. The signals from these sensors are channeled through DAQ system. The transmitted signals are in voltages and have to be translated into the corresponding values of acceleration and displacement, with proper units, using the calibration information supplied. This task is performed by the LabView interface program. The data gathered is stored in a history file along with the control forces obtained from PicPro program, for further processing. A screenshot of the interface of this computer program is presented in Fig. 3.19.

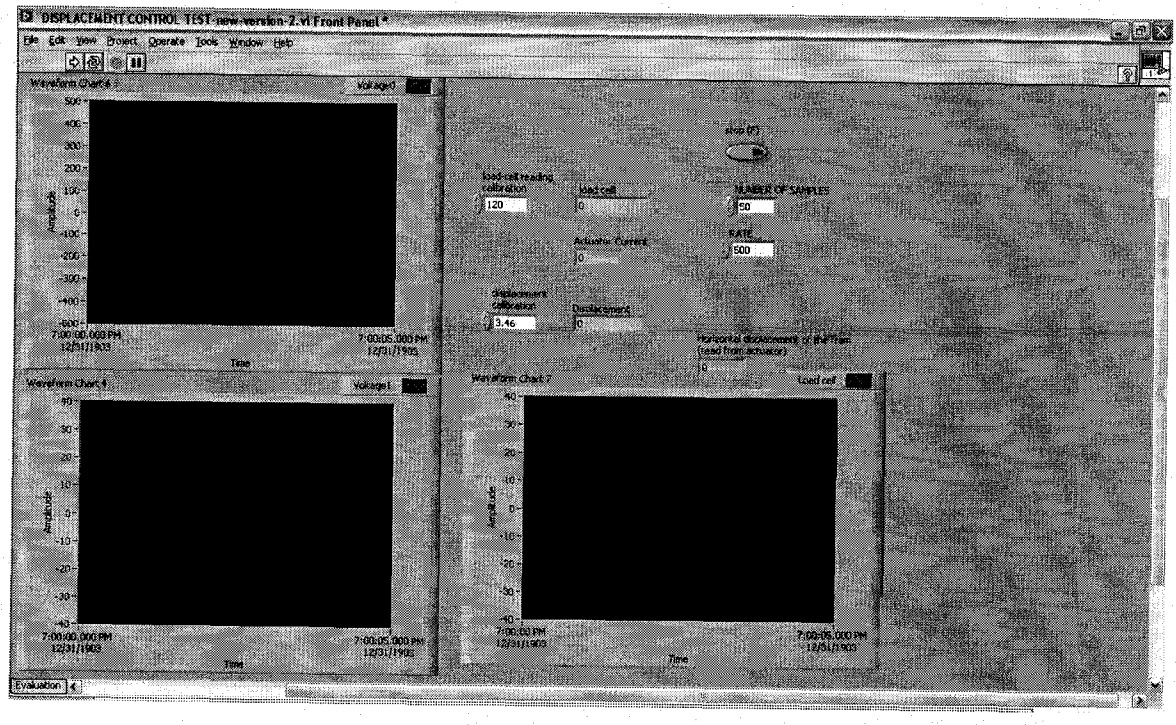

Fig. 3.19 A screenshot of the LabView interface for controlled test

A number of input options are provided on the interface screen for data initialization prior to testing, including; zero load reading of the load cell and zero lateral displacement at the neutral position of frame. In addition, other adjustable input items such as the "rate" and "number of samples" are provided to configure the performance of the data acquisition system. Some graphs are used to provide the user with sufficient visual information to understand the behaviour of the system during testing. These graphs include: the magnitude of control force, the lateral displacement of frame measured by PT-1A and the actuator (shown in separate graphs). There's also an emergency stop button to stop the test in case of equipment malfunction or for any unexpected situation.

3.4.3.2 PicPro interface program

The PicPro interface program was developed using the PicPro programming language, which is a language intended for running machinery and equipment in industry. The language was also suitable for controlling the *EXLAR* electromechanical actuator used in the current experimental project.

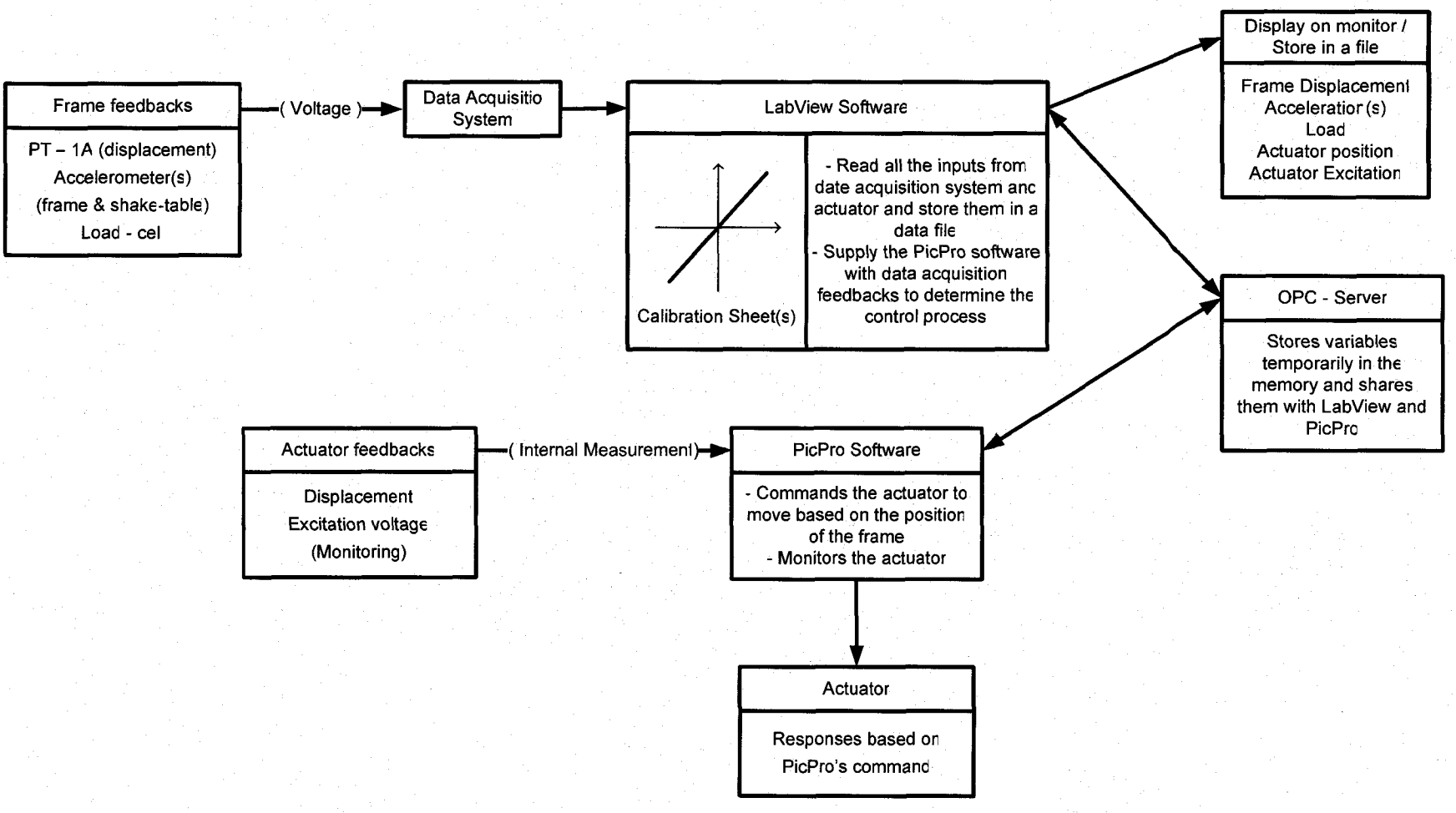

Fig. 3.20 Flowchart of interconnection between computer programs

The program allows the definition of initial displacement and load conditions by the user. Prior to testing, all inputs have to be zero calibrated. Zero-calibration process includes; i) defining neutral position of the actuator by setting the displacement measurement sensor to zero corresponding to zero horizontal displacement of the frame and ii) setting the load-cell externally attached to the actuator to zero before the tests. The PicPro interface was also programmed to activate the actuator beyond a specific threshold value of horizontal frame displacement. This information is input into the program as a "zero-range" value. The zero-range in this research project is defined as the limits within which the actuator will not take any action to constrain or oppose the movement of the frame. These limits are either set by the designer to achieve a certain design philosophy or imposed by technical constraints. The rationale for setting these limits by the structural engineer can be for damage control. For example, if 1% lateral drift ratio is acceptable to the structural engineer as acceptable drift and associated damage level, then 1% of storey height is set as the zero-range for the actuator to trigger structural force control. If the lateral displacement exceeds this zero range, then the actuator starts imposing corrective control forces. The limits set for the technical constraints are associated with the characteristics of the actuator, and can be due to any one of the following reasons:

(a) Hardware accuracy or the minimum movement that is able to trigger the movement of the actuator.

(b) Overshooting problem; depending on the defined acceleration and deceleration rates for the actuator, an overshooting problem might occur. Overshooting occurs if the actuator can not stop within the zero-range and the actuator exceed the range in the opposite direction while trying to stop and remain within the range. This is caused by the momentum of the system. By decreasing the acceleration rate increasing the deceleration rate, the overshooting problem may be overcome.

A software stop switch is defined in the PicPro program for controlling the test. This is needed to stop the test when the displacement of frame exceeds a deformation level that could harm the specimen. This option is set by the user to assure the safety of the frame during testing, as well as during the calibration process. It can be easily disabled in the program at anytime.

3.4.3.3 OPC – Server

OPC-Server program is used to provide a communication link between LabView and PicPro programs. Two different programs in two different environments had to be used for testing mainly because the hardware (actuator) used could only be controlled through the PicPro software. This necessitated the need for a program that had capability to integrate these programs during the real-time experiments. The term "real-time" refers to a situation where all the data transfer is done in a fraction of a millisecond and hence data could be accessed without any time-delay.

The OPC-Server reads and writes data to and from controller(s) and other computer programs through Ethernet connection and stores them in a temporary memory. It allows this data to be accessed and modified through different sources. The controller must have an Ethernet TCP/IP communication module installed and all the device(s) and programs have to be properly configured to recognize OPC-Server and also to be recognized by OPC-Server.

The term OPC is an acronym for OLE for Process Control. OLE stands for Object Linking and Embedding. OLE is a Microsoft technology and is available on Microsoft operating systems, such as Windows NT, 2000, XP. It also can be added to Windows 95/98. OPC-Server details the methods of exchanging data between data source (Also referred to as server) and data users (Also referred to as clients). The data exchange process between a server and a client is possible on the same computer (local server) and/or between server and clients on different computers (remote server). In the experiments conducted as part of the current research project a local server was used to share data locally. A schematic view of a server/client connection is presented in Fig. 3.21.

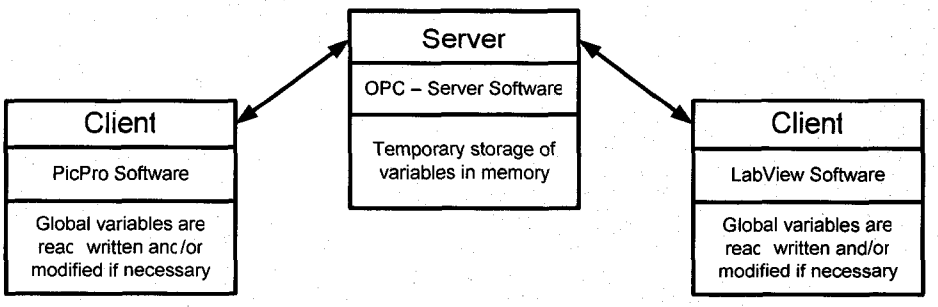

Fig. 3.21 A schematic view of server / client connection

CHAPTER 4

Properties of Model Frames and Test Results

4.1 Introduction

Experimentation is one of the most valuable tools for research to confirm hypotheses, theories and numerical models. The results of these experiments help increase knowledge and help in better predicting the behavior of prototypes in real life. Since experimenting on complex and expensive systems is sometimes impossible or economically unjustifiable and sometimes unsafe, researchers often test scaled models. Basically, the main goal is to predict the behavior of a full-scale system (here; a full-scale frame) by examining the performance of a scaled system (here; a scaled frame). The importance of using models becomes obvious when full-scale experiments involve expensive, time consuming, or complicated and unmanageable system. A good example is aircraft testing.

The results obtained from scaled model tests can only be extended to full-scale systems if the results are properly processed. The similitude theory deals with this problem. In the first place it helps building a model representing the prototype. After testing of the scaled

model, it allows proper scaling up of the results to obtain the performance of the prototype. The similitude model processing is explained in the following section.

4.2 Similitude Model

The similitude theory is used to scale a prototype such that the results obtained on the basis of the model can be processed to represents the performance of the prototype. Basically, this method will help design a scaled-down model frame that will demonstrate similar behaviour as the full-scale frame. In this case, where the model is subjected to ground excitations, the similitude model ensures similar structural response of the full-size frame under the same ground excitation. This scaling process should be done in a way that geometric, kinematic and dynamic similarities are retained. The similitude theory relies on dimensional analysis. In 1914, Buckingham used dimensional analysis to introduce the π-theorem, which forms the basis for the similitude theory. Bridgmann used the term "dimensional analysis" for the first time in his books (1922).

Obtaining the scale factors for basic units is the ultimate goal of dimensional analysis. These scale factors are then used to obtain the scale factors for all other parameters. Also, the dimensionless numbers, referred to as "Pi-numbers", play a key role in the dimensional analysis. The dimensionless mathematical form can be derived by reshaping the equation of motion of the system using Pi-numbers and dimensionless variables.

The first step would be to choose the primary variables representing time (T), Length (L), and mass (M). The dimensions of other variables could be written as a product of these basic units. The height of the center of mass (Z_{cm}), the sprung mass (M) and the frame's natural frequency (ω_0) are chosen as the primary quantities for the frame. In order to find dimensionless Pi-number for each property of the frame, they should be divided by primary quantities to produce a dimensionless number. The representative Pi-numbers for the frame are as follows:

$$\Pi_1 = \frac{K}{M \times \omega^2} \qquad \text{Stiffness Pi-number} \tag{4.1}$$

$$\Pi_2 = \frac{C}{M \times \omega} \qquad \text{Damping Pi-number} \tag{4.2}$$

$$\Pi_3 = \frac{F}{M \times \omega^2 \times L} \qquad \text{Force Pi-number} \tag{4.3}$$

Equations 4.1,4.2 and 4.3 represent Stiffness Pi-number, Damping Pi-number and Force Pi-number, respectively.

According to the similitude theorem, the necessary and sufficient condition to have two similitude models is to have the same dimensionless mathematical form. The dimensionless equations of motion ensure that if two systems have the same Pi-numbers, they have the same dimensionless mathematical model. Also, having the same representative Pi-numbers guarantees that all Pi-numbers of the two systems are the same. The scale factors are defined in a way to satisfy the equality of Pi-numbers for the model and the prototype.

Let C_T, C_L, C_M, C_K, C_C and C_F be the scale factors corresponding to time, length, mass, damping, stiffness and force, respectively. K, M, L, ω, C and F are assumed to be the representative parameters for the full-scale frame, and K', M', L', ω', C' and F' are the parameters representing the small-scale model frame. Then, the stiffness Pi-number for the full-scale frame can be expressed as follows:

$$\Pi_1 = \frac{K}{M\omega^2} \tag{4.4}$$

Writing the full scale frame parameters in terms of their corresponding scaled parameters and their scaling factors results in:

$$\Pi_1 = \frac{C_K C_T^{\,2}}{C_M} \frac{K'}{M'\omega'^2} \tag{4.5}$$

Considering Eq. 4.5, the two Pi-numbers are related with each other through Eq. 4.6:

$$\Pi_1 = \frac{C_K C_T^{\,2}}{C_M} \Pi_1' \tag{4.6}$$

For Π_1 and Π_1' to be equal, the following condition must be met:

$$\frac{C_K C_T^{\,2}}{C_M} = 1 \tag{4.7}$$

Repeating the same steps for damping and force Pi-numbers result in the following equations:

$$\frac{C_C C_T}{C_M} = 1 \tag{4.8}$$

$$\frac{C_F C_T^{\,2}}{C_M C_L} = 1 \tag{4.9}$$

Since it was decided to have a model frame with the same natural period of vibration as the prototype frame, the time factor C_T, is selected as 1.

$$C_T = 1 \tag{4.10}$$

After replacing the C_T value in Eq. 4.8 with unity, one of the scaling rules for similitude models becomes:

$$\frac{C_K}{C_M} = 1 \tag{4.11}$$

Next, C_T is set equal to 1.0 in Eq. 4.9 to obtain the force scaling factor, as shown in Eq. 4.00:

$$C_F = C_M C_L \tag{4.12}$$

It should be noted that the result of one equation can be used in another resulting equation. For example, based on Eq. 4.11, C_M should be equal to C_K and consequently, C_M can be exchanged with C_K in Eq. 4.00. Finally, the last scaling law is obtained as follows:

$$\frac{C_C}{C_M} = 1 \tag{4.13}$$

By satisfying Eq. 4.11, 4.12 and 4.13, based on the similitude theory, it is guaranteed to have a scaled model similar to the original frame.

After considering the following conditions, the scaling factors were chosen to finalize the size of the model.

(a) The scaled model would be manageable;
(b) The size of the model should fit on the shake table available in the Structural Lab of the University of Ottawa;
(c) The height-to-length ratio of the frame should be representative of the range used in practice for a typical prototype frame;
(d) The model frame would be flexible enough to show considerable displacements under dynamic excitations, for simplicity of monitoring.

The specifications of the chosen test models and their scaling factors are presented in the following section.

4.3 Selection of Test Models

Model Frame:

In this experimental research project, two different frames were used, labeled as Frame No. 1 and Frame No. 2. Frame No. 1 represents a prototype frame and hence realistic mass and stiffness characteristics, scaled down to fit the capabilities of the shake table and the test setup. Frame No. 2 was selected to have a considerably reduced flexibility to have a long-period structure to attain high deformations at lower speeds. Certain characteristics of the model frames were selected to have the same properties as those for the prototype structure. First, the column height to beam span ratio was selected to remain the same. Second, the beam was selected to be significantly stiffer than the columns. Therefore, the beam would not deform in any appreciable manner when subjected to lateral forces. This was done to simulate a typical floor diaphragm, stiffened with floor slabs. Third, the reference model frame (Frame No. 1) had the same natural period of vibration as that of the prototype frame. A schematic view of model frames is shown in Fig. 4.1.

The dimensions of Frames No. 1 and No. 2 are presented in Table 4.1 and 4.2. The geometry of the frame is kept constant during the experiments but the mass was changed. The natural period of the structure, as well as the height of the center of mass varied when the frame's sprung mass was changed. Sprung mass is defined as the portion of the mass that participates in the spring action.

Table 4.1 Specifications of Frame No. 1

Column Information		*Beam Information*	
Height	650 mm	*Length*	1050 mm
Width	100 mm	*Width*	100 mm
Thickness	4.75 mm	*Thickness*	12.5 mm
Weight (each Col.)	2.5 kg	*Weight*	10 kg
Frame's height of the center of mass (Z_{cm})		Varying from 55 to 62 depends on the weight of additional mass	

Table 4.2 Specifications of Frame No. 2

Column Info.		*Beam Info.*	
Height	650 mm	*Length*	1050 mm
Width	100 mm	*Width*	100 mm
Thickness	3.2 mm	*Thickness*	10.0 mm
Weight (each Col.)	1.6 kg	*Weight*	8.25 kg
Frame's height of the center of mass (Z_{cm})		Varying from 56 to 62 depends on the weight of additional mass	

The natural frequency of the bare frame was found to be 0.24 sec through a free-vibration test. The relationship between mass, stiffness and natural period is expressed in Eq. 4.14.

$$T = 2\pi\sqrt{\frac{m}{K}} \tag{4.14}$$

Where T is the natural period (sec), m is the sprung mass (kg) and K is the stiffness (N/m). The sprung mass of the model frame includes the weight of the beam plus half of the weight of the columns.

$$m = Beam\ weight + 50\%\ of\ Column\ weight \tag{4.15}$$

$$m = 10.0 + (0.5)\times 2\times 2.5 = 12.5 \quad (kg)$$

Substituting T and m into Eq. 4.14, the value of K is determined as;

$$K = \frac{(2\pi)^2 m}{T^2} \tag{4.16}$$

$$K = \frac{(2\pi)^2 (12.5)}{(0.243)^2} = 8358 \quad (N/m) \tag{4.17}$$

The stiffness of a frame is defined as follows:

$$K = \frac{n.EI_e}{L^3} \tag{4.18}$$

Where n is a multiplier that depends on the end restraints of the supporting columns, E is the modulus of elasticity, I_e is the effective moment of inertia of the frame, and L is the column height. I_e is the summation of the moments of inertia of all the supporting columns. The value of n can be obtained from Eq. 4.19.

$$K = \frac{n \times E_s \times I_{eff}}{L^3} \tag{4.19}$$

$$8358/1000 = \frac{n \times 200,000 \times 2 \times \left(\frac{100 \times 4.75^3}{12} \right)}{650^3} \tag{4.20}$$

$$n = 6.45 \tag{4.21}$$

The value of n in Eq. 4.21 indicates that the end restraint condition for the supporting columns is between full fixity and pinned end which would have corresponding n values of 12.0 and 3.0, respectively.

Prototype Frame:

The prototype frame is a conventional reinforced concrete frame for a low-rise building. The beam is assumed to incorporate the mass and stiffness of the tributary slab. This slab constrains the deformations of the beam significantly to transforms it into a rigid beam. The dimensions of the prototype frame are presented in Table 4.3. This frame has the exact same beam span-to-column height ratio as that for the model frame.

$$(Model\ Frame) \quad \frac{650}{1000} = \frac{3000}{4500} \quad (Prototype\ Frame) \tag{4.22}$$

The next step would be to determine the stiffness, sprung mass, and period of the prototype frame, and compute C_m, C_K, and C_L scale factors. If the calculated scale factors

meet the requirements of the similitude model, then the results obtained from the model frame test can be used to predict the behaviour of the prototype frame under similar conditions.

Table 4.3 Specifications of Prototype Frame

Column Information		*Beam Information*	
Height	3000 mm	*Length*	4500 mm
Width	250 mm	*Width*	250 mm
Thickness	250 mm	*Thickness*	150 mm
Weight (each Col.)	470 kg	*Weight*	422 kg
Slab thickness		150 mm	
Slab tributary width		4000 mm	
Slab Weight		6750 Kg	
Frame's height of the center of mass (Z_{cm})		2830 mmm	

The stiffness of the frame is calculated as follows:

$$K = \frac{12 \times E \times I_{eff}}{L^3} \tag{4.23}$$

Where; I_{eff} is the summation of moments of inertia of all the columns of the frame. I_{eff} (effective moment of inertia, incorporating the effects of concrete cracking) is assumed to be equal to $0.7I_g$, (where I_g is the gross, uncracked moment of inertia), to be consistent with the requirements of CSA A23.1-1994 for columns. The stiffness of the frame is computed as follows:

$$K = \frac{12 \times 25000 \times \left(2 \times \frac{250^4}{12} \times 0.7\right)}{3000^3} = 5064 \quad (kN/m) \tag{4.24}$$

The sprung mass of the prototype frame, M, is computed by the following equation.

$$m = (0.5) \times 2 \times 470 + 422 + 6750 = 7642 \quad (kg) \tag{4.25}$$

Stiffness scale factor, C_K, mass scale factor, C_m, length scaling factor, C_L, and force scaling factor, C_F, are computed in Eq. 4.26 to 4.29 respectively.

$$C_K = \frac{5064}{8.358} = 606 \tag{4.26}$$

$$C_m = \frac{7642}{12.5} = 611 \tag{4.27}$$

$$C_L = \frac{2830}{550} = 5.1 \tag{4.28}$$

$$C_F = C_M . C_L = 3100 \tag{4.29}$$

It is necessary for C_K and C_m to be equal to each other to satisfy the similitude model condition. The scaling factors obtained show acceptable agreement with the similitude model requirements. The natural period of the prototype frame is calculated in Eq. 4.30.

$$T = 2\pi\sqrt{\frac{m}{K}} = 2\pi\sqrt{\frac{7642}{5064\times1000}} = 0.244 \quad (Sec) \tag{4.30}$$

The modeling technique employed resulted in the matching of the natural period of vibration of the prototype frame and the scaled model.

4.4 Test Parameters

Having established the dimensions of the model test frames with two different stiffnesses, the test variables were established for an experimental parametric investigation. The primary response quantities were established for recording and monitoring. It was decided to vary the structural mass, stiffness and ground excitation characteristics. As for the test results, frame displacement response and the magnitude of control forces were of interest. More details on the test variables are provided in the following sections.

4.4.1 Effect of mass

Mass is one of the test parameters that was expected to influence the results significantly. The change in mass has a direct effect on the natural frequency of frame. The increase in mass while keeping all other parameters constant would lengthen the natural period of the frame. In addition, it is known that the magnitude of earthquake-induced inertia forces have a direct relationship with mass. Consequently, a structure with a higher mass

requires a higher control force. This results in increased displacement under constant stiffness. Uniformly distributed mass was added on top of the frame, representing a realistic distribution of structural mass. The additional mass was provided by adding small steel plates on top of the frame. The plates weighed one kilogram each. Placing four plates covered the entire beam. Any desired mass can be superimposed on top of the frame by stacking up these additional masses. A schematic view of this set-up is shown in Fig. 4.2.

During the experiments, it was decided to have the following variation of mass:

Frame No. 1:

- Bare frame (No additional mass);
- 12 kg additional mass (4 set of 3kg stacked steel plates);
- 20 kg additional mass (4 set of 5kg stacked steel plates);
- 28 kg additional mass (4 set of 7kg stacked steel plates).

Frame No. 2:

- Bare frame (No additional mass);
- 12 kg additional mass (4 set of 3kg stacked steel plates);
- 20 kg additional mass (4 set of 5kg stacked steel plates).

4.4.2 Effect of stiffness

The test frames were selected to have somewhat longer periods than typical single-storey buildings. This was done intentionally to monitor the performance of the structure during testing. It would be easier to provide the proof of concept on frames with exaggerated flexibility.

Two sets of frames were selected for testing. One set (Frame No. 1) had columns with higher stiffness, and had a more rigid beam. This frame was a better representative of the actual prototype frame. It was expected that, with increased stiffness, the natural period would be shorter and the lateral displacement would be reduced.

The second frame (Frame No. 2) was selected to be softer to investigate the effects of varying stiffness on the frame. A complete set of testing, with different structural mass, was conducted under different ground excitations.

4.4.3 Effects of dynamic characteristics of ground excitation

Structural response depends on the magnitude and characteristics of ground excitations, as well as their interactions with dynamic characteristics of the structure. A specific earthquake that might cause severe damage in a given structure may induce minor or no damage in another structure. If during a seismic excitation the natural period of the excitation approaches to that of the structure, a phenomenon known as "resonance" may occur. In such a situation, the structure could easily get out of control and experience enormous destructive deformations.

A complete range of sinusoidal excitations was imposed to obtain a wide range of structural response for the frames tested. This task was performed to establish the relationship between structural frequency and the frequency of the ground excitation. The shake table was driven by computer software that used the amplitude and frequency of sinusoidal excitation as inputs. During the tests, constant amplitude (travel distance of actuator) of motion was used. This implies that the ground acceleration increased every time the frequency was increased under constant amplitude.

After finding the response of the frames to sinusoidal excitation, it was desired to see the response of the frame to an actual earthquake record. The 1940 El-Centro N-S record was selected for this purpose. Because the deformations of the selected structures were relatively small, the accelerogram was amplified by a factor of 3.0.

4.4.4 Effects of structural control

The selected model structures were tested with and without the control actuator in place. The first series of experiments for each structure was conducted on an uncontrolled

frame. The same frame was then tested with the electromechanical actuator in place, but not connected (or connected through a sliding bearing connection) so that it would not apply a reactive force, but its mass would be present for possible interference with structural mass. Next, the actuator was connected to the frame. It was activated in a pulse-control mode to apply control forces as necessary in order to stabilize the structure within the deformation range specified.

4.5 Processing of test data

In real-time experimentation several parameters vary continuously. A history file is created to record the changes that occur during testing. This type of experiment is highly sensitive to time lags and the precision of time at which data is recorded. Therefore, it was decided to increase the refreshment rate to have a better control over the system with minimal time lag. Accordingly, the status of the system is updated every two milliseconds as the data is recorded in a history file. Each experiment lasted about a few minutes. This means that the history file of each experiment contains several hundred thousand lines, with several columns of data, each representing one of the feedbacks from the system. It was obvious that the test results could not be processed during the test and needed further processing after the completion of tests. Analysis and processing of a file with several hundred thousand lines is a time-consuming and demanding task. In addition, it is not necessary to process the data for every time step and even one out of several consecutive readings would provide sufficient accuracy for understanding of the behaviour of the system. Therefore, a small computer program was developed in MATLAB language to reduce the number of lines to a more manageable level for ease in processing. However, this reduction was done with caution to ensure that this reduction would not decrease the accuracy of test results. The proper reduction process was found empirically and the results were verified to assure consistency in the accuracy of readings.

Output files from the MATLAB program were exported to Excel software for further processing. This process included the removal of noise from signals through appropriate zero-calibration, when necessary, and presenting the results in the form of graphs. An

example of noise in the reading is demonstrated in Fig. 4.3. The graphs helped better understand the test results, while also helping distinguish the noise in readings. The noise could be avoided by properly monitoring the graphical output.

The peak points of graphs were used to produce response spectrum for each test. A schematic view of a basic analysis process of a sample experiment is shown in Fig. 4.4.

4.6 Test Results

The two model frames with different structural mass were tested on the shake table, under either sinusoidal ground excitations of different frequency and acceleration or a previously recorded actual earthquake record. Bare frames (uncontrolled), frames with a diagonally placed non-active actuator attached using a sliding bearing fixture (also uncontrolled) and frames equipped with the electromechanical actuator in the active mode, applying structural control (controlled frames) were tested. The structural behaviour was monitored and the results were recorded in terms of horizontal floor displacements and the magnitude of the control force (when present). As an example, the status of Frame No. 1 under 2.5 Hz sinusoidal excitation is presented in Fig. 4.5.

4.6.1 Frame Displacements

Frame No. 1, with the natural period of 0.24 seconds, was first subjected to sinusoidal excitations with different frequencies. The frequency of the sinusoidal excitation started at 1.0 Hz and was gradually increased up to 8.0 Hz. The displacement response of the frame was recorded and given in Fig. 4.6(a). It was observed that during the 4Hz excitation, which was close to the natural frequency of the frame, the maximum displacement of 98 millimeters was recorded. This can be explained by the resonance phenomenon. Accordingly, when the frequency of the excitation approaches to the natural frequency of the structure, the displacements increase rapidly and theoretically become infinity under ideal conditions, in the absence of damping. Similar phenomenon was observed in all test cases (Frames No.1 and No.2, with different masses).

The effect of varying mass was investigated though experimental parametric investigation. Three different levels of mass, consisting of 12, 20, and 28 kg were investigated. The test results are presented in Figs. 4.6 (b), (c) and (d), respectively. It was observed that the increase in mass resulted in an increase in the natural period of vibration, as expected. The natural frequency was increased from 0.24 seconds to 0.32, 0.35 and 0.40 seconds. Furthermore, the maximum displacement of the frame was also increased from 98 mm for a bare-frame to 107, 111 and 117 mm for frames with 12, 20 and 28 kg additional masses, respectively.

The lateral displacement of Frame No.2 under sinusoidal excitation is presented in Fig. 4.7. Frame No.2 has a natural period of 0.32 sec and experienced a maximum deflection of 208 millimeters at 3.1 Hz excitation. The effect of the variation in mass was investigated by placing an additional mass of 12 and 20 kg, over and above the mass of the structure. The natural period was lengthened to 0.47 and 0.59 sec and the horizontal displacement increased to 223 and 235 mm, respectively.

It is observed that although Uncontrolled Frame No.1 with 12 kg additional mass and Uncontrolled Frame No.2 with no additional mass have the same natural period of 0.32 seconds, the maximum recorded displacements of these two frames show significant differences. The maximum deformation of Frame No.1 was 107 mm whereas it was 208 mm for Frame No.2 though theoretically the deformations were expected to be the same (assuming equal damping) since both structures had the same fundamental period. The responses of these two frames are compared in Fig. 4.8 and show good agreement before and after the resonance frequency. The difference in maximum displacements recorded, amplified within the resonance frequency range, was attributed to possible differences in damping of the two structures having different stiffness and mass properties. Furthermore, the flexible frame had a relatively more flexible beam, which may have violated the rigid floor assumption, based on which the period of structures was computed. The actual structural period could have been somewhat different than the computed value, although the computed values were verified against free-vibration tests

conducted within the small deformation range. During resonance response, the flexible structure visibly deformed excessively, with some possible deformations in the beam.

Although sinusoidal excitations were used initially, because of the ease in controlling the frequency of excitation, it was felt important to also consider an actual earthquake record to assess the performance of model structures under actual seismic excitations. For this purpose, El-Centro 1940 N-S acceleration record was used conveniently, because the record had already been entered in the MTS controller. To amplify the structural response, to be able to observe deformations and the importance of structural control on deformation magnitudes, the accelerogram was amplified 3.0 times before it was used. A maximum displacement of 22.5 mm was recorded in Frame No. 1, when no additional mass was present. The effect of changing mass was investigated subsequently. The earthquake inertia force is directly related to mass and acceleration. Since the mass was increased, and the earthquake record was kept constant, it was expected to observe higher deformation levels due to the increased inertia forces. Maximum lateral displacements of 29.5, 34.0 and 37.0 mm were recorded for frames with 12, 20 and 28 kg of additional masses, respectively. The deformation of Frame No.2 under the same earthquake record is presented in Fig. 4.10. Maximum displacements of 26, 41 and 45 mm were recorded for Frame No.2 with zero (bare-frame), 12 kg and 20 kg additional masses, respectively.

Having completed the bare-frame tests for uncontrolled frames and before the tests of controlled frames have begun, the effect of the presence of inactive actuator attached to the structure and its mass was questioned. Therefore, another set of tests were conducted, with the actuator in place, but without activating its power. In order to eliminate the restraining effect of a non-powered electro-mechanical actuator, the actuator was connected to the frame through a sliding bearing connection. This would allow the actuator to slide without developing a reactive force as the frame deformed under the excitation of the shaking table. It would also ensure the contribution of the actuator mass, however small it would be, to the structural mass on the beam. However, a small friction force that would have been developed along the sliding bearing could not be eliminated.

The response of Frame No. 1, with the actuator in place, but connected through the sliding bearing, is presented in Fig. 4.11 under a sinusoidal excitation. The test results show that the natural period of the frame slightly increased in comparison with the bare-frame. Also, the maximum deflection has slightly decreased as a consequence of the inherent friction and the resulting damping of the structure.

The effect of varying mass on structural response was investigated by gradually increasing the additional mass placed on the beam. The same pattern of displacement response, as that observed in the uncontrolled bare-frame, was observed. The same tests were subsequently conducted on Frame No.2. The results are presented in Fig. 4.12. During this series of tests, with the flexible Frame No. 2, the deformation level exceeded the 200 mm of allowable extension length of the sliding bearing, when the mass was increased. Hence, the tests were limited to the frequencies that resulted in deformations within the allowable range.

Next, the response of the frame with non-active actuator connector was investigated under amplified El-Centro Earthquake. The test results for Frames No.1 and No.2 are presented in Figs. 4.13 and 4.14, respectively. The lateral displacement increased as the additional mass increased. Since Frame No.2 was more flexible, adding mass on top of the frame had more pronounced effect on lateral displacement.

The third series of tests were performed on controlled frames. Active control was employed through a pulse-control mode of the electromechanical actuator, placed within one of the diagonals, acting in both tension and compression mode. This type of application is also equivalent to the use of two actuators, one in each diagonal direction, or an actuator cable system that can only apply tension in each direction, i.e., the compression mode of the diagonally positioned single actuator was representative of a second actuator placed along the opposite diagonal, applying tension forces only. The application of control forces resulted in a drastic reduction in horizontal displacements of both Frames No. 1 and No.2. This is illustrated in Figs. 4.15 to 4.18. For example, in Frame No. 1 with no additional mass, the maximum displacement of 98 mm was reduced

to approximately 5.5 mm. This translates into a 94% reduction in maximum displacement. Considerable reductions were also observed in other controlled frames. An average reduction of approximately 90% was observed for sinusoidal excitations. As for the earthquake simulations, a minimum displacement reduction of 65% was recorded.

The test results are further compared in Figs. 4.19 through 4.27 to illustrate the significance of test parameters. Figs. 4.19 shows the effect of structural stiffness on displacement response. Frame No.1, with higher stiffness, does exhibit reduced maximum displacement under each frequency of excitation, when compared with the more flexible Frame No. 2. Similarly the effect of structural mass is compared in Figs. 4.20 to 4.21 for uncontrolled and controlled structures. As can be see, the increase in mass reduces the natural frequency and increases the maximum displacement due to the higher inertia forces associated with increased mass.

The effect of control forces on displacement response is illustrated in Figs. 4.24 to 4.27. Accordingly, the two uncontrolled cases considered, i.e., with and without in-active actuators, did not result in a significantly different displacement response. However, when the actuator was activated and applied control pulses, the displacement response was reduced significantly, as discussed earlier.

4.6.2 Control Forces

The magnitude of applied control forces was monitored and recorded during testing. The level of control force required for a given combination of ground excitation and structural mass is important in assessing the capacity requirements of control actuators. Fig. 4.28 displays recorded control forces for Frame No.1 with different masses, subjected to sinusoidal excitation of different frequencies. The results show an increasing trend in the magnitude of control forces with an increase in the excitation frequency. As the excitation frequency approached the natural frequency, it was expected to get stronger control forces due to the stronger response. This trend was observed as expected. However, when the excitation frequency exceeded the natural frequency, it was expected to record a descending trend in the magnitude of control forces as response would

become weaker. But this did not occur contrary to expectations. A closer look at the characteristics of ground excitations revealed that the ground acceleration also changed with excitation frequency when the sinusoidal ground motion was employed. The MTS controller used to run the shake table was designed to make up for the loss in time at ground displacement reversals. For higher frequencies, because the number of cycles increased, the acceleration of the excitation would also increase to be able to apply the required number of cycles per second. Consequently, the increase in excitation frequency was accompanied with an increase in excitation acceleration. In other words, the MTS computer program, which was used to run the shake-table for sinusoidal excitation required two inputs; i) travel distance, and ii) excitation frequency. The travel distance refers to the summation of all the movements of the hydraulic actuator in one second. For the experiment, this value was set to 100 mm. The program computed the amplitude of the sinusoidal excitation based on the required excitation frequency. For example, if the excitation frequency was set to 1.0 Hz, the amplitude would be 50 mm; or for 2.0 Hz, the amplitude would be 25 mm. Consequently, the MTS software would calculate the necessary acceleration rate to produce the required excitation. The acceleration and deceleration rate varies for different frequencies. The above explanation was verified experimentally. The recorded acceleration of the shake-table during a sinusoidal excitation is shown in Fig. 4.34. The figure illustrates that as the frequency increases, the excitation acceleration also increases. Having higher acceleration levels would lead to higher inertia forces. Increased inertia forces would necessitate higher control forces to limit the frame's movement. This provides an explanation for the observed increase in control forces with increase frequency.

The control actuator is expected to allow deformations of the frame within the zero-range and apply control forces beyond the range. This implies that the actuator would follow the frame without applying any force. However, this may not be feasible due to the technique employed in manufacturing the electromechanical actuator used and the gear mechanism implemented. In order to overcome this shortcoming, the actuator was programmed to maintain zero-load within the zero-range and follow the movement of the frame. The performance of the actuator was investigated for different values of zero-

ranges and a satisfactory response was obtained. However, due to the minor time lag in response, a small force of up to 40 N was recorded within the zero-range. This is shown in Fig. 4.35. This corresponds to approximately 20% of the control force used at the lower end of the values obtained and 6% at the higher end. The magnitude of this force is expected to remain constant for large size applications, reducing the significance of the potential error introduced.

It has to be noted that the structural control philosophy in the pulse-control algorithm is completely different than any other active control system. In optimum active control systems, the algorithms used provides a tradeoff between the displacements to be controlled and the magnitude of the control force required. Therefore, the dynamic equation of motion is solved while employing the control algorithm. Usually the displacement is observed and recorded and the magnitude of the control force is computed based on an algorithm and then applied. In a pulse control system, the actuators respond dynamically to overcome any deformation beyond a prescribed deformation threshold. This reactive force is imposed within milliseconds. In other words, it does not allow the buildup of displacements, which would require larger control forces (because of larger deformations). Having higher structural response may lead to higher number of pulse-controlled forces but does not necessarily result in a stronger control force, potentially exceeding the capacity of the actuator.

The control forces for the frames subjected to amplified El-Centro earthquake record is presented in Figs. 4.30 and 4.31. The figures indicate that the magnitude of the control force increases as the mass increases, as expected.

The results of the scaled model tests can be used to assess the response of the prototype, subjected to actual ground excitation. Scaling up of experimentally recorded control force through the force scaling factor, C_F, explained in the previous section, would give yield the required control force for a full-scale prototype frame. For example, to control the effects of an earthquake with three times the magnitude of the El-Centro 1940 N-S

Record, a control force of 200 N was necessary during the shake table test. This value would translate into approximately 600 kN of control force for the prototype structure.

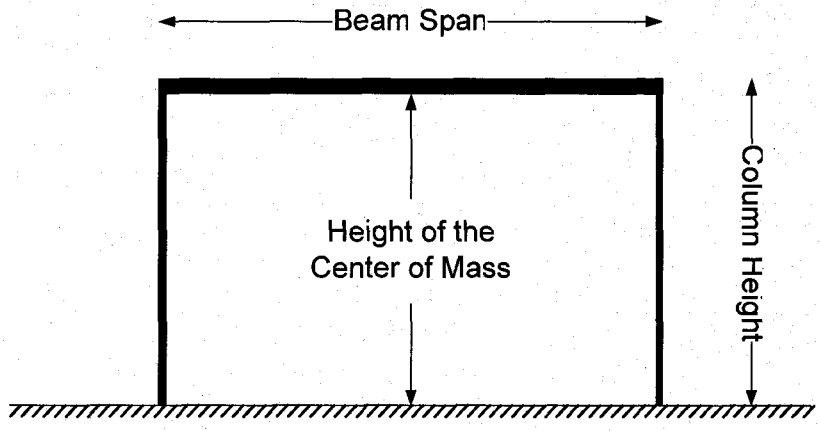

Fig. 4.1 Model frame dimensions

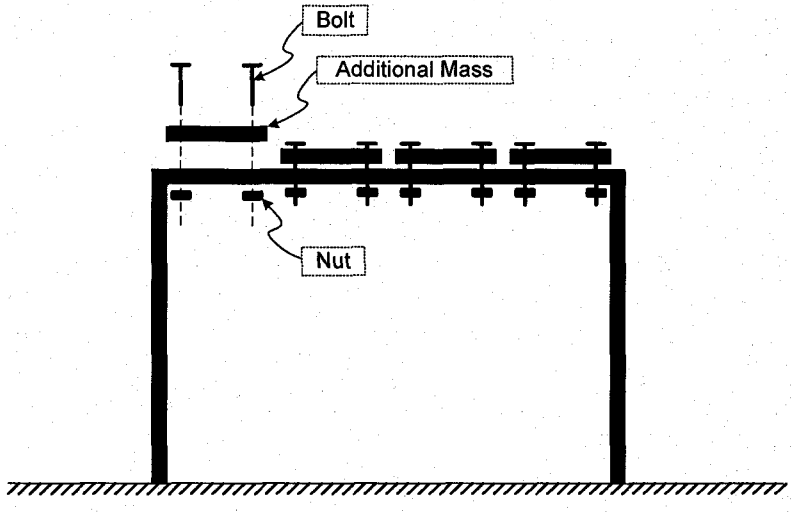

Fig. 4.2 Schematic view of the set-up for structural mass

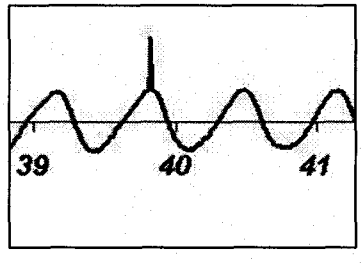

Fig. 4.3 Noise in readings

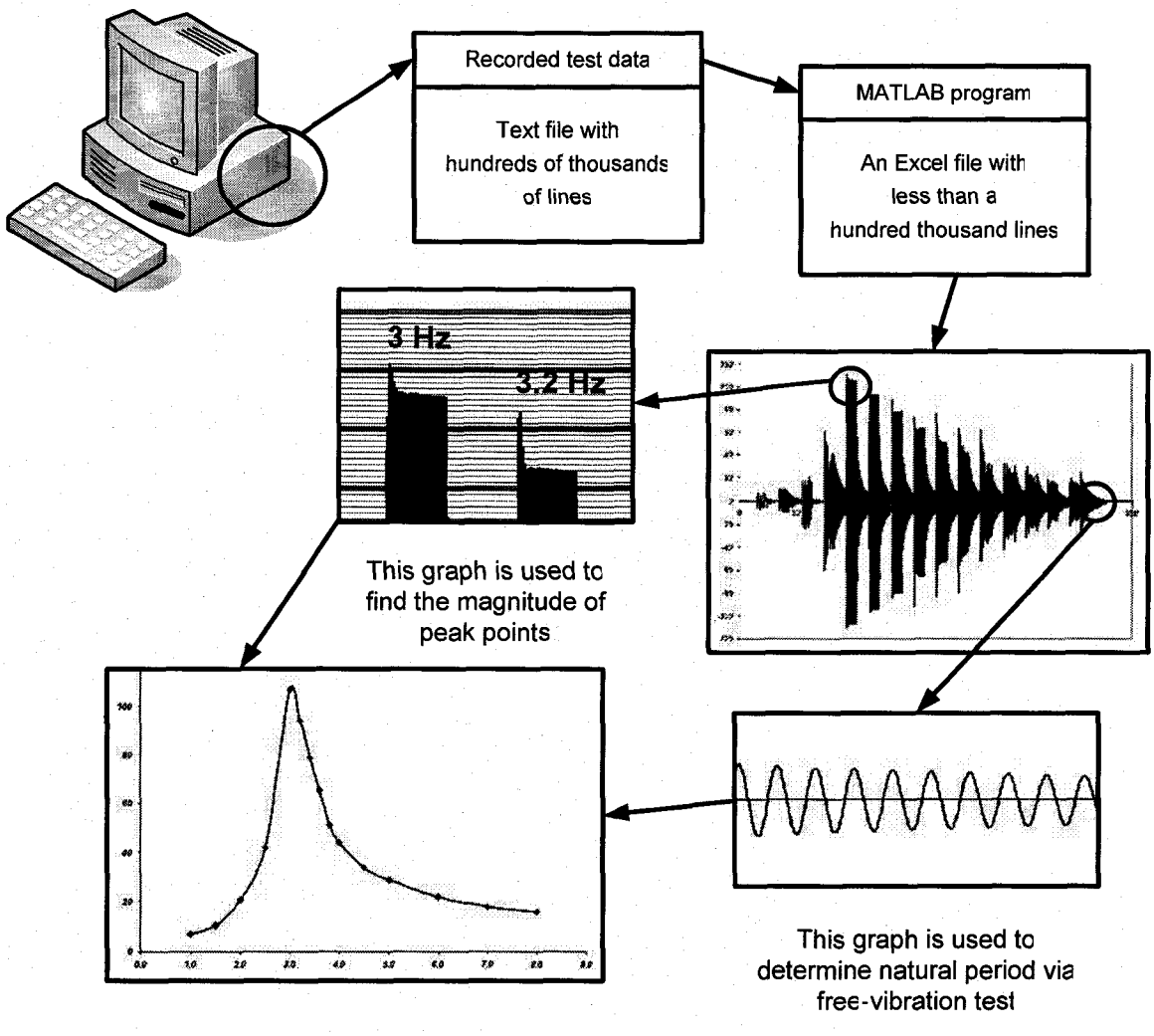

Fig. 4.4 A schematic view of analyzing process for a sample experiment

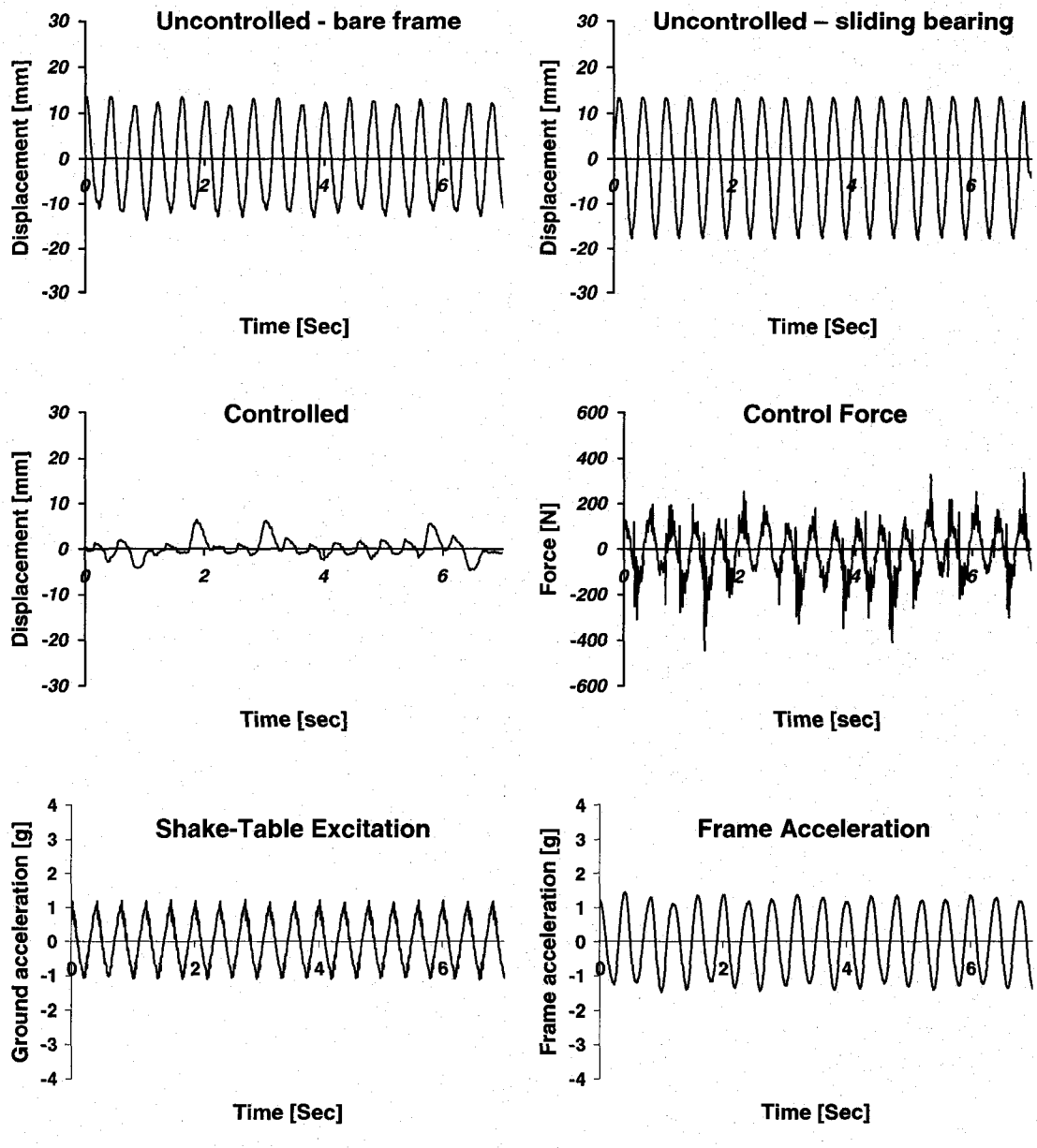

Fig. 4.5 Status of Frame No.1 under 2.5 Hz sinusoidal excitation wave

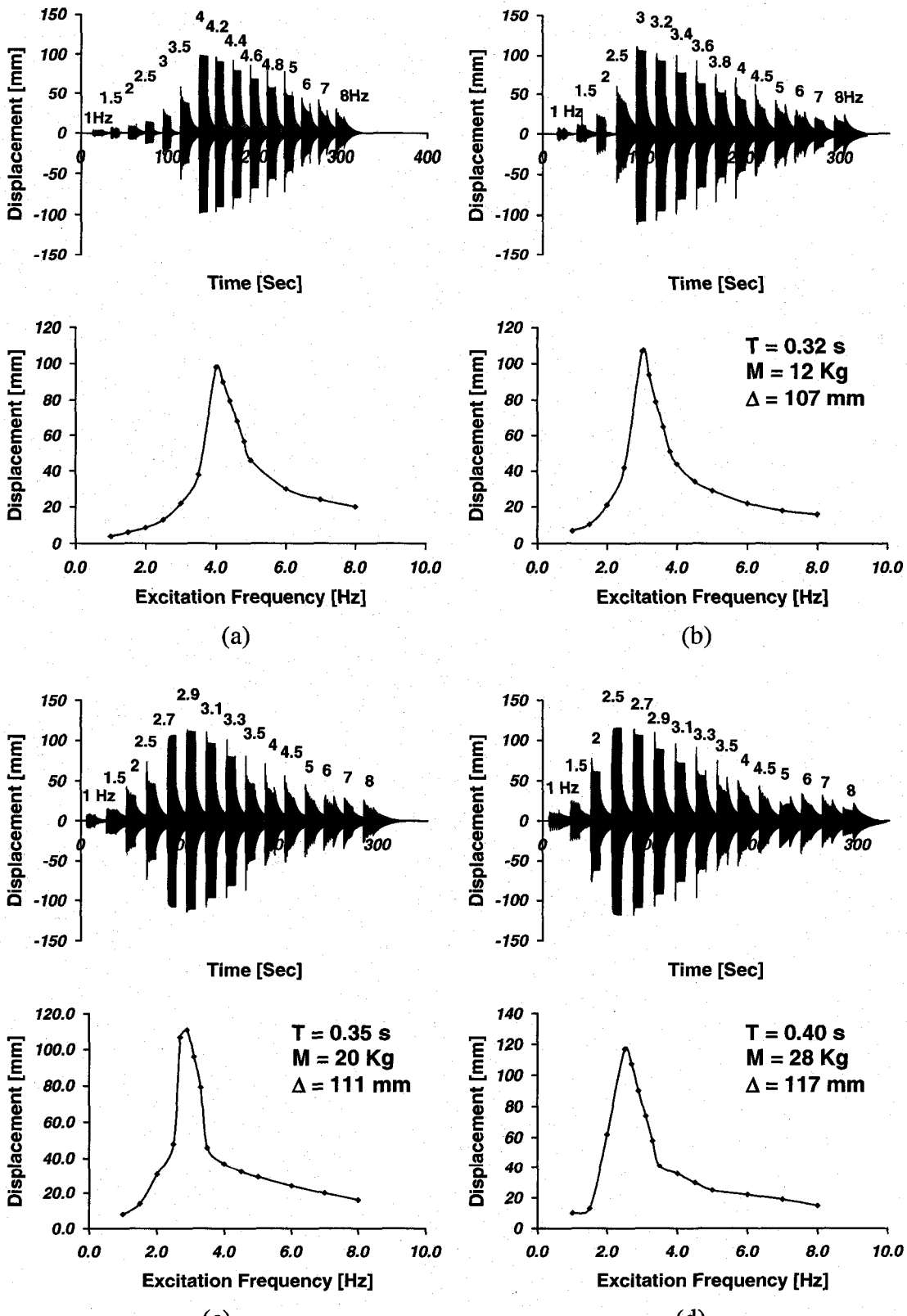

Fig. 4.6 Lateral displacement of Frame No.1 under sinusoidal excitation

Uncontrolled bare frame

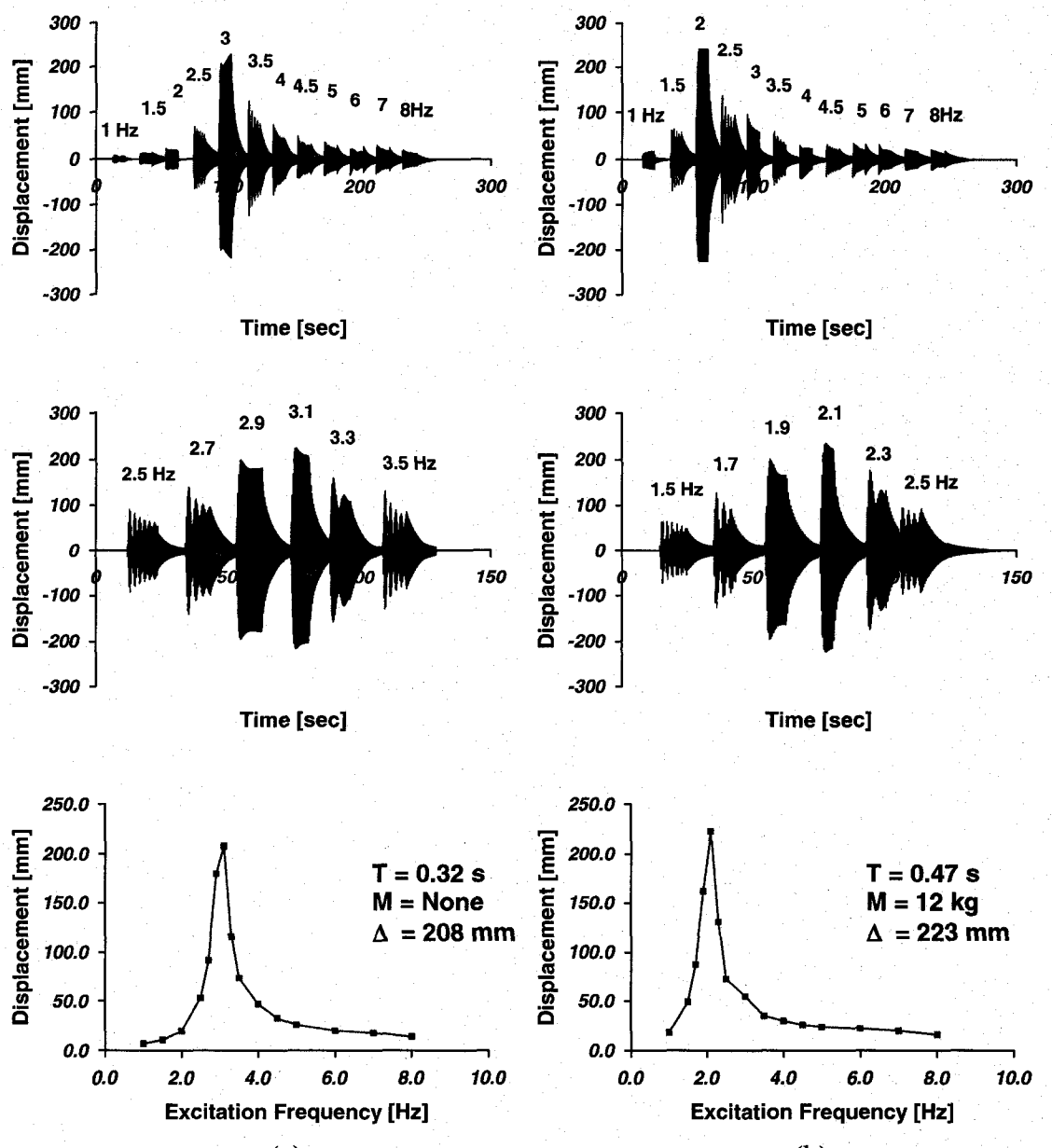

Fig. 4.7 Lateral displacement of Frame No.2 under sinusoidal excitation

Uncontrolled bare frame

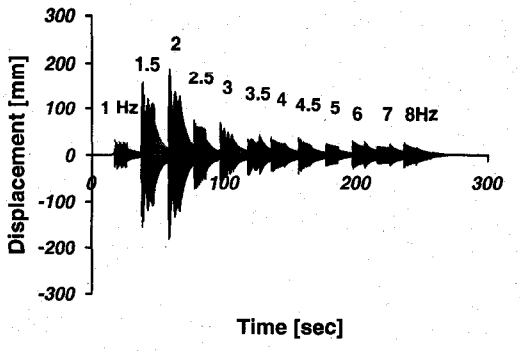

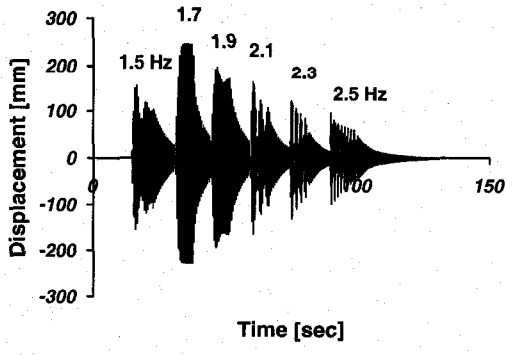

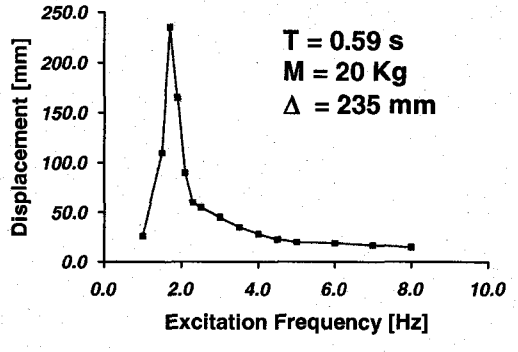

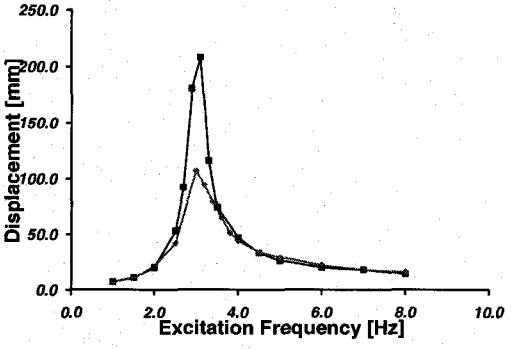

(c)

Fig. 4.7 Lateral displacement of Uncontrolled bare frame (Cont'd)

Fig. 4.8 Comparison of Frame No.1 and 2

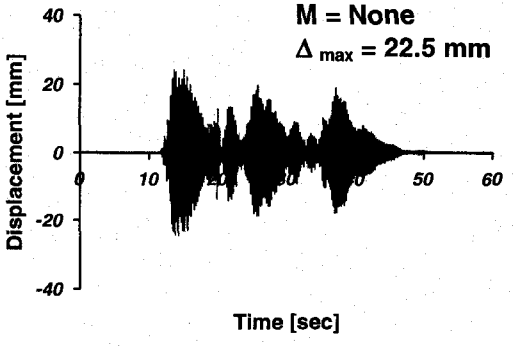

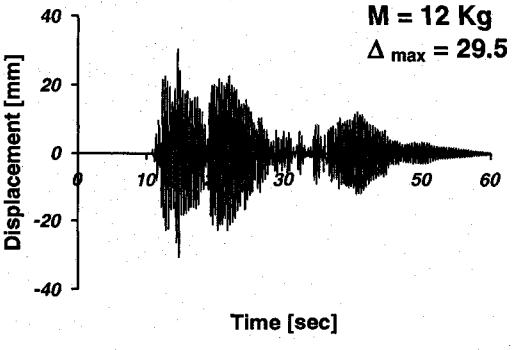

(a) (b)

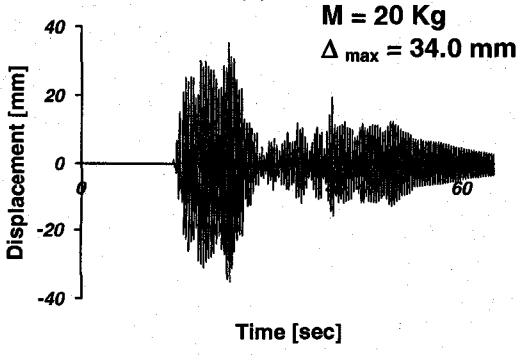

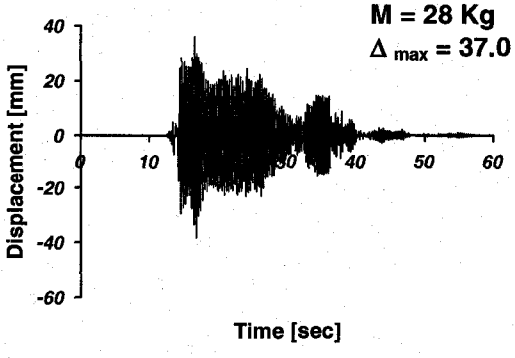

(c) (d)

Fig. 4.9 Lateral displacement of Frame No.1 under amplified El-Centro earthquake Uncontrolled bare frame

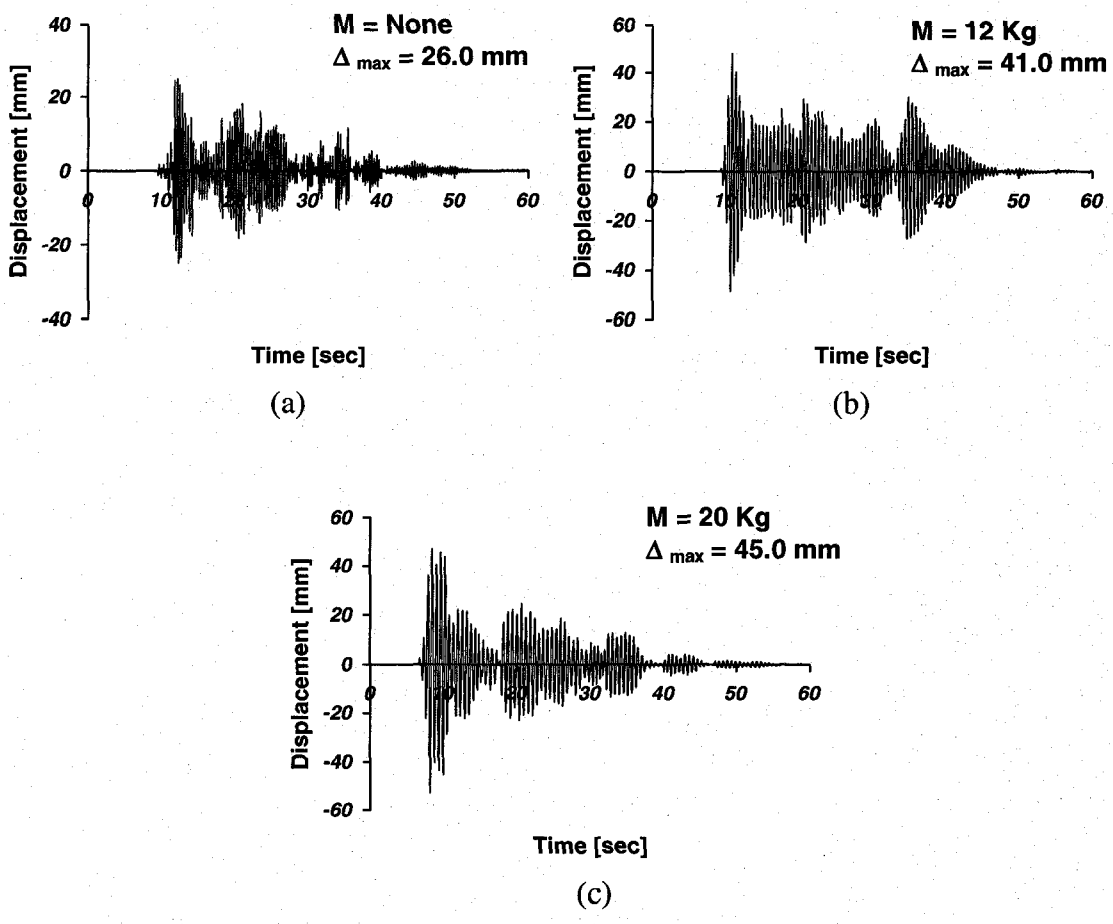

Fig. 4.10 Lateral displacement of Frame No.2 under amplified El-Centro earthquake Uncontrolled bare frame

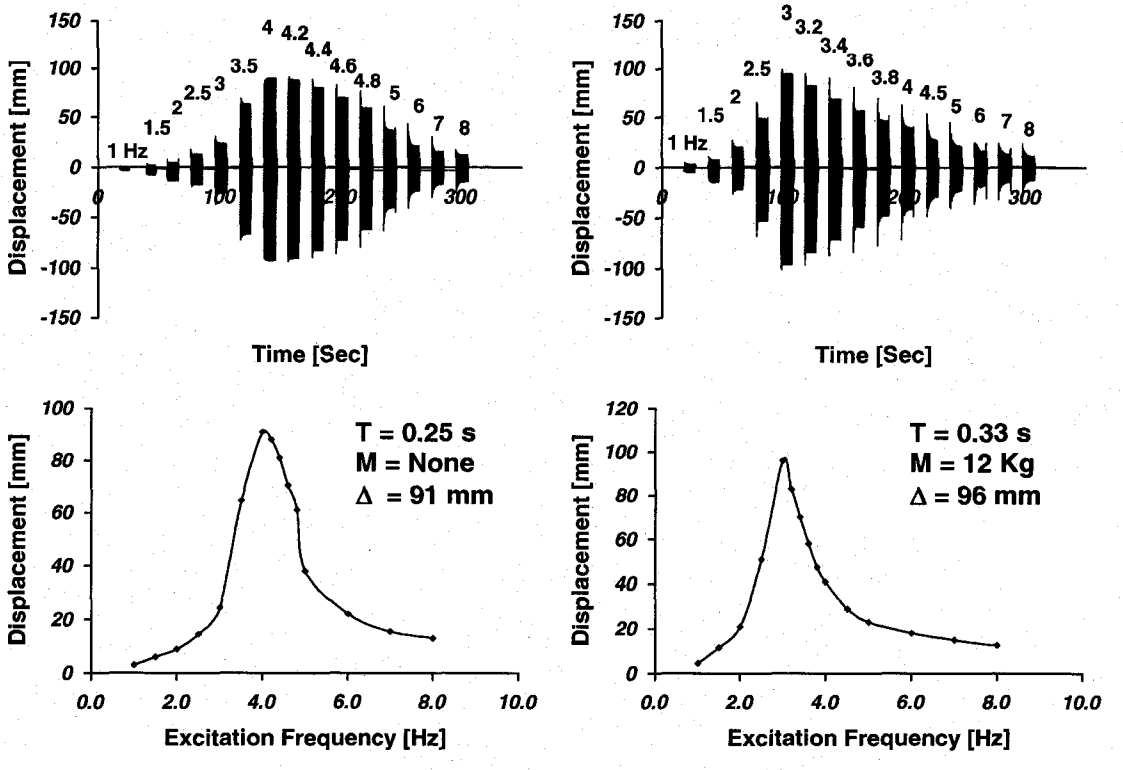

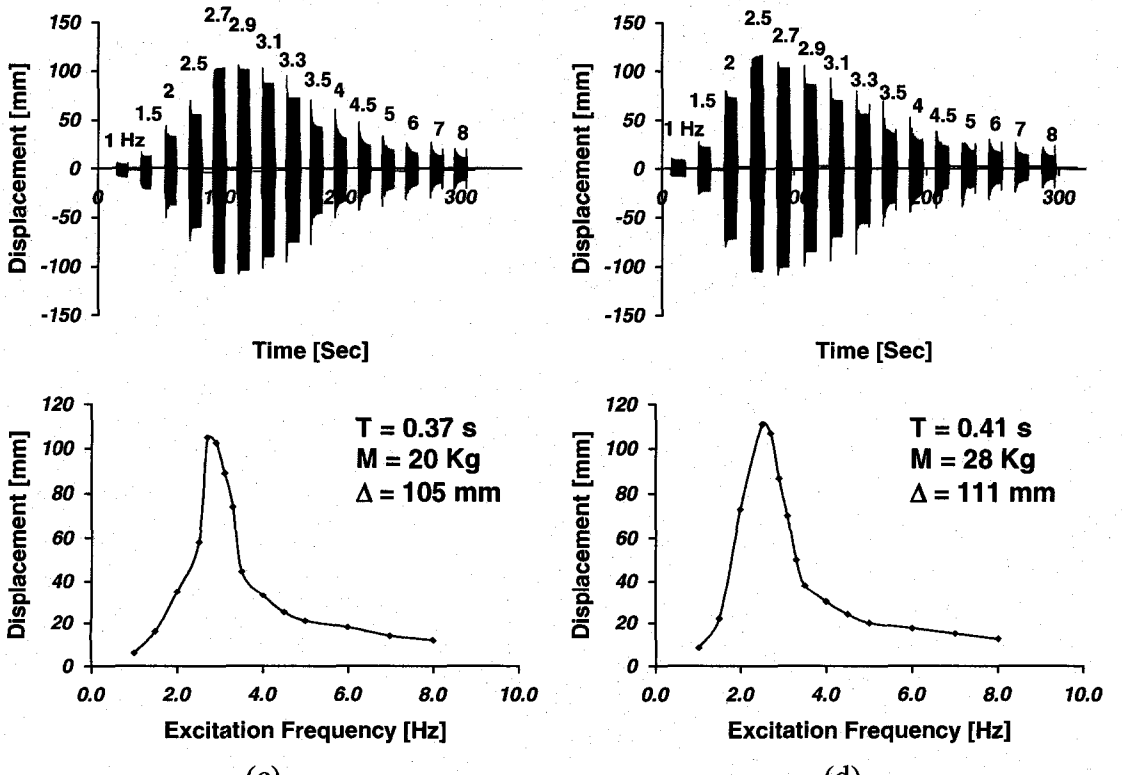

Fig. 4.8 Lateral displacement of Frame No.1 under sinusoidal excitation

Uncontrolled frame where the inactive actuator is connected via sliding bearing

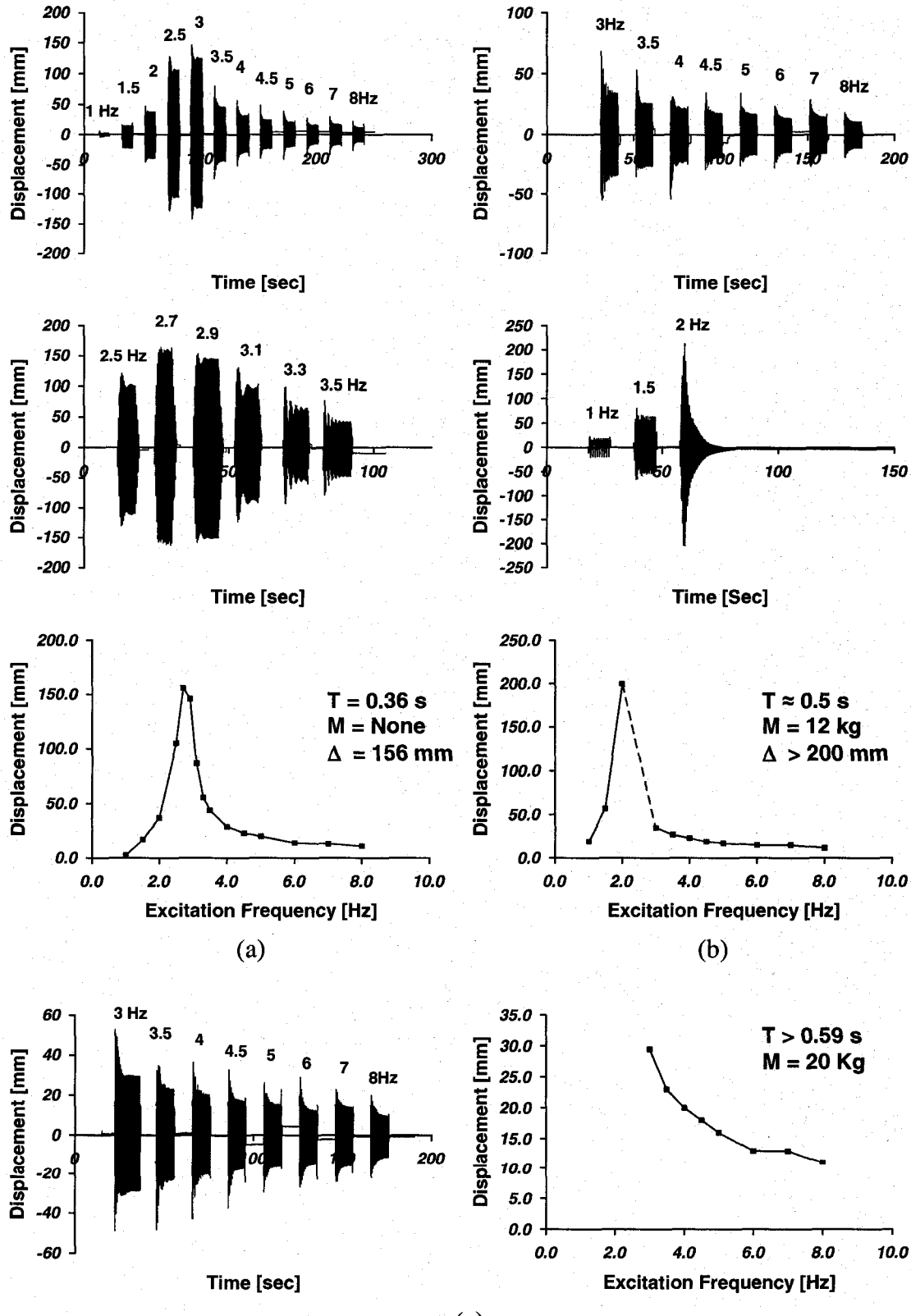

Fig. 4.9 Lateral displacement of Frame No.2 under sinusoidal excitation

Uncontrolled frame where the inactive actuator is connected via sliding bearing

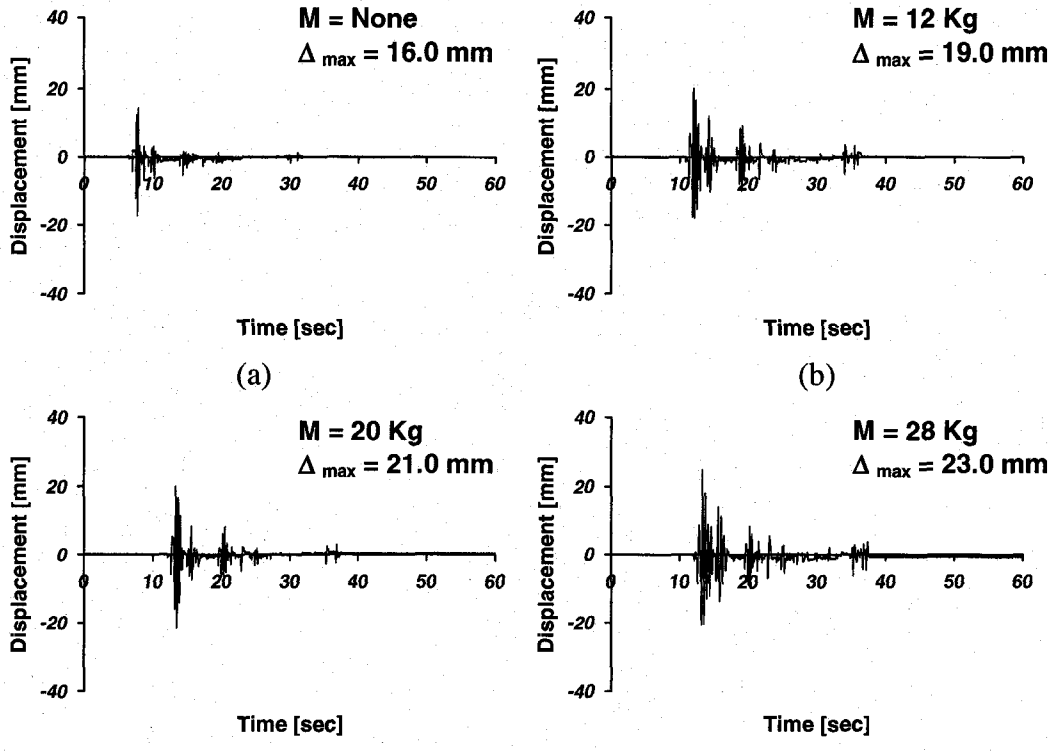

Fig. 4.10 Lateral displacement of Frame No.1 under El-Centro earthquake

Uncontrolled frame where the inactive actuator is connected via sliding bearing

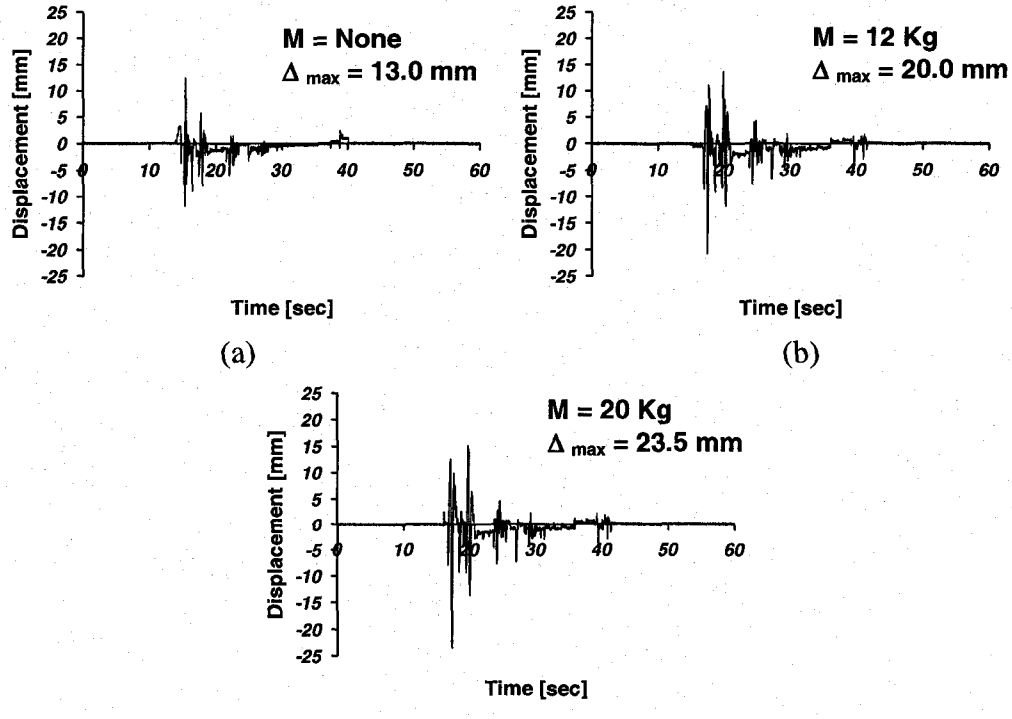

Fig. 4.11 Lateral displacement of Frame No.2 under El-Centro earthquake

Uncontrolled frame where the inactive actuator is connected via sliding bearing

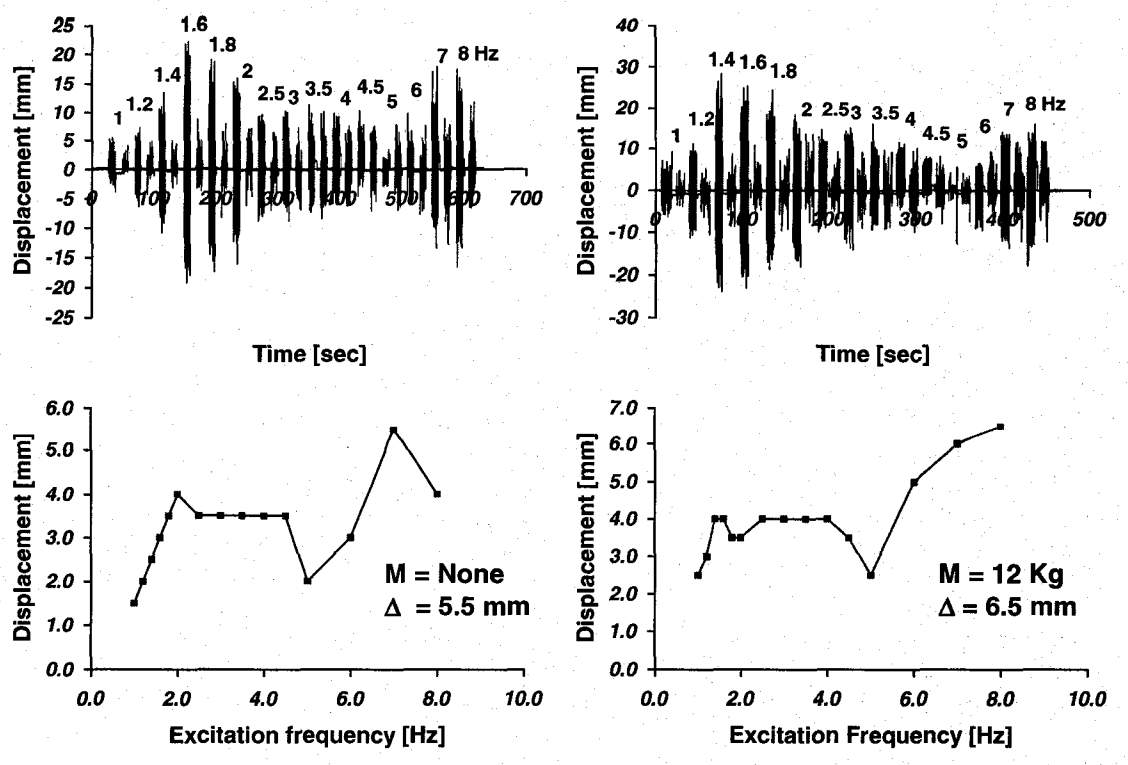

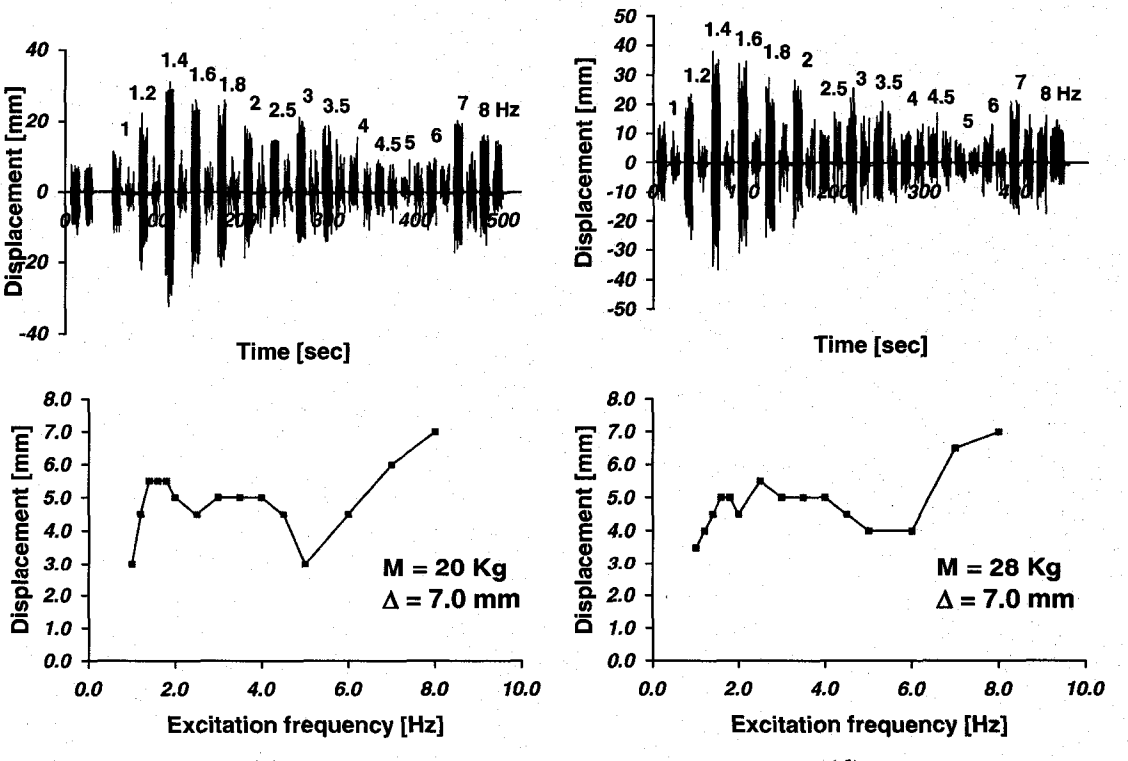

Fig. 4.12 Lateral displacement of Frame No.1 under sinusoidal excitation

Controlled frame

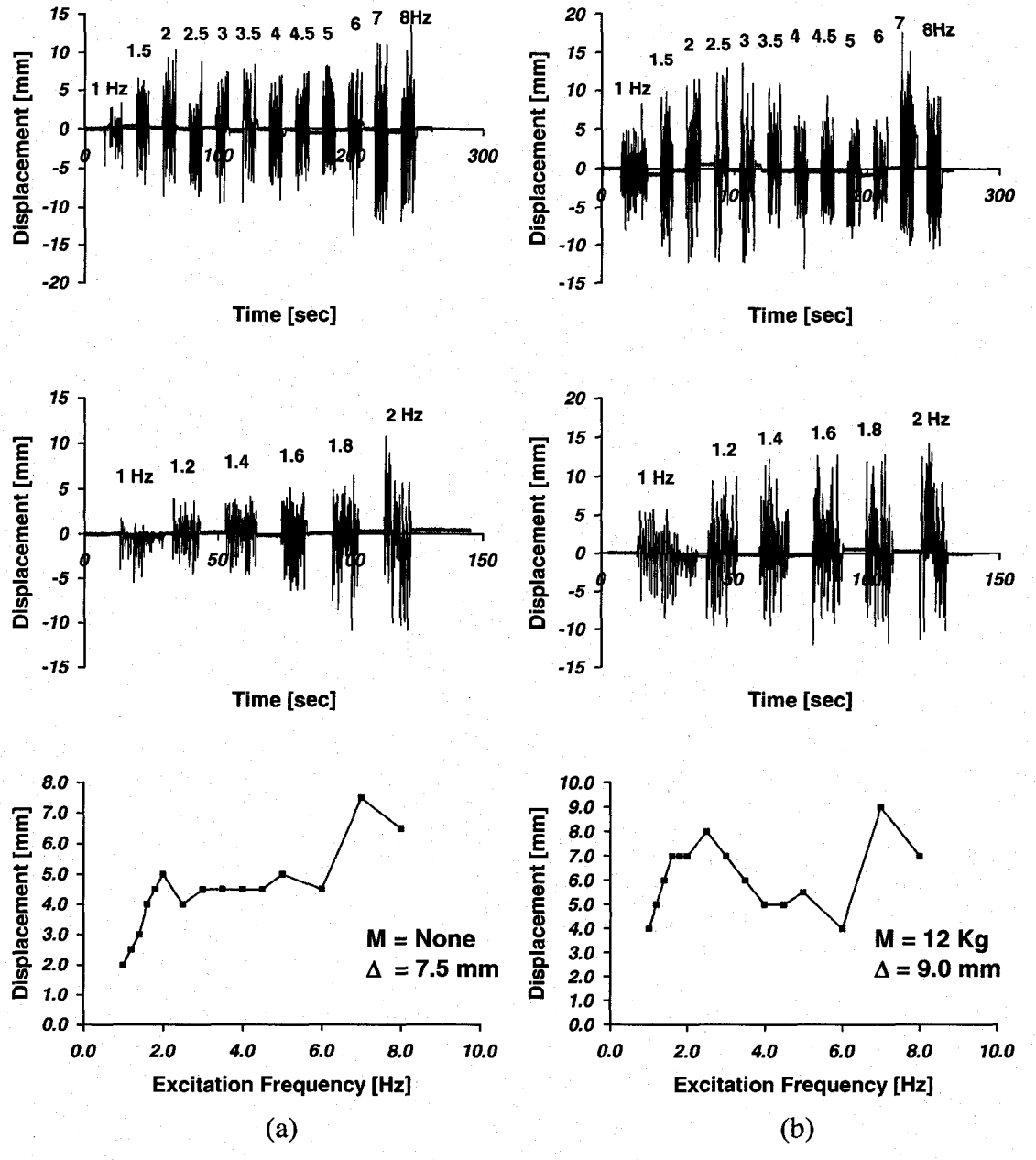

Fig. 4.13 Lateral displacement of Frame No.2 under sinusoidal excitation

Controlled frame

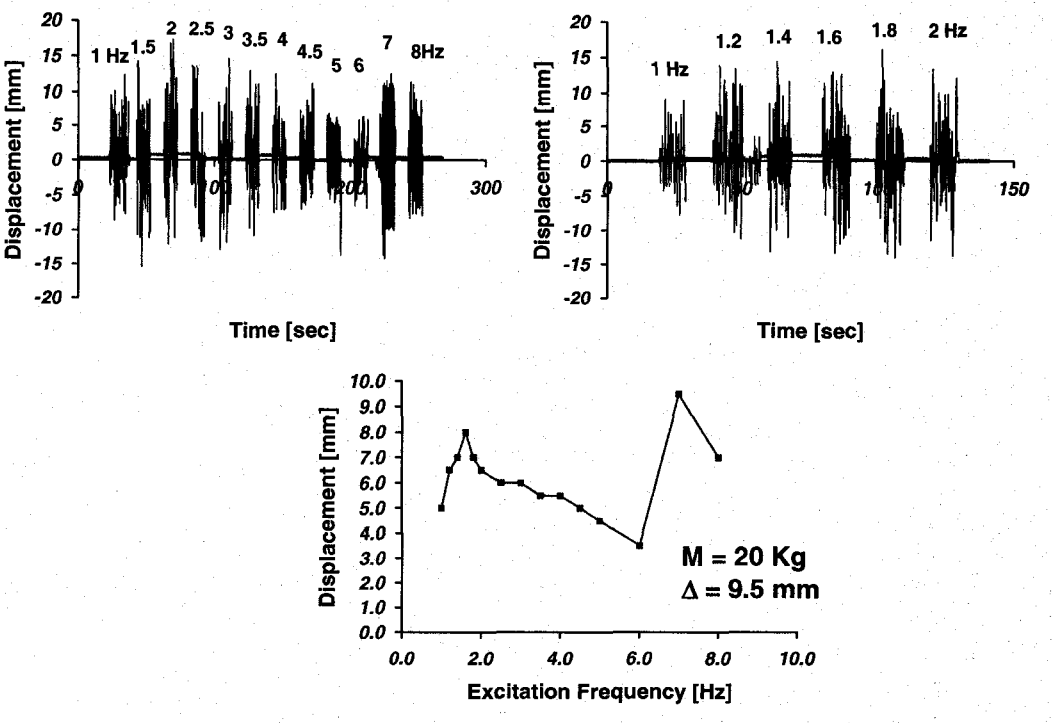

(c)

Fig 4.16 Lateral displacement of Frame No.2 under sinusoidal excitation Controlled frame (Cont'd)

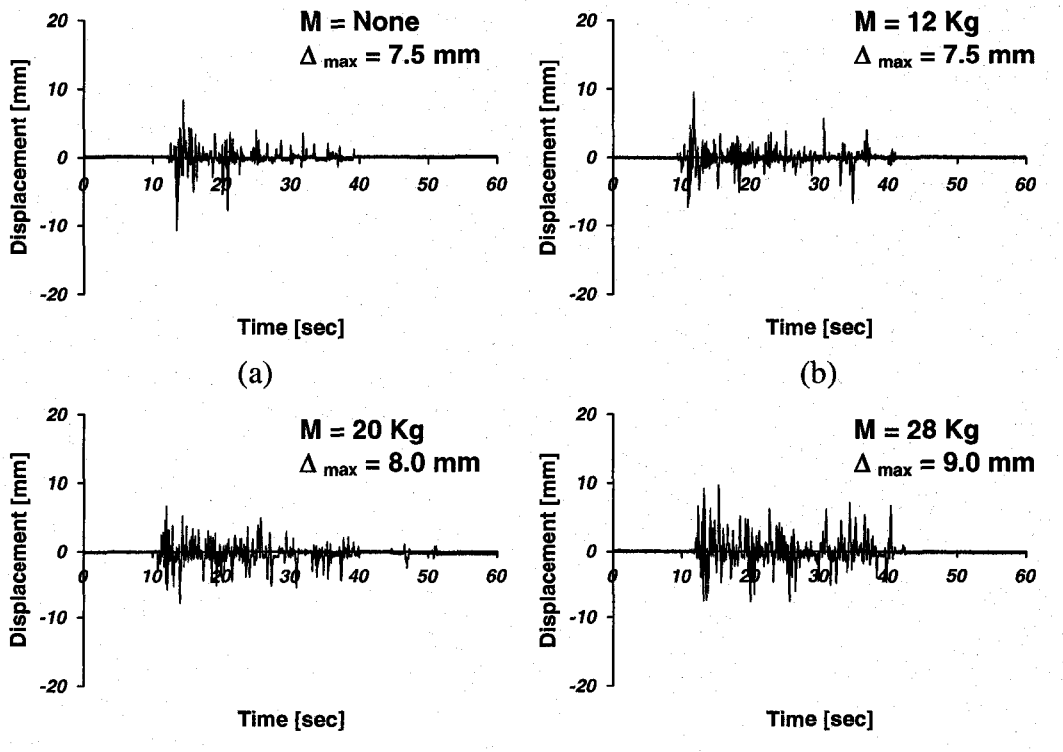

(a) (b)

(c) (d)

Fig. 4.14 Lateral displacement of Frame No.1 under El-Centro earthquake Controlled frame

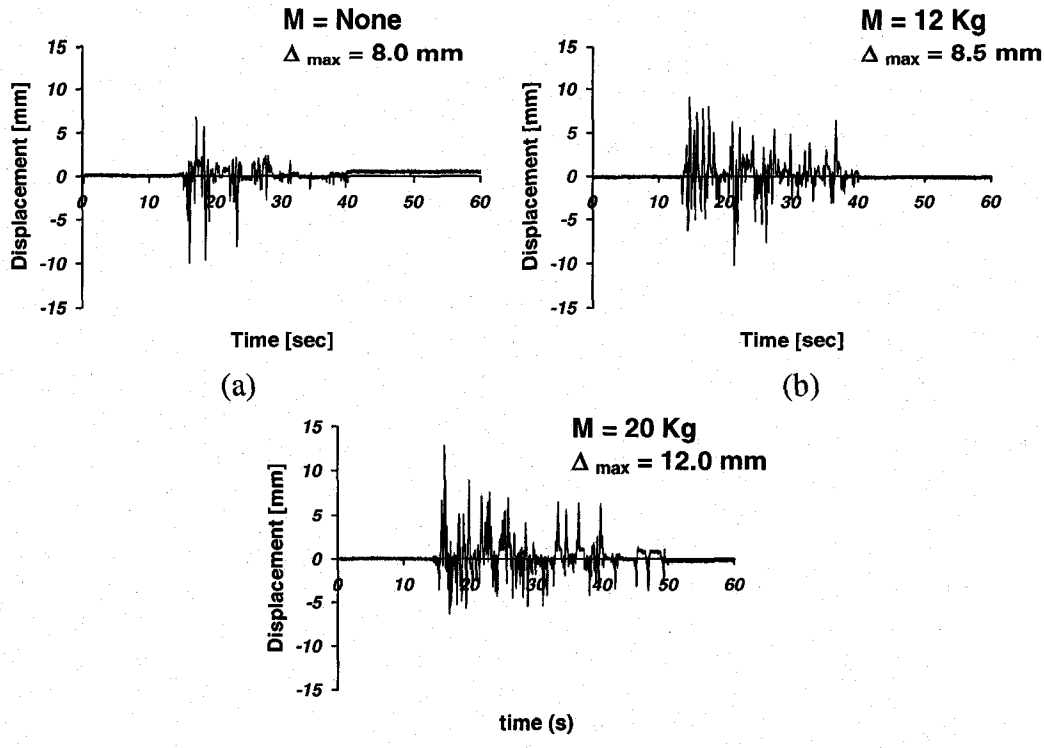

Fig. 4.15 Lateral displacement of Frame No.2 under El-Centro earthquake

Controlled frame

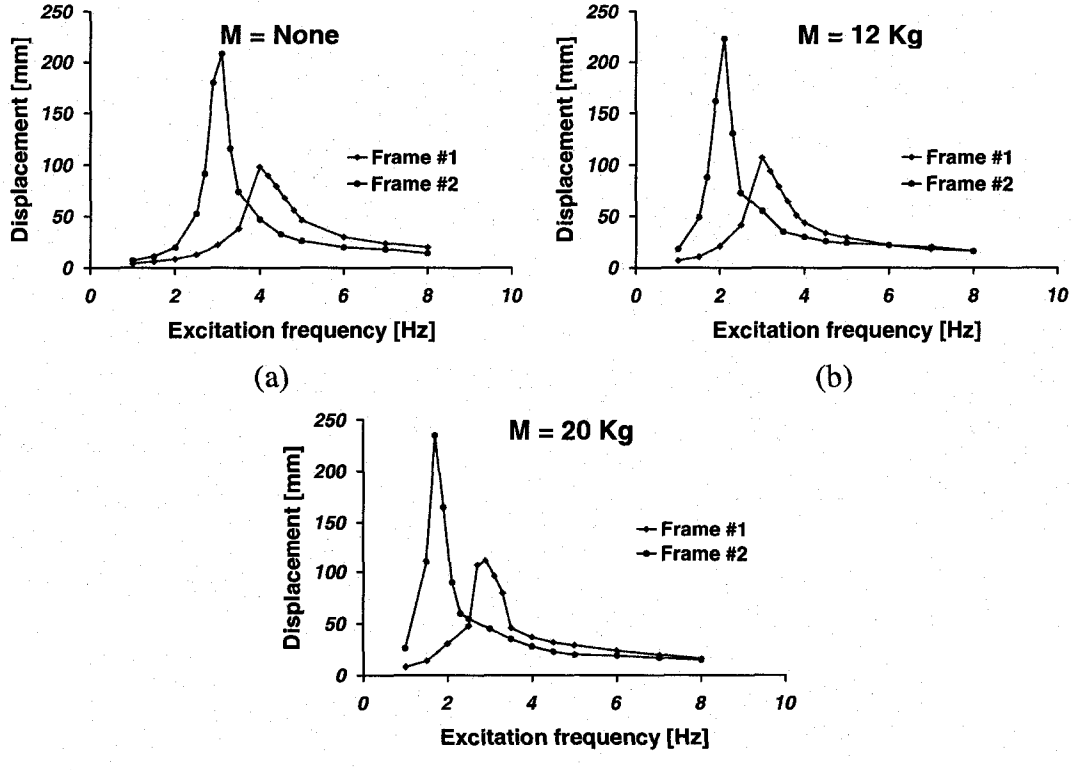

Fig. 4.16 Effect of stiffness on lateral displacement of frame

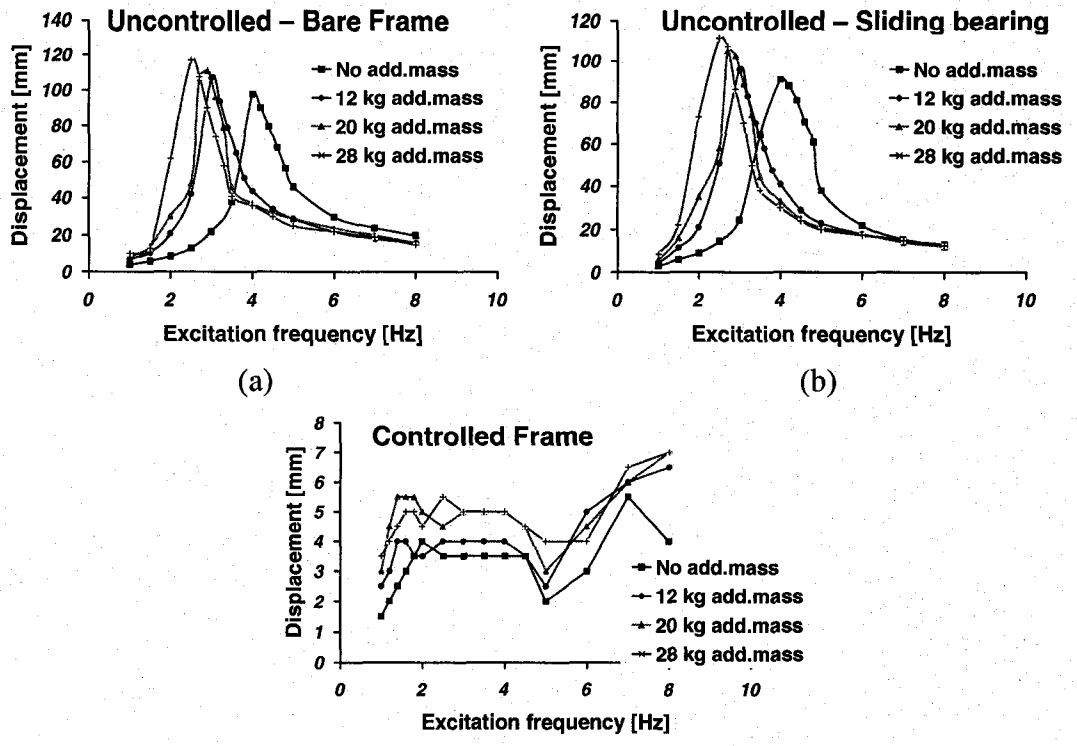

Fig. 4.20 Effect of mass on lateral displacement of Frame No. 1 under sinusoidal excitation

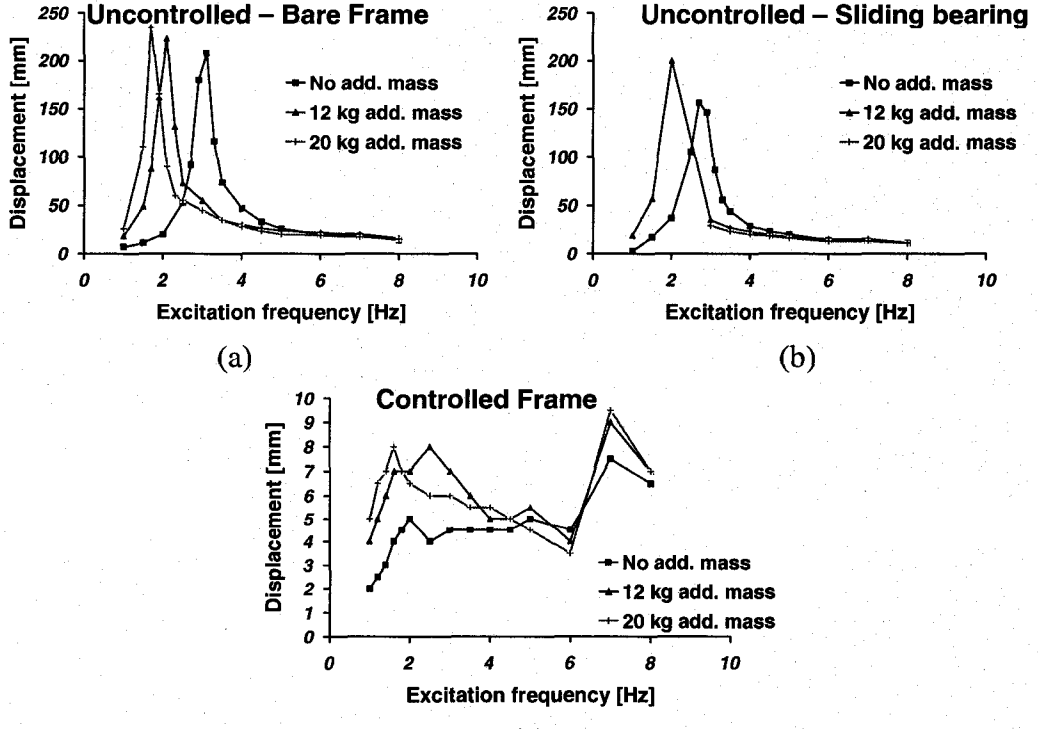

Fig. 4.17 Effect of mass on lateral displacement of Frame No. 2 under sinusoidal excitation

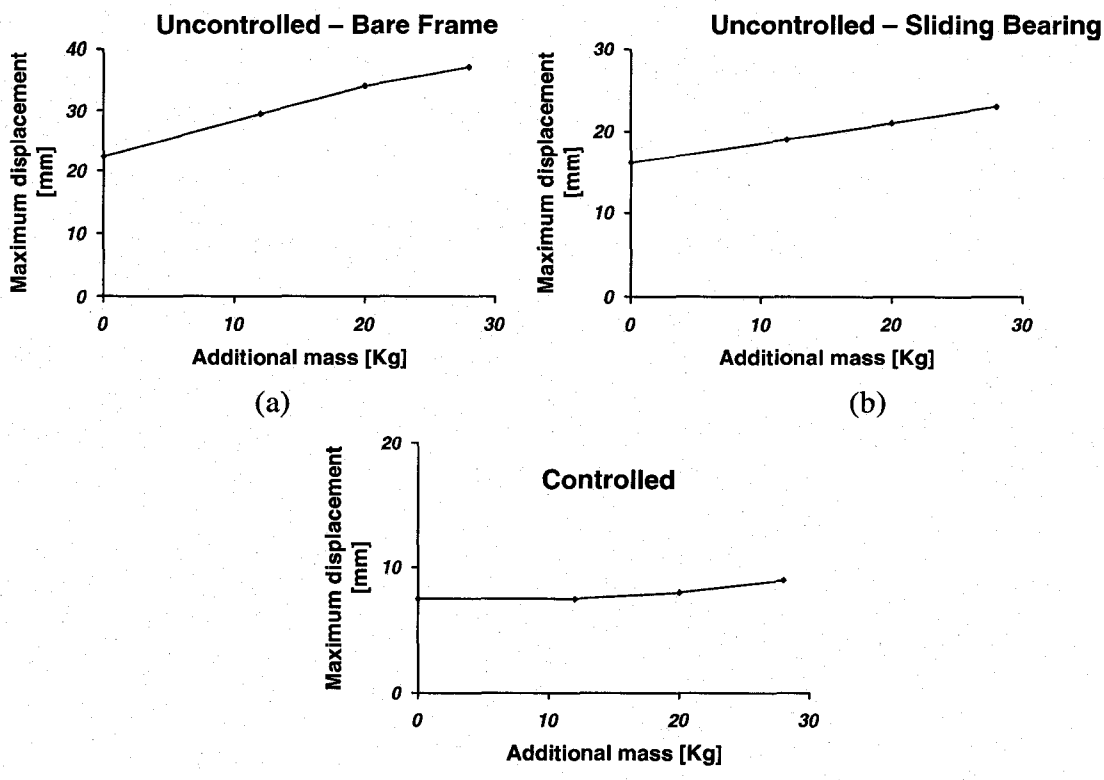

Fig. 4.18 Effect of mass on lateral displacement of Frame No. 1 under El-Centro earthquake

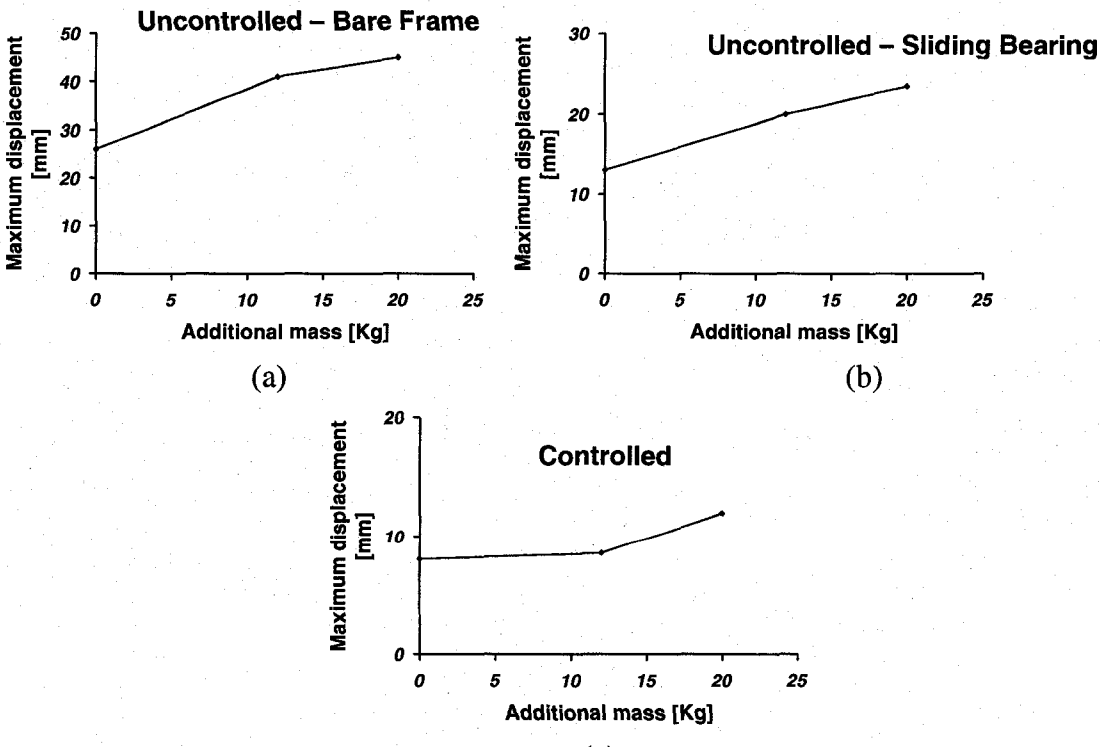

Fig. 4.19 Effect of mass on lateral displacement of Frame No. 2 under El-Centro Earthquake

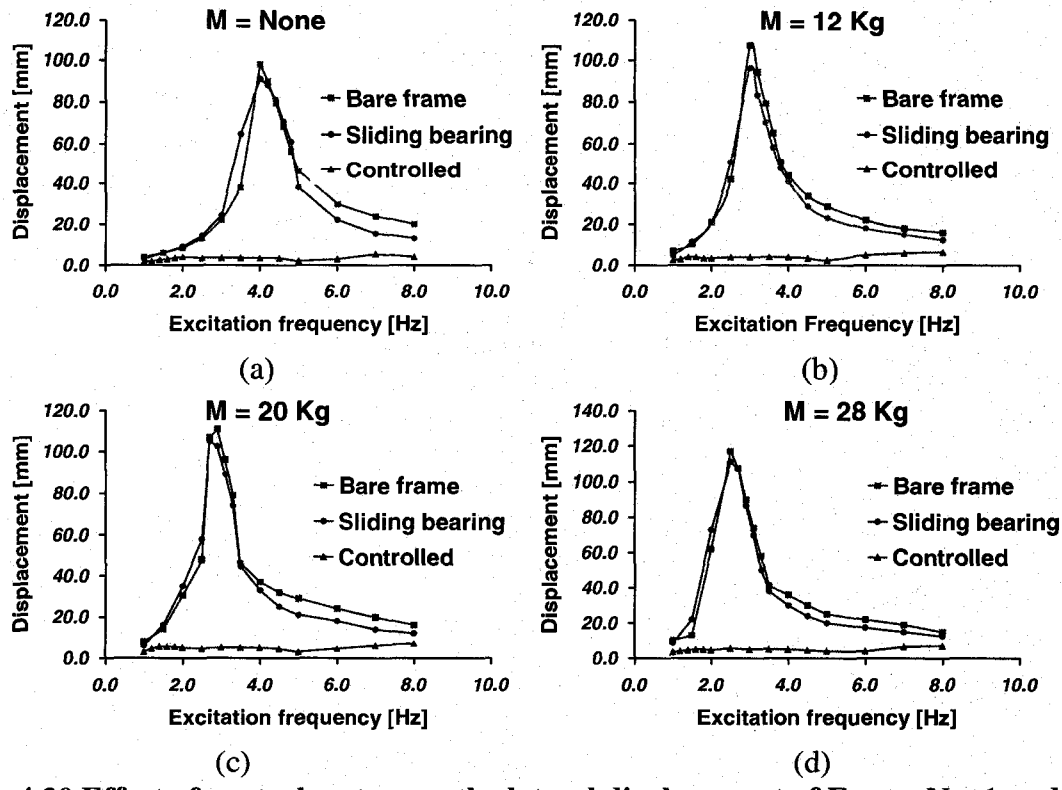

Fig. 4.20 Effect of control system on the lateral displacement of Frame No. 1 under sinusoidal excitation

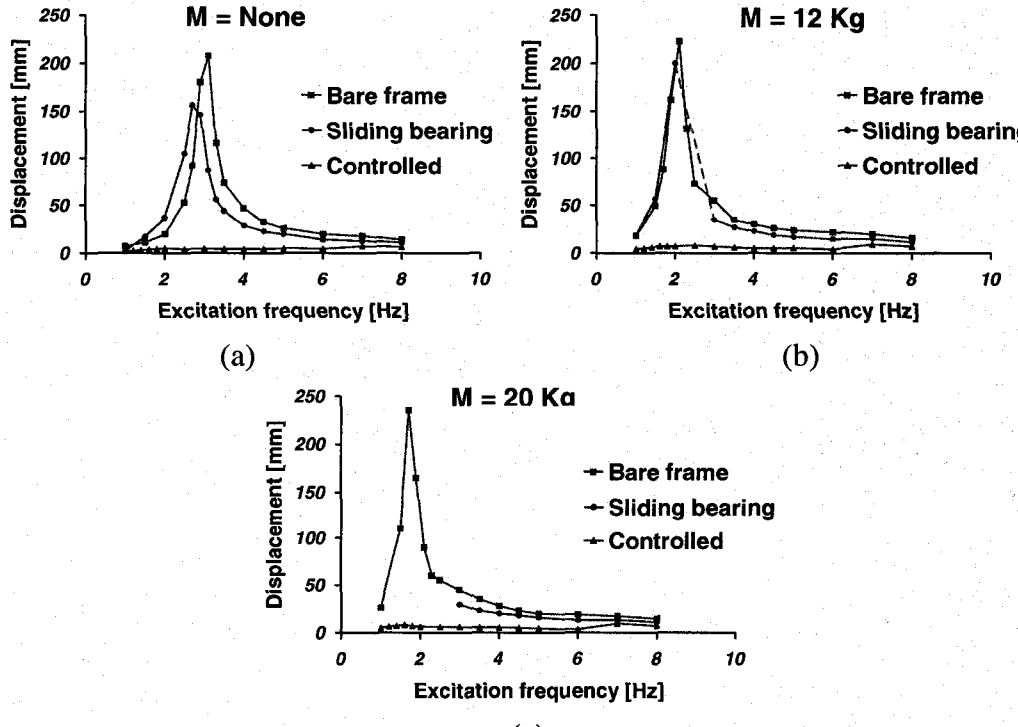

Fig. 4.21 Effect of control system on the lateral displacement of Frame No. 2 under sinusoidal excitation

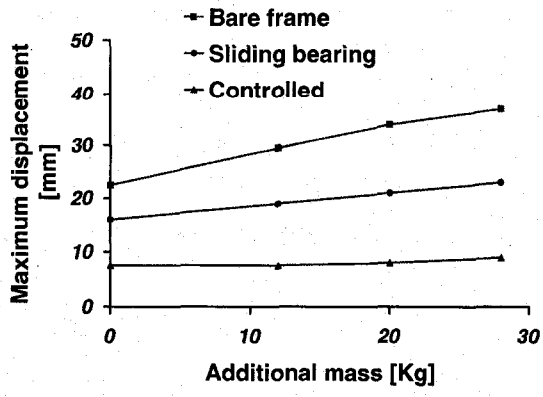

Fig. 4.22 Effect of control system on the lateral displacement of Frame No. 1 under El-Centro Earthquake

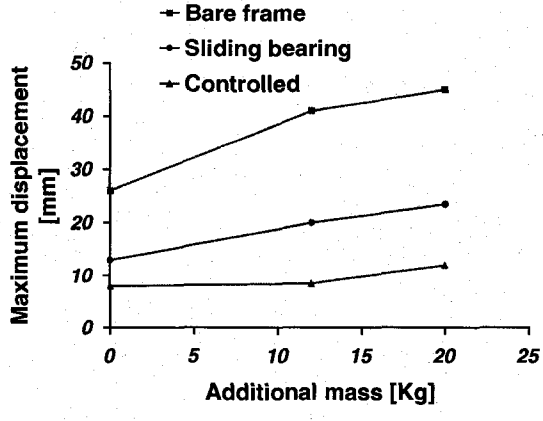

Fig. 4.23 Effect of control system on the lateral displacement of Frame No. 2 under El-Centro Earthquake

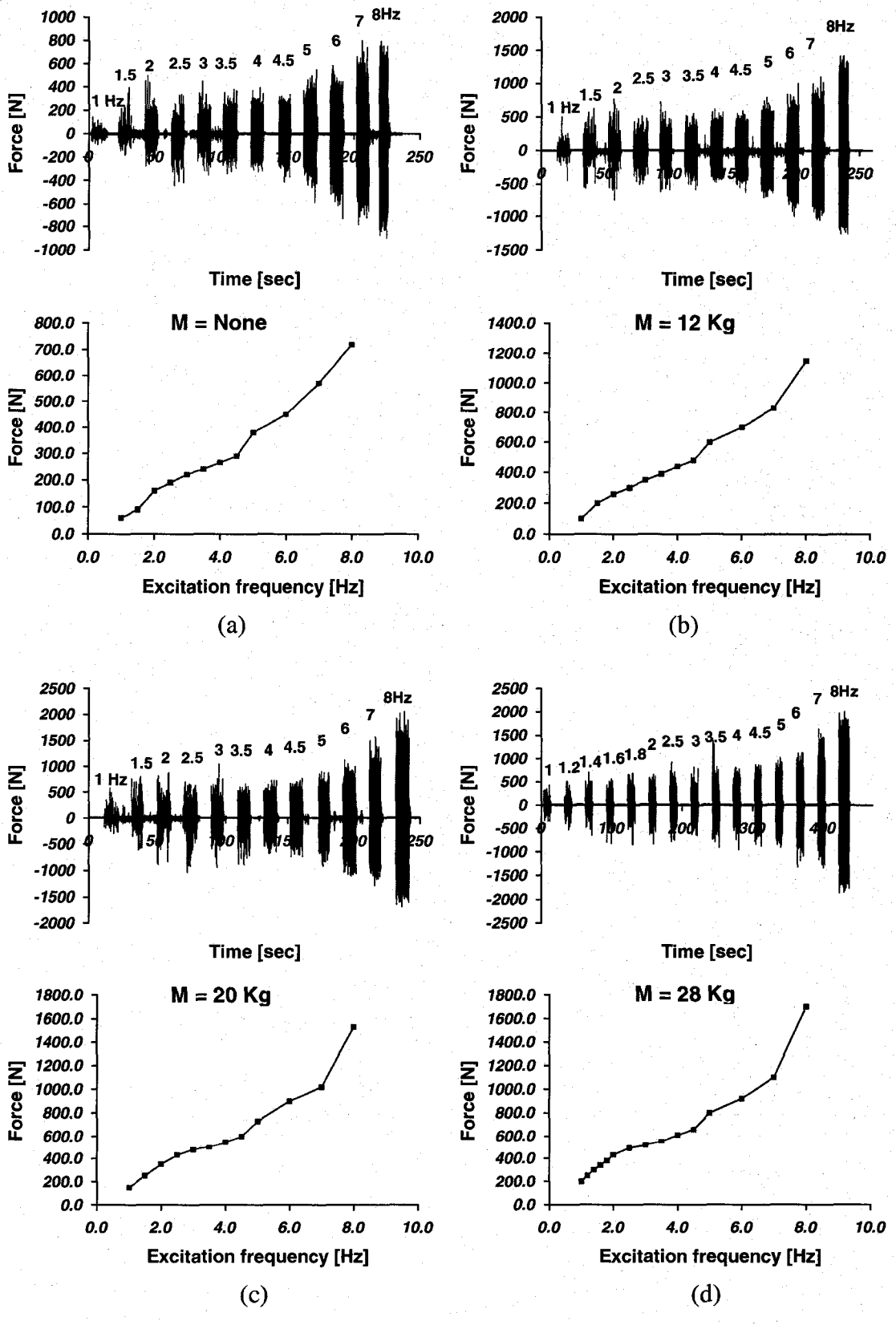

Fig. 4.24 Control forces of Frame No.1 under sinusoidal excitation

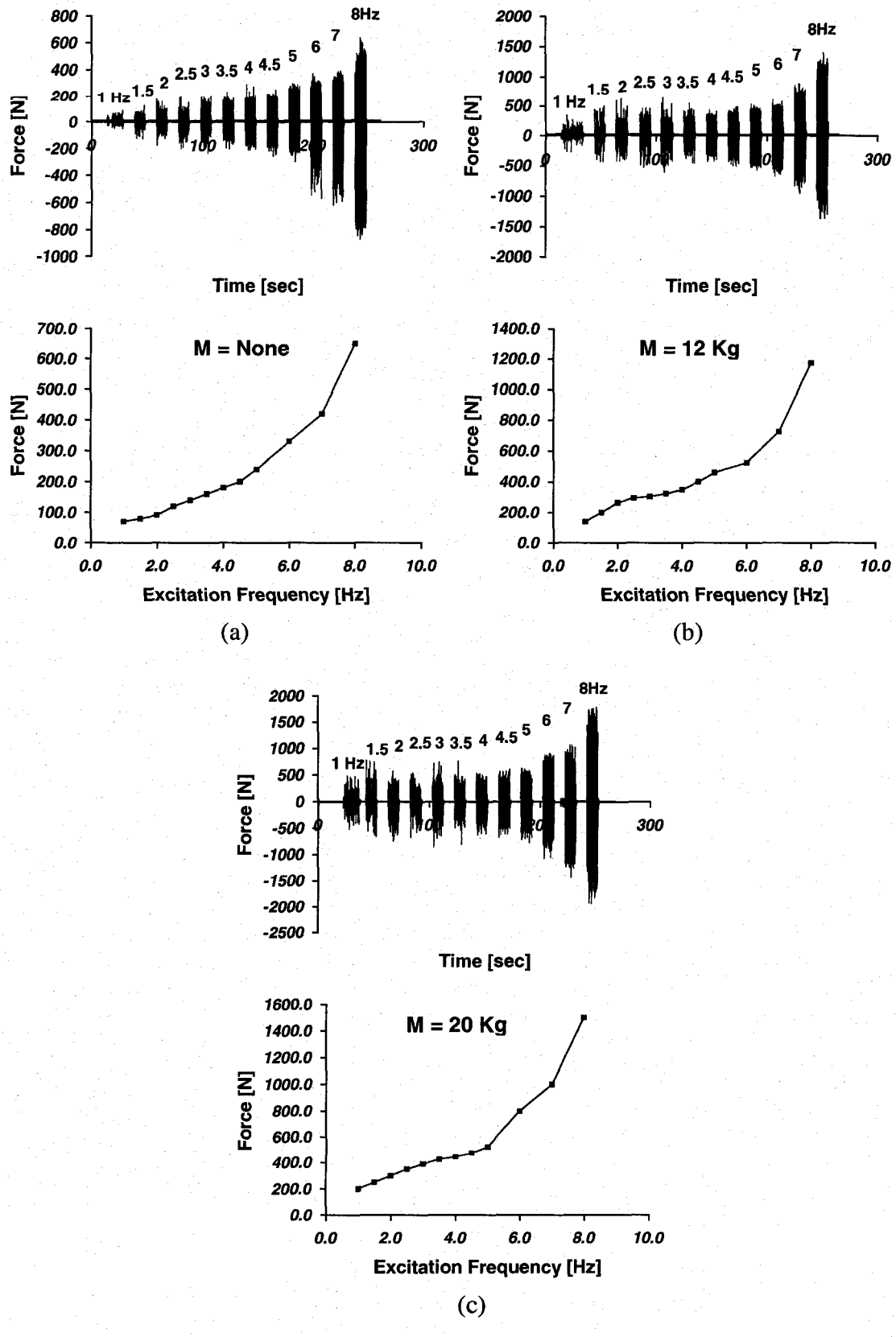

Fig. 4.25 Control forces of Frame No.2 under sinusoidal excitation

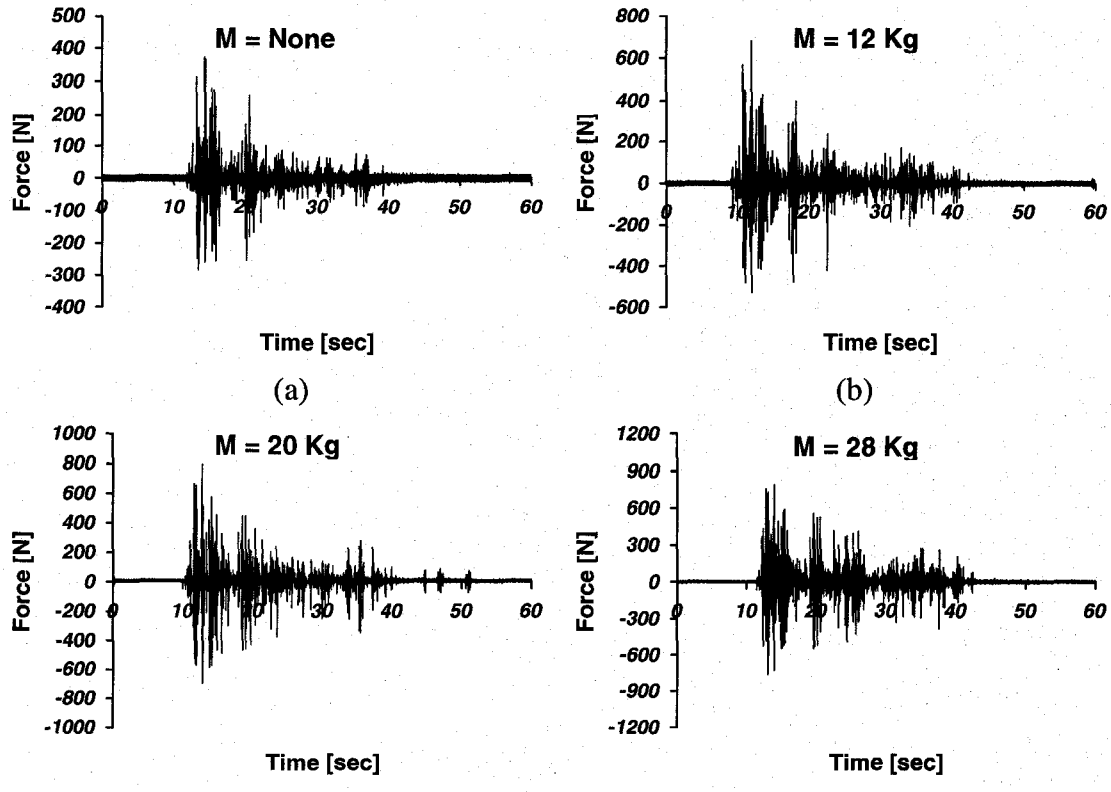

Fig. 4.30 Control forces of Frame No.1 under El-Centro Earthquake

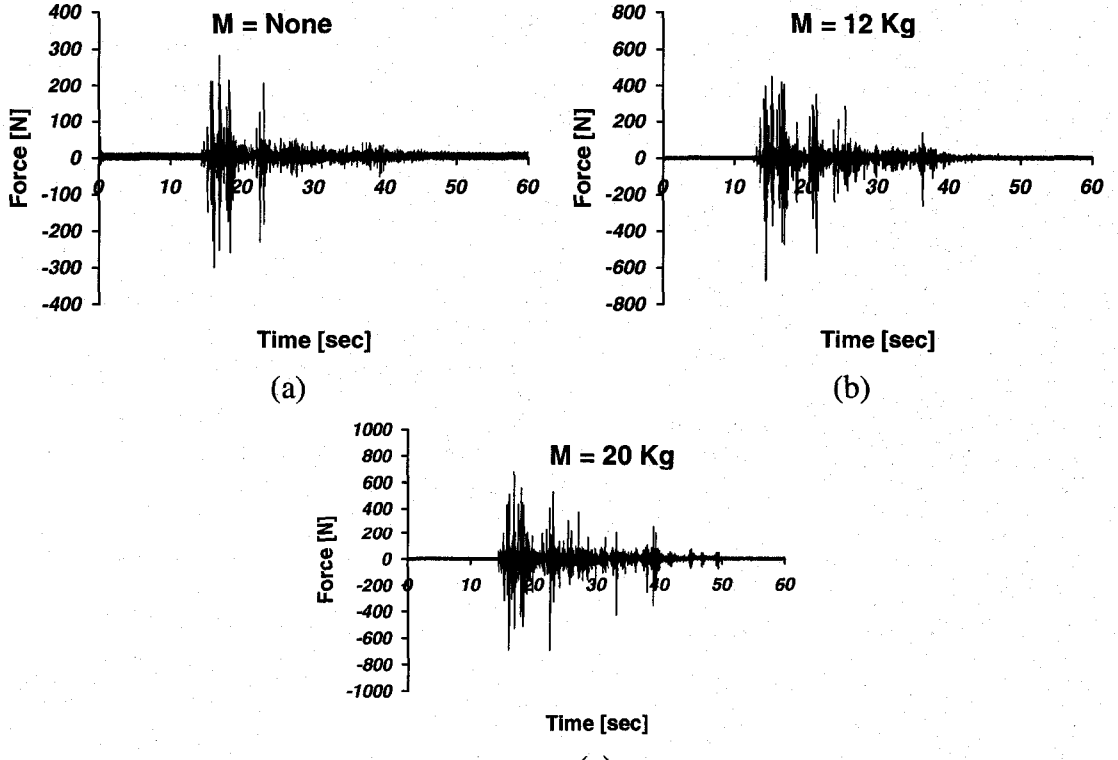

Fig. 4.26 Control forces of Frame No.2 under El-Centro Earthquake

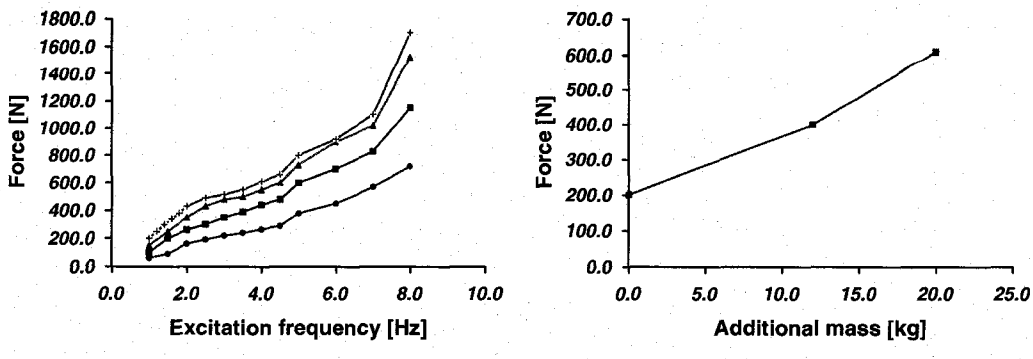

(a) (b)

Fig. 4.27 Effect of additional mass on control forces of Frame No. 1

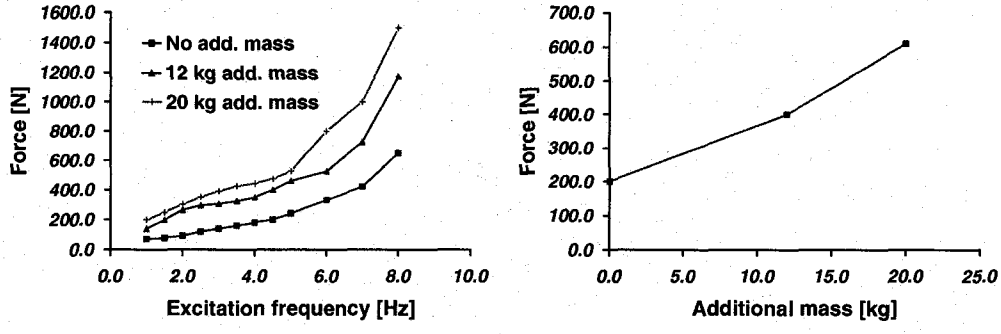

(a) (b)

Fig. 4.28 Effect of additional mass on control forces of Frame No. 2

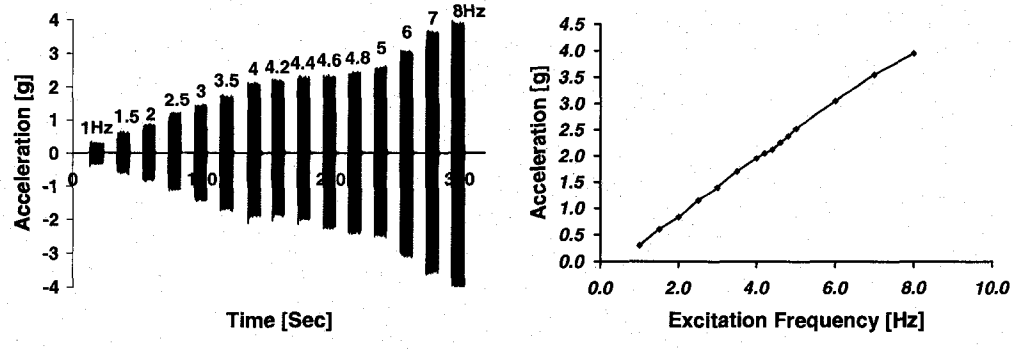

(a) (b)

Fig. 4.29 Shake-table acceleration record during sinusoidal excitation

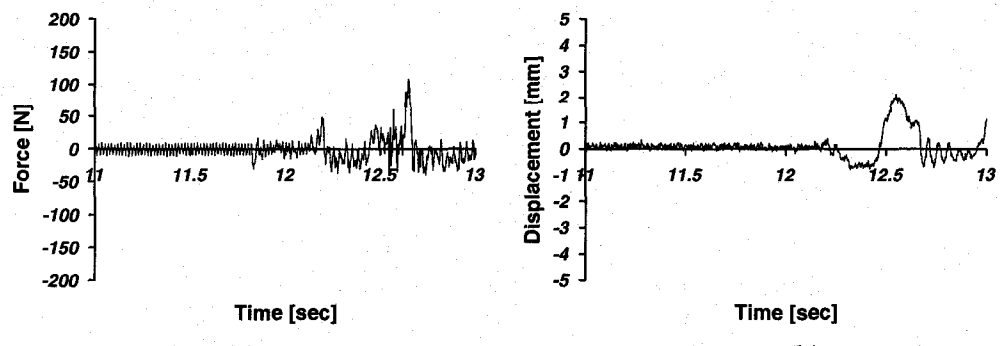

(a) (b)

Fig. 4.30 Shake-table acceleration record during sinusoidal excitation

CHAPTER 5

Summary and Conclusions

5.1 Summary

An experimental research program was undertaken to investigate the feasibility of pulse-generated active force control system for seismic retrofitting. Two single bay-single storey model frames were built and tested on a shake table. The dimensions of the model frames were selected based on a similitude model, representing a low-rise prototype frame building. Their performance, with and without active control, was investigated under sinusoidal excitations of different frequency and a previously recorded earthquake ground motion (the El-Centro 1940 N-S Earthquake Record, amplified three times). The test parameters included the effects of varying mass, stiffness, ground excitation characteristics, and control conditions. The natural periods of vibration of the test frames were increased by adding more sprung mass. The uncontrolled frames were tested in twice, first as bare frames and the second time with the control actuator in place (to include its mass) but inactive so that it would not react to the movements of the frames, with an attachment that allowed free movement. The structural response was monitored and recorded in terms of roof displacement history and the magnitude of control force, when present. The conclusions drawn from the test results are discussed in the following section.

5.2 Conclusions

The following conclusion can be drawn from the experimental research program reported in this thesis:

- There is an intimate relationship between the dynamic characteristics of the frame models tested and the frequency of excitation. The structures with natural frequencies that are significantly different than the frequency of excitation exhibited lower displacement and force response. As the frequency of excitation approached to that of the structure, a significant increase in displacements was observed due to the resonance phenomenon.
- The maximum displacements of frames increased with additional sprung mass. This was attributed to the increase in inertia forces. This was true for all frequencies, since the change in the natural frequency of the structure and its interaction with the frequency of excitation was not as significant as the change in the inertia force.
- For the structures considered, the maximum displacement response of the flexible structure was consistently higher than that of the rigid structure when they were excited at their respective natural frequencies.
- The uncontrolled frames with inactive actuators connected through sliding bearings developed slightly lower response as compared with those of bare frames without the actuators. This was attributed to the increase in damping of the frames with actuators, even though the associated increase in mass attracted higher inertia forces. The frames with inactive actuators also showed lower natural frequencies because of the increased mass.
- The pulse control system employed was very effective in reducing seismic response of structures. The reductions in displacement response were approximately 90% for structures subjected to sinusoidal excitation and 65% to 80% when subjected to three times the 1940 El Centro N-S Record depending on the magnitude of mass.
- The magnitude of control forces changed with the amount of mass placed on the roof. For the model frames considered, the control force showed a variation between approximately 200 N and 600 N when the frames were subjected to three

times the 1940 El Centro Earthquake, N-S Record. The same trend was also observed in frames subjected to sinusoidal excitation. In this case, however the force level was higher since the ground acceleration was higher, reaching up to 4g.

- The pulse control system can be used effectively in seismic retrofit applications.

5.3 Recommendations for Future Research

The following recommendations are made for future research:

- More research is needed to investigate the performance of a pulse-generated active seismic control on large-scale specimens.
- The effect of different zero-range on test results should be investigated. Selecting different zero-ranges will lead to completely different control philosophies. For example, defining a zero-range such that the frame is allowed to move freely within the elastic range can be a viable option which will allow the reduction in force demands associated with structural stiffening due to seismic retrofit.
- Analytical models and computer programs need to be developed to calculate the effects of pulse-control system on structures.
- Further analytical research is needed to extend the results of the small-scale shake table tests conducted in the current investigation to full-scale buildings in practice.

References:

- Abdel-Rohman, M., (1983), "Control of tall buildings response by aerodynamic appendages.", *Journal of Wind Engineering and Industrial Aerodynamics,* 13 (1-3), pp. 253-260.

- Abdel-Rohman, M., (1984), "Optimal control of tall buildings by appendages.", *Journal of Structural Engineering*, 110 (5), pp. 937-947.

- Abdel-Rohman, M., (1987), "Feasibility of active control of tall buildings against wind.", *ASCE Journal of Structural Engineering,* 113, pp.349-362.

- Abdel-Rohman, M. and Leipholz, H. H., (1978), "Structural control by pole assignment method", *ASCE Journal of Engineering Mechanics*, Vol. 104, pp. 1157-1175.

- Abdel-Rohman, M. and Leipholz, H. H., (1983), "Active control of tall buildings.", *ASCE Journal of Structural Engineering,* 109, pp. 628-645.

- Abe, M., Kimura, S., Fujino, Y., (1996), "Control laws for semiactive tuned liquid column dampers with variable orifice openings", *Proceedingsof the 2nd International Workshop on Structural Control.*

- Ahlawat, A.S., Ramaswamy, A., (2001), "Multiobjective optimal structural vibration control using fuzzy logic control system", *Journal of Structural Engineering*, 127 (11), pp. 1330-1337.

- Ahlawat, A.S., Ramaswamy, A., (2002), "Multi-objective optimal design of FLC driven hybrid mass damper for seismically excited structures", *Earthquake Engineering and Structural Dynamics*, 31 (7), pp. 1459-1479.

- Ahlawat, A.S., Ramaswamy, A., (2004), "Multiobjective optimal fuzzy logic control system for response control of wind-excited tall buildings", *Journal of Engineering Mechanics*, 130 (4), pp. 524-530.

- Akbay, Z., Aktan, H.M., (1991), "Actively regulated friction slip devices", *Proceedings of 6th Canadian Conference of Earthquake Engineering*, pp. 367-374.

- Agrawal, A.K., Yang, J.N., Wu, J.C., (1998), "Non-linear control strategies for duffing systems", *International Journal of Non-Linear Mechanics*, 33 (5), pp. 829-841.

- Alt, T.R., Jabbari, F., Yang, J.N., (2000), "Control design for seismically excited buildings: Sensor and actuator reliability", *Earthquake Engineering and Structural Dynamics*, 29 (2), pp. 241-257.

- Ankireddi, S., Yang, H.T.Y., (1996), "Simple ATMD control methodology for tall buildings subject to wind loads", *Journal of Structural Engineering*, 122 (1), pp. 83-91.

- Arco, D.C.D., Aparicio, A.C., (1999), "Improving suspension bridge wind stability with aerodynamic appendages", *Journal of Structural Engineering,* 125 (12), pp. 1367-1375.

- Arco, D.C.D., Aparicio, A.C., (2002), "Improving the wind stability of suspension bridges during construction", *Journal of Structural Engineering*, 127 (8), pp. 869-875.

- Bai, Y., Grigoriadis, K.M., (2005), "H∞ collocated control of structural systems: An analytical bound approach", *Journal of Guidance, Control, and Dynamics*, 28 (5), pp. 850-853.

- Baruh, H., and Meirovitch, L., (1982), "Implementation of the IMSC method by means of a varying number of actuators", *AIAA / AAS / Astrodynamic Conference, San Diego, CA, USA*, Paper No. 82-1035.

- Battaini, M., Casciati, F., Faravelli, L., (1998), "Fuzzy control of structural vibration. An active mass system driven by a fuzzy controller", *Earthquake Engineering and Structural Dynamics*, 27 (11), pp. 1267-1276.

- Betti, R., Panariello, G.F., (1995), "Active tendon control systems for structures subjected to multiple support excitation", *Smart Materials and Structures*, 4 (3), pp. 153-163.

- Buckle, I.G., and Mayes, R.L., (1990), "Seismic isolation history, application, and performance – a would view.", *Earthquake Spectra*, 6, pp. 161–201.

- Carotti, A., DeMiranda, M., and Turci, E., (1987), "An active protection system for wind induced vibrations on pipeline suspension bridge.", *In Leipholz H H E(ed) Structural Control, North Holland, Amsterdam,* pp.76-104.

- Carlson, J.D., Spencer Jr., B.F., (1996), "Magneto-rheological fluid dampers for semi-active seismic control", *Proceedings of 3rd International Conference on Motion and Vibration Control*, 3, pp. 35-40.

- Cao, H., Reinhorn, A.M., Soong, T.T., (1998), "Design of an active mass damper for a tall TV tower in Nanjing, China", *Engineering Structures*, 20 (3), pp. 134-143.

- Chang, C.H., and Soong, T.T., (1980), "Structural control using active tuned mass dampers", *Journal of Engineering Mechanics,* 106 EM6, pp. 1091-1098.

- Chang, J.C.H., and Soong, T.T., (1980), "Use of aerodynamic appendages for tall building control.", *In Leipholz H H E(ed) Structural Control, North Holland, Amsterdam,* pp. 199-210.

- Chang, C.C., Yang, Henry T.Y., (1995), "Control of buildings using active tuned mass dampers", *Journal of Engineering Mechanics*, 121 (3), pp. 355-366.

- Chase, J.G., Smith, H.A., (1996), "Robust H∞ control considering actuator saturation. I: Theory", *Journal of Engineering Mechanics* 122 (10), pp. 976-983.

- Cherry, S., (1994), "Research on friction damping at the University of British Columbia", *Proceedings of International Workshop on Structural Control*, pp. 84-91.

- Chung, L.L., Reinhorn, A.M., and Soong, T.T., (1986), "An expermintal study of active structural control.", *In Hart GC and Nelson R B (eds) Dynamic Response of Structures ASCE, New York,* pp. 795-802.

- Chung, L.L., Reinhorn, A.M., and Soong, T.T., (1988), "Experiments on active control of seismic structures.", *ASCE Journal of Engineering Mechanics,* 114, pp. 241-256.

- Collins, R., Basu, B., Broderick, B., (2006), "Control strategy using bang-bang and minimax principle for FRF with ATMDs", *Engineering Structures*, 28 (3), pp. 349-356

- Dowdell, D.J., Cherry, S., (1994), "Structural control using semiactive friction dampers", *Proceedings of First World Conference on Structural Control*, pp. 59-68.

- Doyle, J., Glover, K., Khargonekar, P., Francis, B., (1988), "State-space solutions to standard H and H control problems.", *Proceedings of the American Control Conference*, 88 pt 1-3, pp. 1691-1696.

- Du, H., Lam, J., Sze, K.Y., (2005), "Non-fragile H∞ vibration control for uncertain structural systems ", *Journal of Sound and Vibration*, 273 (4-5), pp. 1031-1045.

- Dyke, S.J., Spencer, Jr., B.F., Quest, P., Kaspari, Jr., D.C., Sain, M.K., (1994), "Implementation of an AMD using acceleration feedback control", *Microcomputers in Civil Engineering: Special Issue on Active and Hybrid Structural Control.*

- Dyke, S.J., Spencer Jr., B.F., Jr.,Sain, M.K., and Carlson, J.D., (1996), "Modeling and control of magnetorheological dampers for seismic response reduction.", *Smart Materials and Structures*, 5 (5), pp. 565-575.

- Dyke, S.J., Spencer Jr., B.F., Sain, M.K., Carlson, J.D., (1998), "An experimental study of MR dampers for seismic protection", *Smart Materials and Structures*, 7 (5), pp. 693-703.

- Feng, Q. and Shinozuka, M., (1990), "Use of a Variable Damper for Hybrid Control of Bridge Response under Earthquake.", *Proceedings of U.S. National*

Workshop on Structural Control Research., USC Publication No. CE-9013, 107–112.

- Feng, M. Q., Shinozuka, M., and Fujii, S., (1993), "Friction-controllable sliding isolation system", *Journal of Engineering Mechanics*, 119 (9), pp. 1845-1864.

- Garrett, G.T., Chen, G., Cheng, F.Y., Huebner, W., (2001), "Experimental characterization of piezoelectric friction dampers", *Proceedings of 8th SPIE Annual Conference on Smart Structures and Material (SPIE: International Society for Optical Engineering, Bellingham, Washington, United States).*

- Gavin, H., Hoagg, J., Dohossy, M., (2001), "Optimal design of MR Dampers", *Proceedings of U.S.-Japan Workshop on Smart Structures for Improved Seismic Performance in Urban Regions*, pp. 225-236.

- Glover, Keith, Doyle, John C., (1988), "State-Space Formulae for all Stabilizing Controllers that Satisfy an H infinity – Norm Bound and Relations to Risk Sensitivity.", *Systems and Control Letters*, 11 (3), pp. 167-172.

- Guclu, R., Sertbas, A., (2005), "Evaluation of sliding mode and proportional-integral-derivative controlled structures with an active mass damper", *JVC/Journal of Vibration and Control*, 11 (3), pp. 397-406.

- Hall, J. F., ed., (1995), "Northridge earthquake of January 17, 1994 reconnaissance report.", *Earthquake Spectra*, 11, Supplement C, Vol. 1.

- Haroun, M.A., Pires, J.A., Won, A., (1994), "Active orifice control in hybrid liquid column dampers", *Proceedings of First World Conference on Structural Control*, pp. 69-78.

- Heaton, T. H., Hall, J. F., Wald, D. J., and Halling, M. V., (1995), "Response of high-rise and base-isolated buildings in a hypothetical Mw 7.0 blind thrust earthquake.", *Science,* 267, pp. 206–211.

- Hiemenz, G.J., Choi, Y.T., Wereley, N.M., (2003), "Seismic control of civil structures utilizing semi-active MR braces", *Computer-Aided Civil and Infrastructure Engineering*, 18 (1), pp. 31-44.

- Hollot, C.V., Barmish, B.R., (1980), "Optimal quadratic stability of uncertain linear systems", *Proceedings of 18th Allerton Conference.*

- Housner, G.W., Bergman, L.A., Caughey, T.K., Chassiakos, A.G., Claus, R.O., Masri, S.F., Skelton, R.E., Soong, T.T., Spencer, B.F., Yao, J.T.P., (1997), "Structural control: Past, present and future.", *Journal of Engineering Mechanics*, 123 (9), pp. 897–971.

- Hrovat, Davorin, Barak, Pinhas, Rabins, Michael, (1983), "semi-active versus passive of active tuned mass dampers for structural control.", *Journal of Engineering Mechanics*, 109 (3), pp. 691-705.

- Iemura, H., and Izuno, K.,(1994), "Development of the Self-Oscillating TMD and Shaking Table Tests,", *Proceedings of 1st World Conference on Structural Control, Los Angeles, California,* pp. WP2:42–51.

- Iiba, M., (1994), "Shaking table test on seismic response control system by fuzzy optimal logic", *Proceedings of 1st World Conference on Structural Control*, 1, pp. 69-77.

- Imazeki, Masanori, Tanida, Koji, Mutaguchi, Masao, Koike, Yuji, Murata, Tamotsu, Kobori, Takuji, Yamada, Tosikazu, (...), Ohrui, Satoshi, (1995), "Development of V-shaped hybrid mass damper and its application to high-rise

buildings", *American Society of Mechanical Engineers, Design Engineering Division (Publication) DE 84 (3 Pt C).*

- Inaudi, J.A., (1997), "Analysis of hysteretic damping using analytic signals", *Journal of Engineering Mechanics*, 123 (7), pp. 743-745

- Inaudi, J.A., Kelly, J.M., (1990), "Active isolation", *Proceedings of U.S. National Workshop on Structural Control Resolutions.*

- Jabbari, F., Schmitendorf, W.E., Yang, J.N., (1995), "H control for seismic-excited buildings with acceleration feedback", *Journal of Engineering Mechanics - ASCE*, 121 (9), pp. 994-1002.

- Jabbari, F., Bobrow, J.E., (2002), "Vibration suppression with resettable device", *Journal of Engineering Mechanics*, 128 (9), pp. 916-924.

- Jansen, L.M., Dyke, S.J., (2000), "Semiactive control strategies for MR dampers: Comparative study", *Journal of Engineering Mechanics*, 126 (8), pp. 795-803.

- Jin, G., Sain, M.K., Spencer Jr., B.F., (2005), "Nonlinear blackbox modeling of MR-dampers for civil structural control", *IEEE Transactions on Control Systems Technology*, 13 (3), pp. 345-355.

- Joghataie, A., Ghaboussi, J., (1994), "Neural network and fuzzy logic in structural control", *Proceedings of 1st World Conference on Structural Control*, 1, pp. 21-30.

- Johnson, E.A., Christenson, R.E., Spencer Jr, B.F., (2003), "Semiactive damping of cables with sag", *Computer-Aided Civil and Infrastructure Engineering*, 18 (2), pp. 132-146.

- Juang, J.N., Sae-Ung, S., and Yang, J.N., (1980), "Active control of large building structures.", *In Leipholz H H E(ed) Structural Control, North Holland, Amsterdam,* pp. 663-676.

- Jung, H.-J., Choi, K.-M., Spencer Jr., B.F., Lee, I.-W., (2006), "Application of some semi-active control algorithms to a smart base-isolated building employing MR dampers", *Structural Control and Health Monitoring,* 13 (2-3), pp. 693-704

- Kannan, S., Uras, H.M., Aktan, H.M., (1995), "Active control of building seismic response by energy dissipation", *Earthquake Engineering & Structural Dynamics*, 24 (5), pp. 747-759.

- Karkoub, M.A., Zribi, M., (2006), "Active/semi-active suspension control using magnetorheological actuators", *International Journal of Systems Science*, 37 (1), pp. 35-44.

- Kawashima, K., Unjoh, S., (1994), "Seismic response control of bridges by variable dampers", *Journal of Structural Engineering - ASCE*, 120 (9), pp. 2583-2601.

- Kelly, J. M., (1999b), "The current state of base isolation in the United States.", *Proc., 2nd World Conf. on Structural Control, Kyoto, Japan*, Vol. 1, pp. 1043-1052.

- Khargonekar, Pramod P., Petersen, Ian R., Zhou, Kemin, (1990), "Robust stabilization of uncertain linear systems: Quadratic stabilizability and H control theory", *IEEE Transactions on Automatic Control*, 35 (3), pp. 356-361.

- Khot, N.S., Öz, H., (1997), "Structural-control optimization with H2 and H∞ norm bounds", *Optimal Control Applications and Methods,* 18 (4), pp. 297-311.

- Klein, R.E., Cusano, C., and Slukel, J.V., (1972), "Investigation of a method to stabilize wind induced oscillations in large structures.", *ASME Annual Meeting, New York*, Paper No. 72-WA / AUT-11.

- Klein, R.E., and Salhi, H., (1980), "Time optimal control of wind induced structural vibrations using active appendages.", *In Leipholz H H E (ed) Structural Control, North Holland, Amsterdam*, pp. 415-430.

- Kobori, T., Takahashi, M., Nasu, T., Niwa, N., Ogasawara, K., (1993), "Seismic response controlled structure with active variable stiffness system", *Earthquake Engineering and Structural Dynamics*, 22 (11), pp. 925-941.

- Kobori, T., (1994), "Future Direction on Research and Development of Seismic-Response-Controlled Structure.", *Proceedings of 1st World Conference on Structural Control, Los Angeles, California*, pp. 19–31.

- Kose, I.E., Schmitendorf, W.E., Jabbari, F., Yang, J.N., (1996), "H active seismic response control using static output feedback", *Journal of Engineering Mechanics*, 122 (7), pp. 651-659.

- Kose, I.E., Jabbari, F., Schmitendorf, W.E., Yang, J.N., (1998), "Controllers for quadratic stability and performance of a benchmark problem", *Earthquake Engineering and Structural Dynamics*, 27 (11), pp. 1385-1397.

- Kurata, N., Kobori, T., Takahashi, M., Niwa, N., Midorikawa, H., (1999), "Actual seismic response controlled building with semi-active damper system", *Earthquake Engineering and Structural Dynamics*, 28 (11), pp. 1427-1447.

- Kurata, N., Kobori, T., Takahashi, M., Ishibashi, T., Niwa, N., Tagami, J., Midorikawa, H., (2000), "Forced vibration test of a building with semi-active

damper system", *Earthquake Engineering and Structural Dynamics*, 29 (5), pp. 629-645.

- Kuriowa, H., and Aizawa, S., (1987), Private communication, May 1987.

- Li, C., (2004), "Evaluation of the lever-type active tuned mass damper for structures", *Structural Control and Health Monitoring*, 11 (4), pp. 259-271.

- Li, C., Liu, Y., Wang, Z., (2003), "Active multiple tuned mass dampers: A new control strategy", *Journal of Structural Engineering*, 129 (7), pp. 972-977.

- Li, C., Zhang, L., (2004), "Adjustable lever-type active tuned mass damper: A new ATMD model", *Acta Mechanica Solida Sinica,* 17 (1), pp. 74-82.

- Li, C., Zhou, D., (2004), "Evaluation of multiple active lever-type tuned mass dampers for structures under ground acceleration ", *Engineering Structures*, 26 (3), pp. 303-317.

- Liang, Z., Tong, M., Lee, G.C., (1995), "Real-time structural parameter modification (RSPM): Development of innervated structures", *Technical Report NCEER-95-0012 (National Center for Earthquake Engineering Research, Buffalo, New York).*

- Loh, C.-H., Chang, C.-M., (2006), "Vibration control assessment of ASCE benchmark model of cable-stayed bridge ", *Structural Control and Health Monitoring,* 13 (4), pp. 825-848.

- Lou, J.Y.K., Lutes, L.D., Li, J.J., (1994), "Active tuned liquid damper for structural control", *Proceedings of First World Conference on Structural Control*, pp. 70-79.

- Lund, R. A., (1979), "Active damping of large structures in wind", *ASCE Convention and Exposition.*

- Lynch, J.P., (1998), "Active structural control research at Kajima Corporation", PhD Dissertation, Department of Civil and Environmental Engineering, Stanford University.

- Mackriell, L.E., Kwok, K.C.S., Samali, B., (1997), "Critical mode control of a wind-loaded tall building using an active tuned mass damper", *Engineering Structures*, 19 (10), pp. 834-842

- Madden, G.J., Symans, M.D., Wongprasert, N., (2002), "Experimental verification of seismic response of building frame with adaptive sliding base-isolation system", *Journal of Structural Engineering*, 128 (8), pp. 1037-1045.

- Madden, G.J., Wongprasert, N., Symans, M.D., (2003), "Analytical and numerical study of a smart sliding base isolation system for seismic protection of buildings", *Computer-Aided Civil and Infrastructure Engineering*, 18 (1), pp. 19-30.

- Makris, N., (1997), "Rigidity-plasticity-viscosity: Can electrorheological dampers protect base-isolated structures from near-source earthquakes.", *Earthquake Engineering and Structural Dynamics,* 26 (5), pp. 571–591.

- Martin, C. R., and Soong, T. T., (1976), "Modal control of multistory structures", *ASCE Journal of Engineering Mechanics*, Vol. 102, pp. 613-623.

- Masri, S.F., Bekey, G.A., and Udwadia, F.E., (1980), "On-line control of tall buildings.", *In Leipholz H H E(ed) Structural Control, North Holland, Amsterdam,* pp. 471-492.

- Masri, S.F., Bekey, G.A., and Caughey, T.K., (1981), "Optimal pulse control of flexible structures.", *ASME Journal of Applied Mechanics,* 48, pp. 619-626.

- Masri, S.F., Bekey, G.A., and Caughey, T.K., (1982), "On-line control of nonlinear flexible structures.", *ASME Journal of Applied Mechanics,* 49, pp. 877-884.

- Miller, R.K., Masri, S.F., Dehghanyar, T.J., and Caughey, T.K., (1988), "Active vibration control of large civil structures.", *ASCE Journal of Engineering Mechanics,* 114, pp. 1542-1570.

- Morison, J., and Karnopp, D., (1973), "Comparison of optimized active and passive vibration absorbers", *14th Annual Joint Automatic Control Conference,* pp. 928-932.

- Nagarajaiah, S., (1994), "Fuzzy controller for structures with hybrid isolation system", *Proceedings of 2nd World Conference on Structural Control*, TA2, pp. 67-76.

- Nagarajaiah, S., Mate, D., (1998), "Semi-active control of continuously variable stiffness system", *Proceedings of 2nd World Conference of Structural Control*, 1, pp. 397-405.

- Nagarajaiah, S., and Sun, X., (2000), "Response of base-isolated USC hospital building in Northridge Earthquake.", *Journal of structural engineering New York*, 126 (10), pp. 1177–1186.

- Nagarajaiah, S., Varadarajan, N., (2000), "Novel semiactive variable stiffness tuned mass damper with real time tuning capability", *Proceedings of 13th Engineering Mechanics Conference (CD-Rom).*

- Nagarajaiah, S., Sahasrabudhe, S., Iyer, R., (2000), "Seismic response of sliding isolated bridges with MR dampers", *Proceedings of American Control Conference (CD ROM).*

- Nagarajaiah, S., Sahasrabudhe, S., (2006), "Seismic response control of smart sliding isolated buildings using variable stiffness systems: An experimental and numerical study", *Earthquake Engineering and Structural Dynamics*, 35 (2), pp. 177-197.

- Ni, Y.Q., Ying, Z.G., Wang, J.Y., Ko, J.M., Spencer Jr., B.F., (2004), "Stochastic optimal control of wind-excited tall buildings using semi-active MR-TLCDs", *Probabilistic Engineering Mechanics*, 19 (3), pp. 269-277.

- Nishimura, I., Kobori, T., Sakamoto, M., Koshika, N., Sasaki, K., Ohrul, S., (1992), "Active tuned mass damper", *Journal of Smart Material Structures,* 1, pp. 306-311.

- Nissen, H.D., Sørensen, P.H., Jannerup, O., (2004), "Active aerodynamic stabilisation of long suspension bridges", *Journal of Wind Engineering and Industrial Aerodynamics,* 92(10), pp. 829-847.

- *Newsletter of the International Association for Structural Control*, (1997). "New life for the Walnut Creek Bridge via semi-active vibration control", 2 (1), pp. 4-5.

- Ohrui, S., Kobori, T., Sakamoto, M., Koshika, N., Nishimura, I., Sasaki, K., Kondo, A., and Fukushima, I. (1994). "Development of Active-Passive Composite Tuned Mass Damper and an Application to the High Rise Building." *First World Conference on Structural Control, Los Angeles, CA,* TP1-100 - TP1-109.

- Patten, W.N., He, Q., Kuo, C.C., Liu, L., Sack, R.L., (1994), "Suppression of vehicle induced bridge vibration via hydraulic semiactive vibration dampers", *Proceedings of First World Conference on Structural Control*, pp. 3-38.

- Patten W.N., (1998), "The I-35 Walnut Creek Bridge: an intelligent highway bridge via semi-active structural control.", *Proceeding of 2nd World Conference on Structural Control*, pp.427–436.

- Patten, W.N., Sun, J., Li, G., Kuehn, J., Song, G., (1999), "Field test of an intelligent stiffener for bridges at the I-35 Walnut Creek Bridge.", *Earthquake Engineering and Structural Dynamics*, 28 (2), pp. 109-126.

- Petersen, Jan R., (1985), "Riccati equation approach to the design of stabilizing controllers and observers for a class of uncertain linear systems.", *IEEE Transactions on Automatic Control*, AC-30 (9), pp. 904-907.

- Peterson, Ian R., (1987), "Disturbance attenuation and h infinity optimization: a method design based on the algebraic Riccati equation.", *IEEE Transactions on Automatic Control*, AC-32 (5), pp. 427-429.

- Petersen, Ian R., Hollot, Christopher V., (1986), "Riccati equation approach to the stabilization of uncertain linear systems.", *Automatica*, 22 (4), pp. 397-411.

- Phillips, R.W., (1969), "Engineering applications of fluids with a variable yield stress.", Ph.D. thesis, University of California, Berkeley, California.

- Prucz, Z., and Soong, T.T., (1983), "On reliability and active control of tension leg platforms.", *In Chen W.F. and Lewis A.D.M. (eds) Recent Advances in Engineering Mechanics and Their Impact on Civil Engineering Practice,* 2, pp. 903-906.

- Ramallo, J.C., Johnson, E.A, Spencer, B.F., (2002), "Smart base isolation systems", *Journal of Engineering Mechanics*, 128 (10), pp. 1088-1100.

- Reinhorn, A.M., Soong, T.T., and Manolis, G.D., (1986), "Disaster prevention of deep water offshore structures by means of active control.", *Proceedings of ASME 5th OMAE Conference, Tokyo, Japan,* pp. 39-44.

- Reinhorn, A.M., Soong, T.T., and Wen, C.Y., (1987a), "Base isolated structures with active control.", *Proceedings of ASME PVD Conference, San Diego, CA,* pp. 413-420.

- Reinhorn, A.M, Manolis, G.D., and Wen, C.Y., (1987b), "Active control inelastic structures.", *ASCE Journal of Engineering Mechanics,* 113, pp. 315-333.

- Roorda, J., (1975), "Tendon control in tall structures.", *ASCE Journal of Structural Division,* 101, pp. 505-521.

- Sack, R.L., Patten, W., (1993), "Semiactive hydraulic structural control", *Proceedings of International Workshop on Structural Control*, pp. 417-431.

- Sahasrabudhe, S., Nagarajaiah, S., Hard, C., (2000), "Experimental study of sliding isolated buildings with smart dampers subjected to near source ground motions", *Proceedings of 13th Engineering Mechanics Conference (CD ROM).*

- Sahasrabudhe, S., Nagarajaiah, S., (2005), "Effectiveness of variable stiffness systems in base-isolated bridges subjected to near-fault earthquakes: An experimental and analytical study", *Journal of Intelligent Material Systems and Structures*, 16 (9), pp. 743-756.

- Samali, B., Yang, J.N., and Yeh, C.T., (1985a), "Control of coupled lateral-torsional motion of wind-excited buildings.", *ASCE Journal of Engineering Mechanics,* 111, pp. 779-796.

- Samali, B., Yang, J.N., and Liu, S.C., (1985b), "Control of lateral-torsional motion of buildings under seismic load.", *ASCE Journal of Structural Engineering,* 111, pp. 2165-2180.

- Schmitendorf, W.E., Kose, I.E., Jabbari, F., Yang, J.N., (1994), "H∞ control of seismic excited buildings using direct output feedback", *Proceedings of 1st World Conference on Structural Control.*

- Shooshtari, M., (2005), "Active seismic control of reinforced concrete structures", Ph.D. dissertation, University of Ottawa, Ottawa, Ontario, Canada.

- Smith, H.A., Chase, J.G., (1994), "Robust disturbance rejection using H∞ control for civil structures", *Proceedings of 1st World Conference on Structural Control.*

- Soong, T.T., Reinhorn, A.M., and Yang, J.N., (1987), "A standardized model for structural control experiments and some experiments and some experimental results.", *In Leipholz H H E(ed) Structural Control Martinus Nijhoff, Amsterdam,* pp. 669-693.

- Soong, T.T., (1990), "Active structural control", John Wiley and Sons, Inc., New York.

- Soong, T.T., and Costantinou, M.C., (1994), "*Passive and Active Structural Vibration Control in Civil Engineering*", Springer-Verlag Wien, New York.

- Soong, T.T., and Dargush, G.F., (1997), "Passive Energy Dissipation Systems in Structural Engineering", John Wiley & Sons, England.

- Soong, T.T., and Skinner, G.T., (1981), "Experimental study of active structural control.", *ASCE Journal of Engineering Mechanics Devision,* 107, pp. 1057-1068.

- Soong, T.T., Spencer, B.F., (2002), "Supplemental energy dissipation: State-of-the-art and state-of-the-practice", *Engineering Structures*, 24 (3), pp. 243-259.

- Spencer Jr., B.F., Sain, M.K., (1997), "Controlling buildings: A new frontier in feedback", *IEEE Control Systems Magazine*, 17 (6), pp. 19-35.

- Spencer Jr., B.F., Dyke, S.J., Sain, M.K., Carlson, J.D., (1997), "Phenomenological model for magnetorheological dampers", *Journal of Engineering Mechanics*, 123 (3), pp. 230-238.

- Spencer Jr., B.F., Dyke, S.J., Deoskar, H.S., (1998), "Benchmark problems in structural control: Part I-active mass driver system", *Earthquake Engineering and Structural Dynamics*, 27 (11), pp. 1127-1139.

- Spencer Jr., B.F., Yang, G., Carlson, J.D., Sain, M.K., (1999), "Smart dampers for seismic protection of structures: A full-scale study", *Proceedings of 2nd World Conference of Structural Control*, 1, pp. 417-426.

- Spencer Jr., B.F., Johnson, E.A., Ramallo, J.C., (2000), "Smart isolation for seismic control", *JSME International Journal, Series C: Mechanical Systems, Machine Elements and Manufacturing*, 43 (3), pp. 704-711.

- Spencer Jr., B.F., (2002), "Civil engineering applications of smart damping technology", *Proceedings of 5th International Conference on Vibration Engineering*, pp. 771-782.

- Spencer Jr., B.F., Nagarajaiah, S., (2003), "State of the art of structural control", *Journal of Structural Engineering*, 129 (7), pp. 845-856.

- Subramaniam, R.S., Reinhorn, A.M., Riley, M.A., Nagarajaiah, S., (1996), "Hybrid control of structures using fuzzy logic", *Microcomputers in Civil Engineering*, 11 (1), pp. 1-17.

- Sun, J., Shahin, A.R., (1999), "Optimal H∞ control of structural vibrations using shape memory alloy actuators", *American Society of Mechanical Engineers, Aerospace Division (Publication)*, AD 59, pp. 161-174.

- Symans, M.D., Constantinou, M.C., Taylor, D.P., and Garnjost, K.D., (1994), "Semi-active fluid viscous dampers for seismic response control.", *Proceedings of 1st World Conference on Structural Control*, pp. 3–12.

- Symans, M.D., Constantinou, M.C., (1997), "Seismic testing of a building structure with a semi-active fluid damper control system", *Earthquake Engineering and Structural Dynamics*, 26 (7), pp. 759-777.

- Symans, M. D., and Constantinou, M. C. (1999), "Semi-active control systems for seismic protection of structures: A state-of-the-art review.", *Engineering Structures*, 21 (6), pp. 469–487.

- Symans, M.D., Kelly, S.W., (1999), "Fuzzy logic control of bridge structures using intelligent semi-active seismic isolation systems", *Earthquake Engineering and Structural Dynamics*, 28 (1), pp. 37-60.

- Taran, V. A., (1964), "Improving the dynamic properties of automatic control systems by means of nonlinear corrections and variable structures", *Automat Remote control*, 25, pp. 140-149.

- Traina, M.I., et al. (1988), "An experimental study of the earthquake response of building models provided with active damping devices.", *Proceedings of the 9th World Conference on Earthquake Engineering, Japan,* VIII, pp. 447-452.

- Uang, C-M., and Bertero, V.V., (1988), "Use of energy as a design criterion in earthquake-resistant design.", *Report No. UCB/EERC-88/18,* University of California, Berkeley.

- Udwadia, F.E., and Tabaie, S., (1981a), "Pulse control of a single-degree-of-freedom system.", *ASCE Journal of Engineering Mechanics,* 107, pp. 997-1010.

- Udwadia, F.E., and Tabaie, S., (1981b), "Pulse control of structural and mechanical systems.", *ASCE Journal of Engineering Mechanics,* 107, pp.1011-1028.

- Utkin, V. I., (1977), "Variable structure systems with sliding mode, a survey", *IEEE Trans Automat Control,* 22, pp. 212-222.

- Utkin, V.I., (1992), "*Sliding Modes in Control Optimization*", Springer, Berlin.

- Varadarajan, N., Nagarajaiah, S., (2003), "Wind response control of building with variable stiffness tuned mass damper using empirical mode decomposition/Hilbert transform", *Journal of Engineering Mechanics*, 130 (4), pp. 451-458.

- Veillette, R.J., Medanic, J.V., Perkins, W.R., (1989), "Robust stabilization and disturbance rejection for systems with structured uncertainty", *Proceedings of 28th Conference on Decision and Control.*

- Wu, J.-C., (2003), "Experiments on a full-scale building model using modified sliding mode control", *Journal of Engineering Mechanics*, 129 (4), pp. 363-372.

- Wu, J.C., Yang, J.N., (1998), "Active control of transmission tower under stochastic wind", *Journal of Structural Engineering*, 124 (11), pp. 1302-1312.

- Wu, J.C., Yang, J.N., Agrawal, A.K., (1998), "Applications of sliding mode control to benchmark problems", *Earthquake Engineering and Structural Dynamics*, 27 (11), pp. 1247-1265.

- Wu, J.-C., Yang, J.N., (2004), "Modified sliding mode control for wind-excited benchmark problem", *Journal of Engineering Mechanics*, 130 (4), pp. 499-504.

- Xie, Lihua, de Souza, Carlos E., (1992), "Robust H control for linear systems with norm-bounded time-varying uncertainty", *IEEE Transactions on Automatic Control*, 37 (8 pt I), pp. 1188-1191.

- Yalla, S.K., Kareem, A., (2003), "Semiactive tuned liquid column dampers: Experimental study", *Journal of Structural Engineering*, 129 (7), pp. 960-971.

- Yalla, S.K., Kareem, A., Kantor, J.C., (2001), "Semi-active tuned liquid column dampers for vibration control of structures", *Engineering Structures*, 23 (11), pp. 1469-1479.

- Yan, N., Wang, C.M., Balendra, T., (1999), "Optimal damper characteristics of ATMD for buildings under wind loads", *Journal of Structural Engineering*, 125 (12), pp. 1376-1383.

- Yan, S., Zhang, H., (2005), "Smart vibration control analysis of seismic response using MR dampers in the elevated highway bridge structures ", *Proceedings of SPIE (The International Society for Optical Engineering)*, 5765 (P2), pp. 1053-1060.

- Yan, G., Zhou, L.L., (2006), "Integrated fuzzy logic and genetic algorithms for multi-objective control of structures using MR dampers ", *Journal of Sound and Vibration,* 296 (1-2), pp. 368-382.

- Yang, J.N., Giannopoulos, F., (1978), "Active tendon control of structures.", *ASCE Journal of Engineering Mechanics Division,* 104, pp. 551-568.

- Yang, J.N., Giannopoulos, F., (1979a), "Active control and stability of cable stayed bridge.", *ASCE Journal of Engineering Mechanics Division*, 105, pp. 677-694.

- Yang, J.N., Giannopoulos, F., (1979b), "Active control of two-cable stayed bridge.", *ASCE Journal of Engineering Mechanics Division*, 105, pp. 795-810.

- Yang, J.N., (1982), "Control of tall buildings under earthquake excitations.", *ASCE Journal of Engineering Mechanics Division,*108, pp. 50-68.

- Yang, J.N., and Lin, M.J., (1983), "Building critical-mode control: Nonstationary Earthquakes.", *ASCE Journal of Engineering Mechanics Division,* 109, pp. 1375-1389.

- Yang, J.N., Akbarpour, A., Ghaemmaghami, P., (1986), "New optimal control algorithms for structural control", *ASCE Journal of Engineering Mechanics*, Vol. 113, pp. 1369-1386.

- Yang, J.N., Wu, J.C., Hsu, S.Y., (1994a), "Parametric control of seismic-excited structures", *Proceedings of First World Conference Structural Control.*

- Yang, J.N., Wu, J.C., Reinhorn, A.M., Riley, M., Schmitendorf, W.E., Jabbari, F., (1994b), "Experimental verification of H∞ and sliding mode control for seismic excited structures", Proceedings of 1st World Conference on Structural Control.

- Yang, J.N., Wu, J.C., Agrawal, A.K., Li, Z., (1994c), "Sliding Mode Control of Seismic-excited Linear and Nonlinear Civil Engineering Structures.", *Technical Rep. NCEER-94-0017, National Center for Earthquake Engineering Research, Buffalo, N.Y.*

- Yang, G., Spencer, B.F., Carlson, J.D., Sain, M.K., (1995a), "Hybrid control of seismic-excited bridge structures", *Earthquake Engineering and Structural Dynamics*, 24 (11), pp. 1437-1451.

- Yang, J.N., Wu, J.C., Agrawal, A.K., (1995b), "Sliding mode control for seismically excited linear structures", *Journal of Engineering Mechanics*, 121 (12), pp. 1386-1390.

- Yang, J.N., Wu, J.C., Agrawal, A.K., (1995c), "Sliding mode control for nonlinear and hysteretic structures", *Journal of Engineering Mechanics*, 121 (12), pp. 1330-1339.

- Yang, J.N., Wu, J.C., Reinhorn, A.M., Riley, M., Schmitendorf, W.E., Jabbari, F., (1996a), "Experimental verifications of H and sliding mode control for seismically excited buildings", *Journal of Structural Engineering*, 122 (1), pp. 69-75.

- Yang, J.N., Wu, J.C., Reinhorn, A.M., Riley, M., (1996b), "Control of sliding-isolated buildings using sliding-mode control", *Journal of Structural Engineering*, 122 (2), pp. 179-186.

- Yang, J.N., Wu, J.C., Agrawal, A.K., Hsu, S.Y., (1997), "Sliding Mode Control with compensator for wind and seismic response control", *Earthquake Engineering and Structural Dynamics*, 26 (11), pp. 1137-1156.

- Yang, J.N., Kim, J.-H., Agrawal, A.K., (2000), "Resetting semiactive stiffness damper for seismic response control", *Journal of structural engineering New York, N.Y.*, 126 (12), pp. 1427-1433.

- Yang, G., (2001), "Large-scale magnetorheological fluid dampers for vibration mitigation: modeling, testing and control", Ph.D. dissertation, University of Notre Dame, Indiana, United States.

- Yang, J.N., Agrawal, A.K., (2002), "Semi-active hybrid control systems for nonlinear buildings against near-field earthquakes", *Engineering Structures*, 24 (3), pp. 271-280.

- Yang, G., Spencer, B.F., Carlson, J.D., Sain, M.K., (2002a), "Large-scale MR fluid dampers: Modeling and dynamic performance considerations", *Engineering Structures*, 24 (3), pp. 309-323.

- Yang, J.N., Lin, S., Kim, J. H., Agrawal, A. K., (2002b), "Optimal design of passive energy dissipation system based on H_∞ and H_2 performances", *Earthquake Engineering and Structural Dynamics,* 31 (4), pp. 921-936.

- Yang, G., Spencer Jr., B.F., Jung, H.-J., Carlson, J.D., (2004), "Dynamic modeling of large-scale magnetorheological damper systems for civil engineering applications", *Journal of Engineering Mechanics*, 130 (9), pp. 1107-1114.

- Yi, F., and Dyke, S.J., (2000), "Structural control systems: performance assessment.", *Proceedings of American Control Conference*, Chicago, IL.

- Yi, F., Dyke, S.J., Caicedo, J.M., Carlson, J.D., (2001), "Experimental verification of multiinput seismic control strategies for smart dampers", *Journal of Engineering Mechanics*, 127 (11), pp. 1152-1164.

- Ying, Z., Ni, Y., Ko, J., (2004), "A new stochastic optimal control strategy for hysteretic MR dampers ", *Acta Mechanica Solida Sinica*, 17 (3) , pp. 223-229.

- Yoshioka, H., Ramallo, J.C., and Spencer Jr., B.F., (2002), "Smart base isolation strategies employing magnetorheological dampers.", *Journal of Engineering Mechanics*, 128 (5), pp. 540-551.

- Xu, Y.L., Qu, W.L., Ko, J.M., (2000), "Seismic response control of frame structures using magnetorheological/electrorheological dampers", *Earthquake Engineering and Structural Dynamics*, 29 (5), pp. 557-575.

- Zames, G., (1981), "Feedback and optimal sensitivity - model reference transformations, multiplicative seminorms, and approximate inverses.", *IEEE Transactions on Automatic Control*, AC-26 (2), pp. 301-320.

- Zhou, Q., Nielsen, S.R.K., Qu, W.L., (2006), "Semi-active control of three-dimensional vibrations of an inclined sag cable with magnetorheological dampers", *Journal of Sound and Vibration,* 296 (1-2), pp. 1-22.